1990

Model Potential Studies of Perfect and Defect Properties of Some Alkali Metal Hydride and Deuteride Crystals

Haque, Md. Enamul

University of Rajshahi

MODEL POTENTIAL STUDIES OF PERFECT AND DEFECT PROPERTIES OF SOME ALKALI METAL HYDRIDE AND DEUTERIDE CRYSTALS.

By

Md. Enamul Haque

A Thesis Submitted to the University of Rajshahi in Candidature for the Degree of Doctor of Philosophy.

Condensed Matter Research Laboratory
Department of Physics
University of Rajshahi
Rajshahi - 6205
Bangladesh

August 1990

The author also wishes to acknowledge the award of a Research Fellowship by the University Grants Commission, Bangladesh and the University of Rajshahi for granting him the study leave.

Finally, the author takes pleasure in extending his thanks to all the members of his family for their encouragement and sacrifice over the years.

The preparation of this thesis owes much to other works which are listed as references.

A B S T R A C T

The work in this thesis describes an investigation of the static, dynamic, and defect properties of hydrides and deuterides of lighter lithium in addition to a heavier sodium alkali metal. A combination of various theoretical techniques are utilized to obtain a potential model that gives a good unified description of all the properties, e.g. static, dynamic, and defect properties of the lighter as well as the least studied heavier compounds.

The first part of the work reviews the directions along which the study on crystal interactions is progressing on the basis of the phenomenological and microscopic theories. The basic theories of these models have been reviewed with a view to developing an interaction potential applicable in all respects in the field of alkali metal hydrides and deuterides.

The second part of the work is concerned with the development of a set of interionic potentials of the Born-Mayer form using the shell model. Some of the earlier potentials suffer from serious drawbacks particularly when applied to dynamic and defect properties. These deficiencies are taken into cosideration in the present study. The development is carried out through using a combination of theoretical techniques, empirical fit, and a few plausible assumptions.

The third part of the work assesses the derived potentials by calculating the lattice statics and dynamics of the crystals and then by comparing results with experimental data (where available) and with other calculations. The potentials are found

to describe the elastic and dielectric properties reasonably well. The phonon dispersion curves of hydrides and deuterides of lithium and sodium are compared with the observed data (where available) and the calculations of Dyck and Jex based on force constant model approach and the results discussed. For the assessment of the potential, in case of a defect lattice the energies of formation of Schottky and Frenkel defects are calculated together with activation energies for defect migration mechanisms. The predicted anion vacancy activation energies are smaller and comparable with the cation value. The values , thus, obtained are insufficient to explain the curvature in the conductivity plot of ionic compounds. From this study it is suggested that both interstitial and vacancy play an important role in ionic conduction in all these four compounds. Finally, the good agreement with the observed data (where available) shows the validity and reliability of the derived potentials.

C O N T E N T S

CHAPTER 1

INTRODUCTION

1.1 General Introduction:

Metal hydrides possess properties that make them desirable for nuclear applications, for chemical reducing agents, for deoxidation and desulphurization of molten ferrous alloys, and for use as high energy fuels. Some of the hydrides can be used as portable sources of hydrogen[1].The hydrides of the alkali metals are all quite similar in their overall physical and chemical properties. LiH is a material unique in its simplicity of electronic structure and its nuclear preparation. Thus it is not surprising to find that there are considerably more literature pertaining to LiH AND LiD[1-11] than to any of the other saline hydrides. A survey of literature shows that both theoretical and experimental investigations on the perfect and defect properties of the hydride and deuteride of lithium have been made. Pandey and Stoneham[11] reported both the perfect (static and dynamic) and defect lattice properties of the lightest hydride and deuteride. Verble et al.[12] have investigated rigid ion model and shell model and presented the phonon dispersion in LiD, also Jaswal et al.[6] and Jaswal and Dilly[7] have calculated the phonon dispersion of LiH and LiD using the deformation dipole model as well as the extended form of this model,the deformable-ion model. Experimental studies on the phonon dispersion in LiD and the frequency distribution function of LiH and LiD were performed on the basis of inelastic neutron scattering by Verble et al.[12] and Zemnialov et al.[13], respectively. Raman and infrared measurements

on both the compounds have been reported[3,6,14,15], the elastic constants[15-18] and the specific heat[19] of the crystals, LiH and LiD, have been published. Singh[20] and Laplaze[21] have carried out theoretical investigation on rigid and deformable shell models, respectively. From the survey of literature it has been found that a limited number of lattice properties of perfect crystals of heavier hydrides and deuterides have been made. Following LiH, more is known of NaH and CaH_2, the remaining saline hydrides fall into a category about which relatively little specific information is available. This is not surprising since, because of the similarity among the hydrides, the hydrides that was most readily available and least expensive would naturally be chosen for a particular application.

Most of the theoretical investigations on the properties of perfect crystal (static and dynamic) and defect lattice have been concentrated on the alkali halides. Also from the experimental point of view, a good description of these compounds are available in literature. However, less attention has been paid on the study of these properties for alkali hydride crystals. This may be due to the nonavailability of experimental data. The author feels that more study of these crystals is necessary because they possess simple structure and important application. Hydride ion possesses a noble gas electron configuration and so the alkali hydrides are considered to be very close to the ideal picture of alkali halides as far as the nature of chemical bond and the crystal structure are concerned. The alkali hydrides are then considered to be the members of the alkali halide family.

The nature of binding in ionic crystals plays an important role in solid state physics and it is possible to describe a crystal in all respects if the true nature of binding between the ions of the crystal is known. The development of potentials for hydrides and deuterides has been largely driven by the increased use of modelling methods in studying both structural and defect properties of these materials. The works of several investigators[11,22-26] have clearly established the predictive role of defect calculations and have shown that the reliability is largely limited by the quality of the interatomic potentials used in the simulation.

Force constant models have been developed from the rigid ion model of Kellermann[27] through the shell model of Dick and Overhauser[28], Woods et al.[29] to the breathing shell model of Schroder or its extension[30-33] in order to explain the dynamical behaviour of crystal lattices. But such potentials are of little use outside this sphere and hence are not suitable for static or defect properties. Observed values for the hydrogen centres in alkali halides are available in literature. One can estimate the local mode frequencies for isolated and H^- substitutional (U-centre) and interstitial impurities, H^--cation impurity and H^--anion impurity pairs in alkali halides, because the modelling of interstitial H^- serves as a good test for any interionic potential. A sharply defined single mode property, e.g. local- (or gap-) mode frequencies yields an excellent and stringent test of the transferability of the derived potentials in dynamical application. There are several physical differences between the

parameters used in the force constant models and those used in the potential models[34]. In fact, new parameters are introduced at each stage of such development. The ultimate goal of all such calculations should be to develop a fully unified approach, in which the same model and interionic potentials are used consistently for all these types of calculations, e.g. static lattice, lattice vibration, and defect properties.

Bowman[35] derived empirical potentials for alkali hydrides and deuterides using the Born-Mayer model and reported cohesive energies which are in excellent agreement with the observed data. The results indicate a constant value for the hardness parameter, ρ determined from LiH (LiD) compressibility data and showed an adequate description of alkali hydride (deuteride) short-range forces when next nearest neighbour and van der Waals terms are included in the model. Although the potentials yield lattice energies in good agreement with the experimental values, their use in other calculations shows serious drawbacks in the calculation. As will be shown later the potentials fail miserably to describe elastic, dielectric, and defect properties. In fact, defect energy calculation on the basis of these potentials was not possible owing to the invalidity of minimisation caused by the potentials which give excessive shell displacement and it is a serious deficiency in the potential. Pandey and Stoneham[11] also presented a model potential and reported values for the perfect and defect crystals of LiH and LiD compound. Prior to PS[11] work, nearly all investigations were made for the lattice dynamics of LiH and LiD only except the work of Dyck and Jex[9] who for the

first time calculated the phonon dispersion curves for the heavier alkali metal hydride and deuteride compounds. As mentioned earlier all these works [9,30] involve shell model, distortion dipole model and their extended versions. The models were shown to be reasonable for the lattice dynamics of LiH and LiD which may successfully be used for the calculation of any physical properties of these crystals that is related to the lattice dynamics. But these are not suitable for defect calculation including some static calculation.

Recently Hussain and Sangster[36] has extended an existing set of model potentials for alkali halides (S-A) to incorporate alkali hydrides. The important feature of the potentials for alkali halides is that all pair interaction potentials are specified solely in terms of parameters of the ions involved. The undesirable thing is the use of LiH data for the scheme since dielectric data and optic frequencies for heavier hydrides are not available. The choice is the least favourable because lithium halides are the salts least well represented in the S-A scheme. A further problem arises from the chosen form of parametrization which necessitates relaxation of the restriction on Pauling parameter β_{--} to unacceptable value. There is also a difficulty in fitting cohesive energy with a reasonable choice of σ_{-}. They had to increase σ_{-}, with corresponding reduction in S_{-} in order to reduce the value of β_{--}, which then improved the fit to cohesive energy without seriously degrading the fit to lattice parameters of the hydrides except CsH[36]. Although cohesive energy, dielectric, and lattice dynamic properties are

represented in LiD by virtue of a fit to ε_0, ε_∞, ω_0, the elastic constants predicted by the model (calculated by the author) are too high. The significant differences between different potentials in predicting both cation migration and, even more important, the relative values of the Schottky and Frenkel formation energies in ionic compound[24,37] serve to emphasize the importance of using potentials that simulate both the dielectric and elastic properties as closely as possible. The lattice constants found by Hussain and Sangster[36] for NaH and CsH are higher. Also the use of a non-integral value of Z is less transparent physically and introduces various problems associated with the definition of the energies of charged defects[11].

Some potentials are more complex than others. The more complex potentials have been set up specifically to account for the Cauchy violation, yet these do not predict better defect calculations[37]. The breathing shell models or extensions of these models fitted to phonon spectra to account for finer details of these spectra do not require the lattice to be in equilibrium, whereas for defect calculations it is absolutely necessary to ensure this[37]. In view of the problems associated with the potentials as described above, it seems that an accurate evaluation of the interatomic potential will be a major work. This is particularly true if there are insufficient experimental data to derive a reliable potential.

Defects which require a good potential for their estimation, do determine many of the technologically important properties of solids and the knowledge of defect study will be applicable in the fields where technical requirements demand materials with

high ionic conduction, viz. in solid state batteries and fuel cells. Hence an ever increasing amount of attention is being devoted to the study of interionic potential.

The work presented in the thesis is to derive, using a combination of different approaches, a potential model that would describe not only the static but also lattice dynamic and defect properties for the lighter and heavier alkali hydrides and deuterides.

The plan of the thesis is as follows:

Chapter 2 is concerned with the structure and bonding of the alkali hydride and deuteride crystals. Chapter 3 describes various theoretical models of ionic crystals,e.g. rigid ion model, point polarizable ion model and shell model, together with a discussion of theoretical techniques which helped to formulate the present potential model. A brief account of the static and a detailed description of the dynamical properties of the perfect lattice including estimation of the phonon dispersion relations in principal symmetry directions have been given in chapter 4. The work on defect lattice which largely consists of computer simulation studies of transport properties, used in comparisons and interpretations of conductivity and diffusion experiments, and investigating mechanistic features of defect migration, etc. have been presented in chapter 5. Chapter 6 is concerned with the calculations and discussions of the results obtained on the basis of the derived potential. The conclusions and suggestions which provide a definite guideline for future work have been given in chapter 7.

CHAPTER 2

STRUCTURE AND BONDING

2.1 Introduction:

The solids have a long range-order or spatial periodicity of atoms in three dimensions. In solids the atoms are, in general, rigidly fixed at their positions or sites except for small vibrations (or sometimes localised group rotation). Such solids are called crystals, and the arrangement of atoms is termed the crystal structure. The properties of crystals are closely related to their structures. The basis on which crystals are distinguished from non-crystals is that the atoms in crystals are arranged in the form of a periodic array. Such an array consists of a representative unit of the structure which can be repeated in many different ways satisfying the basic requirement of periodicity. The internal regularity of atom placement in solids often leads to a symmetry of their external shapes. Rock salt crystals, e.g. rectangular parallelopipeds with faces which are identical when looked at from several different directions and which possess a high degree of symmetry. On the other hand, the glasses are not crystalline at all and the structure has a short-range order; in a fluid the order is confined to an extremely small range or it is absent completely. Section 2.2 is concerned with the Bonding in Solids. Section 2.3 discusses the structure of the crystals and the final section describes the Cohesive Energy of Ionic Crystals.

2.2 Bonding in Solids:

As solid exists in equilibrium at temperatures lower than those of the corresponding liquids and gases, they must have the lowest (free) energy configuration at the low temperatures. Furthermore, since solids do possess symmetry, a symmetrical spatial arrangement of atoms must be of lower energy than a random spatial arrangement. As the atoms of a solid do stick together and as they do not collapse to a very high density, there must be an attractive force counter-balanced by a repulsive force. There are several mechanisms which can give rise to an attractive force between atoms. The nucleus of an atom is surrounded by clouds or shells of electronic charge distribution. The stability of a shell is greater when it has a specified number of electrons in it. This situation is only possible by losing electrons from the outermost valence shells or acquiring some electrons to fill a shell. Most of the mechanisms available in literature to bind atoms are concerned with the manner in which the closed shell structure is attained. The solids are classified according to the types of binding, a description of which is presented below:

(a) Ionic: Atoms are bounded together and attain the stable equilibrium of closed shell structure by the loss or by the addition of one or more electrons. Consequently, the ionic bond is the result of the Coulombic type attraction between the essentially spherically distributed charges of opposite sign. Owing to the spherical symmetry this ionic bond is non-directional and the ions have a tendency to surround themselves

with as many ions of opposite sign as can possibly fit around the central ion. The surrounding ions are of like sign and tend to repel each other, but in practice, some types of compromise is attained. Each ion has a tendency to surround itself in the same way and instead of forming small discrete molecules they form the crystal through the continuous network of ions. In other words, a block of crystal is not made up of many individual molecules, rather the entire block is one gigantic molecule in which the effect on a given ion of all other ions is significant. This ionic bond is relatively strong and the crystals are characterized by their strength, hardness, high melting points and low coefficient of expansion.

(b) Covalent: In this type of bonding the electrons are shared between binding atoms without transferring the electrons from one to another. The electrons are shared in such a way that there is no way to say definitely whether the electron now belongs to any particular atom. The shells of all the atoms are then completely filled. The covalent bond is usually formed from two electrons, one from each atom participating in the bond. The electrons from the bond tend to be partly localised in the region between the two atoms joined by the bond. This covalent bond is directional and the sharing makes the bond very strong; the solids are, thus, hard with high melting points.

(c) Metallic: Here, the electron clouds associated with the atoms can escape and freely migrate from one atom to another instead of being confined to the neighbouring atom. Positively charged ion cores are then held together by their attraction to

the free electrons which form a cloud between them. The metallic crystals have high electrical and thermal conductivity, high optical reflection and absorption coefficients.

(d) Hydrogen Bonding: Hydrogen has only one electron and it should then form a covalent bond with only one other atom. Under certain conditions an atom of hydrogen is attracted by strong forces to two atoms. If the second atom is strongly electronegative, then the electron of the hydrogen atom is mostly transferred to it and leaves the atom positively charged. This is then attracted by another neighbouring electronegative ion and form the bond.

(e) van der Waals Bonding: In case of atoms with closed shell structures, high energy is required to remove an electron from their shells to make it available for sharing or transfer. Such atoms are held together to from a solid by the forces which arise from some relative motion between the electrons around an atom and the positively charged core. The electrostatic field then, fluctuates with the movement of the electrons. When two atoms approach each other this gives rise to a set of fluctuating dipoles with the result of an attractive force between the two. The van der Waals binding is weak and the solids, thus, formed are generally soft with low melting points.

2.3 The Structure of Crystals:

The structure adopted by a particular crystalline compound depends, to a great extent, on three main factors:(a) the general formula of the compound and the valencies of the elements

present, (b) the nature of bonding between the atoms, and (c) the relative size of the atoms or ions. A description of the above factors is presented below:

(a) The General Formula: The term General Formula is used here to denote the relative number of atoms of each type that are present, without specifying what the atoms are. As for example, the formula associated with the compound A_XB_Y gives the values of x and y without identifying A and B. Here, the coordination numbers of A and B are related directly to the general formula. In this connection, the general rule is that: the coordination numbers of A and B are in the ratio y:x, provided that direct A-A or B-B contacts do not occur. The rule does not predict absolute coordination numbers for a given formula but it imposes restriction on the combination of coordination numbers that are possible in a structure.

In a compound $A_XB_YC_Z$, in which the atoms A and B are cations and coordinated only to anions C, the average cation coordination number (CN) is related to the anion coordination number by

$$\frac{\text{Average cation CN}}{\text{Anion CN}} = \frac{Z}{X+Y} \qquad (2\text{-}1)$$

Here, the average cation CN is expressed by

$$\frac{X\ (\text{CN of A}) + Y\ (\text{CN of B})}{X+Y} \qquad (2\text{-}2)$$

Using (2-2) in (2-1), the eqn. stands as

$$X\ (\text{CN of A}) + Y\ (\text{CN of B}) = Z\ (\text{CN of C}) \qquad (2\text{-}3)$$

The relationship between general formula and coordination number has little importance in the absence of structural information and breaks down when bonding occurs between atoms of the same type. These comments are applicable to the relative coordination numbers in a compound and take no account of the valency of the atoms. In molecular crystals, however, the absolute coordination numbers are controlled by the valency and this is due to the electron pair covalent bonds hold the molecules together. Unless multiple or partial bonds occur, the number of bonds to a particular atom in a molecule is equal to the coordination number which is then equal to the valency of that ion. In molecular crystals although the valency of an atom or ion has its importance in controlling the general formula of the compound, it does not have a direct bearing on coordination number and structure.

(b) Bonding: The nature of bonding between atoms affects considerably the coordination number of the atoms and it has, thus, a major influence on the crystal structure. The structures with ionic bonding possess high symmetry and involve coordination numbers as high as possible. In this way, the net electrostatic attractive force which holds crystals together (and hence the lattice energy) is maximized. In contrast, covalent bonding is highly directional and one or all of the atoms of the compound has a definite preference for a certain coordination environment. The coordination numbers associated with a covalently bonded structure are usually small and may be less than those of corresponding ionic structures.

(c) Size: The relative size of the atoms in a compound plays an important role in the structure, especially, in more ionic structures. The principle that lies here is that the coordination number of a particular ion will be as large as possible, provided that it can be in contact with all of its neighbouring ions of opposite charge. The limiting situation takes place when a cation is too small to fit snugly into a particular hole in the array of anions. In this respect a hypothetical structure is regarded as unstable when a cation is found to rattle inside its holes. The limiting size of the interstitial hole in various anion arrays, e.g. f.c.c. and b.c.c. can be estimated on the basis of the radius ratio rules, but in reality, exception of the rule also occurs. The general relation between size and coordination number yields a value for the later associated with a structure and, here, the coordination number of the cation increases with the increase of the ratio (cation radius/anion radius).

In molecular materials, however, size considerations are less important. This is partly due to the fact that the coordination numbers in molecular materials are controlled by valency and partly due to the covalent radii of elements which do not show the same spread of values as do the ionic radii.

2.3.1 Ionic Structure:

Purely ionic bonding in crystalline compounds is an idealized or extreme form of bonding. But in reality, this type of bonding exists rarely. Even in structures which are regarded as essentially ionic , there is usually a certain amount of covalent

bonding between cation and anion which in turn reduces the charge on each. The rules which explain the formation of different structures are:

(a) Ions are treated as charged, elastic and polarizable spheres.

(b) Ionic structures are held together by electrostatic forces and hence the ions are arranged in such a way that cations are surrounded by anions, and vice versa.

(c) In order to maximize the net electrostatic attraction between ions in a structure (i.e. the lattice energy) the coordination numbers become as high as possible provided that the central ion maintains contact with all its neighbouring ions of opposite charge.

(d) As next nearest neighbour interactions are between the ions of like nature they are repulsive. Like ions arrange themselves to be as far apart as possible and hence, this leads to structures of high symmetry with a maximized volume.

(e) Around cation or anion sites electroneutrality must be preserved. In other words, the valency of an ion is equal to the sum of the electrostatic bond strengths between it and adjacent ions of opposite charge.

A brief account of the rules is given below:

Ions are charged as it is obvious from the cohesion of the ion. These are also elastic as their size varies with coordination number and are polarizable when departures from

purely ionic bonding occurs. Points (a) and (b) infer that the forces which hold ionic crystal together and the net energy of interaction between the ions are the same. This is obtained by assuming the crystal as a three-dimensional array of point charges and considering the net Coulombic energy of the array. The general Coulomb's law of interaction between any two ions is then applied to each pair of ions in the crystal and evaluation of the resulting force between all the ions leads to the lattice energy of the crystal. According to (c), the nearest neighbour ions should be in contact with each other. From the nature of the electron density distributions in ionic crystals, it is, in practice, hard to quantify what is meant by in contact. It is, however, an important factor since, although the variation in apparent size of ions with the coordination number occurs, most ions, especially, smaller ones, appear to have a maximum coordination number, e.g. for Be^{2+} this is four whereas for Li it is six. Ions are, therefore, flexible, but expand or contract only within fairly narrow limits. Point (d) on the maximization of volume of ionic crystals is not expected, on the ground that one is accustomed to regarding ionic structures and derivative close packed structures, especially, as having minimum volume. However, conflict does not exist. The prime bonding force in ionic crystals is the nearest neighbour cation-anion attractive force which is maximized at a small cation-anion separation. Also, when the ions are too close, additional repulsive forces come into play and then reduces the net attractive force. The effect of next nearest neighbour repulsive forces between like ions is then superposed on the former force and with the

constraints that (i) cation-anion distances be as short as possible, and (ii) coordination numbers be as large as possible, like ions arrange themselves to be as far apart as possible in order to reduce their mutual repulsion with the result of a regular and highly symmetrical arrays of like ions. The regular arrays of ions, then, tend to possess maximized volumes and that, by distorting the structures, a reduction in volume is possible,which may exist, at least in principle. According to Pauling`s electrostatic rule (e), the charge on a particular ion, e.g. an anion, must be balanced by an equal and opposite charge on the surrounding cations. As these cations are also shared with other anions, it is necessary to estimate the quantity of positive charge which is effectively associated with each cation-anion bond. For a cation M^{m+} surrounded by n anions, X^{n-}, the electrostatic bond strength (e.b.s.) of the cation-anion bond is expressed by

$$e.b.s. = m/n$$

Hence, for each anion, the sum of the electrostatic bond strength of the surrounding cations must balance on negative charge on the anion, i.e.

$$\frac{m}{n} = x$$

2.3.2 Structure of the Crystals under Study:

The hydrides and deuterides of lithium and sodium solidify in the rock salt structure. This structure consists of two face centered cubic sublattices, one of cations and the other of

anions. The unit cell of the structure is shown in fig. 2.1. This is simple cubic if the difference between the cation and anion positions is ignored. In fig. 2.2, the coordination environment of each ion is shown. As shown in fig. 2.2, both the anions and cations are octahedrally coordinated. From the general rule of coordination numbers of A and B associated with A_xB_y, the number must be in the ratio y:x. In this rock salt structure, x=y and therefore, anions and cations have the same coordination number. Here, each octahedron has twelve edges and each edge is shared between two octahedra. In fig. 2.3, a unit cell of one of the compounds under study is outlined (dotted) and is in the same orientation as in fig. 2.1. Octahedra 1 and 2 share a common edge, indicated by the thick dashed line, and octahedra 2 and 3 share a common edge, shown by the thick solid line. As each octahedron is linked by its edges to twelve other octahedra it is very difficult to represent satisfactorily in a drawing.

2.4 Cohesive Energy of Ionic Crystals:

Ionic crystals may be regarded as arrays of positively and negatively charged ions. The forces that hold the crystals together are entirely electrostatic in origin. The interaction potentials are divided, on the basis of ranges over which the individual terms are significant, into two parts:

(a) a short-range part, including both repulsion and van der Waals terms, and

(b) the long-range Coulombic part.

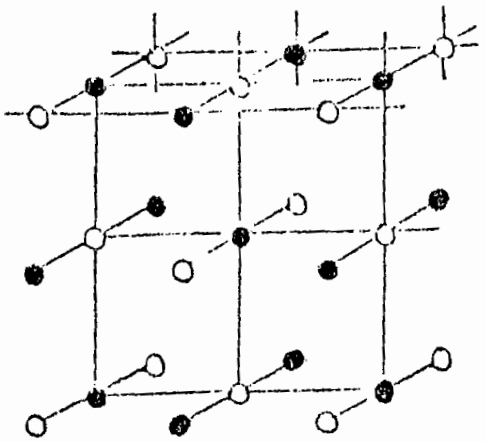

Fig. 2.1: Unit cell for f.c.c. lattices

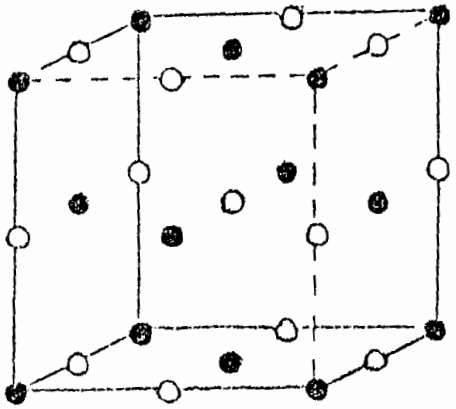

Fig. 2.2 : Coordination numbers of ions in f.c.c. lattices

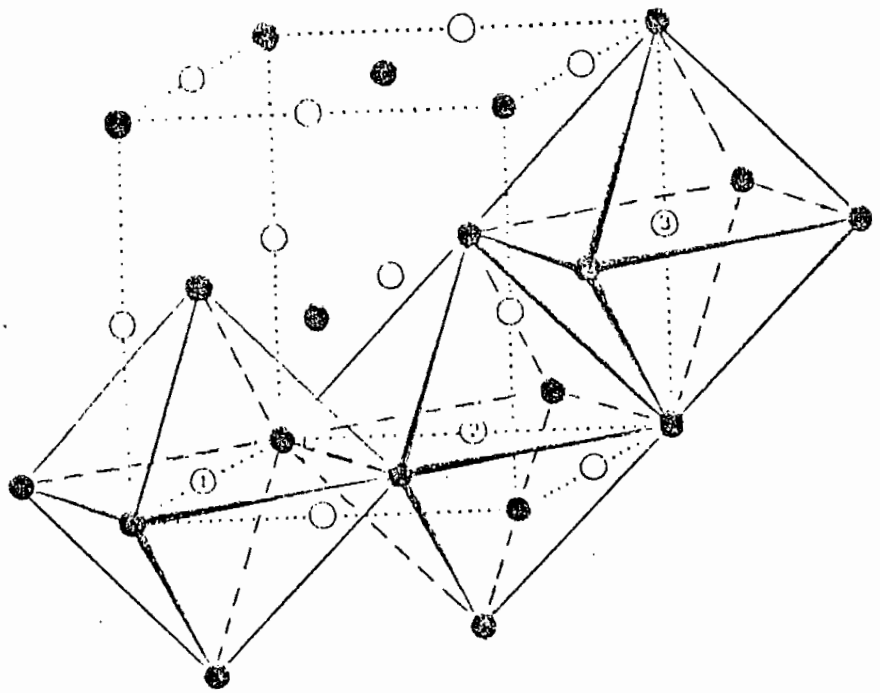

Fig. 2.3: Unit cell of the f.c.c. lattices showing edge sharing of octahedra.

The cohesive energy of a crystal is defined as the net potential energy of the arrangement of crystals that forms the structure. The value of the energy depends on the manner in which the ions are arranged, i.e. structure, the charges on the ions and the inter-nuclear separation between the anion and cation. The calculation of cohesive energy requires summation of both short-range and long-range terms.

It is assumed that the short-range interactions with a particular ion are truncated on a sphere centered on the ion and with the radius of the inscribed sphere of the cubic box. If two particles within the box are labelled by i and j and if their force on the particle i associated with j is required, then in addition to the particle j, all its images are also considered. With the above truncation, the contribution is from at most only one of the set of particles {j} (particle j and all its images). At first, it is required to find the particle from the set {j} which lies closest to i and then the components of the force which this particle exerts on particle i is evaluated. The cohesive energy is given by

$$U = Z_i Z_j \frac{e^2}{r} + \phi_{ij}(r) \qquad (2\text{-}4)$$

where i and j can be either + or -. In this case of alkali halide crystals, the system has been assumed to be fully ionic and the values of Z_i and Z_j are +1; r is used to denote the interionic separation. A detailed description of the short range terms $\phi_{ij}(r)$ has been given in the last part of chapter of 3. Short-range repulsive forces are important when ions are so close

together that their electron clouds begin to overlap. This short-range interactions of an ion with its neighbours are summed directly up to a specified distance beyond which the interaction has a negligible effect. Although significant contributions diminish rapidly with distance, this does not present problems for a real space summation. On the other hand, the long-range electrostatic summation involves great problems and an accurate calculation of the long-range Coulombic part is considerably harder. To obtain the Coulombic force on particle i associated with particle j, contributions from the complete set of particles {j} , as even distant terms are significant, must be taken into consideration. Thus, the summation can not be effectively truncated when handled in real space. However, rapid convergence occurs when it is transferred into reciprocal space. Although two-body, three-body, and higher order terms contribute to short-range interactions, in this study only the two-body terms have been taken into consideration. This is due to the fact that the approximation is valid in these systems of strongly ionic crystals, the alkali halides, but is less secure for more covalent systems. The electrostatic summation is calculated by the Ewald[38] method, a description of the method is given in the next section.

2.4.1 The Ewald Summation Method:

The Coulombic interaction of an array of ions i with a particular ion j is given by

$$\sum_i \frac{Z_i Z_j}{r_i} \qquad (2\text{-}5)$$

where Z_i and Z_j are the charges on ions i and j. Here, r_i indicates the distance between ion i and j.

The convergence in real space is very slow due to the r^{-1} term. Faster convergence is obtained by applying a mathematical transformation developed by Ewald. In this method a Gaussian charge distribution was added and then subtracted to each point charge in the array. In the method the various terms are arranged into rapidly and slowly converging series. By exploiting the periodicity of the lattice, the slowly converging series is Fourier transformed into reciprocal space and a rapid convergence is resulted. The transformation is discussed in most standard solid state texts and applications to crystals are given by Born and Huang[39].

The object of the Ewald method is to calculate the electrostatic potential experienced by one ion, in the presence of all the other basis species. The problem is then simplified by considering the interaction between the reference ion and each sublattice separately and then the summation is evaluated.

The total potential at the reference ion is expressed as the sum of the two potentials:

$$\Psi = \Psi_1 + \Psi_2 \qquad (2\text{-}6)$$

The potential Ψ_1 is that of the sublattice, with a Gaussian distribution of charge replacing each point charge; the Gaussians are taken to have a width of η. The charge distribution on the reference point does not contribute to Ψ and so Ψ_1 may be written as

$$\Psi_1 = \Psi_a - \Psi_b \qquad (2\text{-}7)$$

Ψ_a is the potential of a continuous series of Gaussians and, Ψ_b the Gaussian charge distribution at the reference point. The potential Ψ_2 corresponds to a lattice of point charges with an additional equal but oppositely charged Gaussian distribution. Summation of the two potentials cancels out the Gaussian charge distribution, and thus the potential is independent of the Gaussian width η.

The charge density of the potential Ψ_a is Fourier transformed and as the charge is periodic in the lattice, the transform involves only contributions from reciprocal lattice vectors, i.e. Ψ_a may be written as;

$$\Psi_a = \sum_G C_G e^{iGr} \qquad (2\text{-}8)$$

where G is the reciprocal lattice vector and C_G are the coefficients of the Fourier terms. The charge distribution is then made smooth by the transform and only the neighbouring lattice vectors make a significant contribution to the potential.

A suitable choice of η leads to a rapidly converging series in reciprocal space and Ψ_1 is obtained after subtraction of the charge distribution at the reference point; Ψ_2 is rapidly converging in real space. Although the combined potential is independent of Gaussian width, the choice of η is critical for rapid series convergence. Large values favour fast convergence in reciprocal space, in contrast, small values are suitable for real space convergence. The optimum width is, however, obtained from the balance between the extreme values.

With the help of the above method electrostatic energy is calculated precisely, leaving only the short-range component of the cohesive energy. This short-range part is evaluated by direct summation of the analytical expression used to model short-range interactions.

CHAPTER 3

THEORETICAL MODELS OF IONIC CRYSTALS

3.1 Introduction:

It is known that the conditions for equilibrium of a crystal require that at small separations the inter-particle forces are dominated by repulsive terms. At equilibrium these forces are balanced by the attractive Coulomb terms (and also the van der Waals, interactions). Thus, an interaction potential is required which must accurately model short-range interactions and the physical origin of which lies in the opposition to the overlap of closed electron shells. Although some quantum-mechanical calculations of the repulsive interactions have been performed, these have been found to be restricted to light ion and serve only to provide some justification for assuming a simple functional dependence of interionic distance for the repulsive energy. The short-range requirement has led to the adoption of either inverse power potentials or exponentially decaying potentials (to be discussed in subsequent sections).

Chapter 2 discussed the division of cohesive energy into long-range electrostatic terms and short-range interactions. It has been shown that the long-range part may be exactly evaluated using the Ewald method. On the other hand, accurate calculation of the short-range terms presents a much greater challenge and the limitation on the reliability of lattice simulation techniques is almost exclusively due to these terms. The aim of the present chapter is to highlight the limitations associated

with the old potential models and then to derive a potential model to reproduce the widest range of crystal properties. Section 3.2 consists of a description of The Rigid Ion Model. Section 3.3 discusses The Point Polarizable Ion Model. Section 3.4 is concerned with The Shell Model. Section 3.5 describes the Theoretical Techniques which are used to derive Interionic Interactions, and the final section, 3.6, is concerned with the Present Potential Model.

3.2 The Rigid Ion Model:

In the Rigid Ion Model (RIM) the ions are regarded as the rigid and unpolarizable point ions. They are prevented from collapsing under their mutual Coulomb attraction by the presence of a short-range overlap repulsion.

The energy of the perfect crystal is then given by

$$U = \frac{1}{2} \sum_{i=j} \left[\frac{Z^2 e^2}{r_{ij}} + \phi(r_{ij}) \right] \qquad (3\text{-}1)$$

where Ze is the ionic charge and r_{ij} denotes distance between ions i and j.

In the simplest treatments, the overlap forces are considered to be restricted to nearest neighbour atoms. It is then possible to describe the overlap forces in terms of a single function of the anion-cation distance . The values of the two parameters associated with any convenient energy function are then evaluated on the basis of experimental values of the compounds.

The two principal expressions for ϕ are:

(i) The Born potential $\phi = br^{-n}$ (3-2)

(ii) The Born-Mayer potential $\phi = Ae^{-r/\rho}$ (3-3)

In each case, r denotes the interionic distance . The parameters linking (i) are b and n and those associated with (ii) are A and ρ .

The overlap forces due to second neighbours have been taken into consideration approximately by Pauling[40], Huggins and Mayer[41] and then by Fumi and Tosi[42]. As the overlap energy now involves cation-cation and anion-anion interactions, more parameters are then included in the expression for ϕ unless simplifications are made.

Pauling[40] utilised the crystallographic concept of ionic radii to relate the b-parameters of the Born potential to the radii of the two ions involved in the interaction. According to Pauling the parameter n is used to be the same for all alkali halides. Pauling's expression for the overlap energy between the two ions i and j then takes the form:

$$\phi_{ij}(r) = \beta_{ij}(b_i+b_j) / r^n \qquad (3\text{-}4)$$

where $$\beta_{ij} = 1 + \frac{Z_i}{n_i} + \frac{Z_j}{n_j}$$

Z_i = valency of ion i

n_i = number of valency electrons in outer shells, and

b_i, m, n = parameters to be evaluated.

Tosi and Fumi[43] also investigated a form of the Born-Mayer potential. They allowed the hardness parameter ρ to be varied from crystal to crystal and took b as a constant, According to them the potential is:

$$\Phi_{ij}(r) = \beta_{ij}\, b\, e^{(r_i + r_j - r)/\rho_{ij}} \qquad (3\text{-}5)$$

Here, ρ_{ij} gives the value of the hardness parameter in a crystal composed of ions i and j.

Due to the omission of the polarization effects simulation of high frequency dielectric properties of a lattice is not possible on the basis of the model. At optical frequencies only the electrons (and not the ions) respond to the electric field of light. The electronic polarization gives rise to the dielectric constant ε_∞, as The Rigid Ion model ignores the electronic polarizabilities, it predicts $\varepsilon_\infty = 1$. In contrast, accurate simulation of crystal properties requires inclusion of polarizability. In addition to the above drawback, the model fails to account for the Cauchy violation[44-46], the phonon dispersion[47,48], the Szigeti effective charge[49] and the long-wave optical modes of vibrations[50]. However, the advantage of such a model is the reduction both in the number of parameters and degrees of freedom needed to model a system.

3.3 The Point Polarizable Ion Model:

The simple Rigid Ion Model is not suitable in situations where the ions are polarized, such as the polarization of the lattice by an external electric field or by the field due to a vacancy. The analysis of Kellermann[51] of the lattice vibrations

of alkali halides by means of The Rigid Ion Model was also unsatisfactory because the vibrating ions create an alternating electric field which polarizes the ions themselves. The circumstantial evidences, however, make one to believe that the deficiencies of The Rigid Ion Model can be overcome by the use of a model which takes the electronic polarizability of the ions into account.

Tessman et al.[52] obtained ionic polarizabilities by assuming the molecular polarizability of a given salt to be approximately equal to the sum of the polarizabilities of the component ions. The resulting polarizabilities are different from the free ion polarizabilities owing to the polarization of any ion is constrained by the presence of its neighbours. Thus,

$$\alpha_m = \alpha_i + \alpha_j + \Delta\alpha_m \qquad (3\text{-}6)$$

where α_m = molecular polarizability of the compound consisting of ions i and j,

α_i = ionic polarizability of ion i

$\Delta\alpha_m$ = error in additivity rule.

The molecular polarizabilities were obtained from the high frequency dielectric constant by the relation

$$\alpha_m = V_m \frac{\varepsilon_\infty - 1}{L(\varepsilon_\infty - 1) + 4\pi} \qquad (3\text{-}7)$$

where V_m is the molecular volume.

The Lorentz factor L arises in (3-7) relating the effective field E_{eff} and the applied field E and is expressed by:

$$E_{eff} = E + LP \qquad (3\text{-}8)$$

Using the value of L(=4π/3) the expression for molecular polarizability relating the high frequency dielectric constant is given by

$$\alpha_m = \frac{3V_m}{4\pi} \cdot \frac{\varepsilon_\infty - 1}{\varepsilon_\infty + 2} \qquad (3\text{-}9)$$

The dielectric properties on the basis of the point polarizable ion model (PPI) which incorporates such ionic polarizabilities can be investigated by comparing the atomic equations for longwave infrared vibrations with the corresponding continuum equations.

For an isotropic medium, Huang[39] presented the following continuum equations

$$\ddot{W} = b_{11} W + b_{12} E \qquad (3\text{-}10)$$

$$P = b_{21} W + b_{22} E \qquad (3\text{-}11)$$

where W is given by

$$W = \left(\frac{M_+ M_-}{M_+ + M_-} \right)^{1/2} (u_+ - u_-) \qquad (3\text{-}12)$$

Here, M_+, M_- = masses of the positive and negative ions,

u_+, u_- = displacements of the positive and negative ions

E = electric field vector,

P = polarization vector

It is known in the electromagnetic theory of light that the square of the refractive index is equal to the dielectric constant; the phenomenon of dispersion (the dependence of the refraction of a monochromatic wave on its frequency) follows directly from a frequency dependent dielectric constant. By solving equations (3-10) and (3-11) for the plane waves given by

$$W = W_0 \, e^{i(\omega t - k.r)} \qquad (3\text{-}13)$$

and

$$E = E_0 \, e^{i(\omega t - k.r)} \qquad (3\text{-}14)$$

Born presented the dispersion formula which is an expression for the frequency dependence of the dielectric constant ε and given as under:

$$\varepsilon(\omega) = \varepsilon_\infty + \frac{\varepsilon_0 - \varepsilon_\infty}{1 - (\omega/\omega_0)^2} \qquad (3\text{-}15)$$

where ε_0 is the static dielectric constant and ω_0 is the transverse optical frequency.

A combination of equations (3-10), (3-11) and (3-12) with the Maxwell's equations yields expressions for the longitudinal and two transverse wave solutions. The longitudinal wave has no magnetic field, and its frequency ω_1 does not depend on the wave vector q; Lyddane, Sachs and Teller's[50] relation is then written as

$$\left(\frac{\omega_1}{\omega_0}\right)^2 = \frac{\varepsilon_0}{\varepsilon_\infty} \qquad (3\text{-}16)$$

For the transverse waves, the dispersion relation is given by

$$\frac{(ck)^2}{w^2} = \varepsilon_\infty + \frac{\varepsilon_0 - \varepsilon_\infty}{1 - (w/w_0)^2} \qquad (3\text{-}17)$$

The polarization vector P is given by

$$P = \frac{1}{v} [\, Ze(u_+ - u_-) + (\alpha_+ + \alpha_-) E_{eff} \,] \qquad (3\text{-}18)$$

It is the inclusion of the electronic polarization terms

$$\frac{1}{v} (\alpha_+ + \alpha_-) E_{eff} \qquad (3\text{-}19)$$

in (3-18) which distinguishes the point polarizable ion model from the rigid ion model of the last section.

For sinusoidal waves of frequency W it can be shown that

$$(R - W^2\bar{M})(u_+ - u_-) = Ze\, E_{eff} \qquad (3\text{-}20)$$

Where

$$R = 2 \left[\frac{2\,\phi'(r_0)}{r_0} + \phi''(r_0) \right] \qquad (3\text{-}21)$$

Here, ϕ denotes the non-Coulombic part of the potential. Substituting the values of $u_+ - u_-$ in (3-18) one gets

$$P = \frac{1}{v} \left[\frac{(Ze)^2}{R - \bar{M}W^2} + \alpha_+ + \alpha_- \right] E_{eff} \qquad (3\text{-}22)$$

$$= \frac{\alpha(W)}{v} E_{eff}$$

where $$\alpha(\omega) = \alpha_+ + \alpha_- + \frac{(ze)^2}{R-\bar{M}\omega^2} \qquad (3\text{-}23)$$

The expression for the dielectric constant $\varepsilon(\omega)$ at frequency ω can be written in terms of $\alpha(\omega)$ as:

$$\frac{\varepsilon(\omega) - 1}{\varepsilon(\omega) + 2} = \frac{4\pi}{3v}\,\alpha(\omega) \qquad (3\text{-}24)$$

The expressions for the limiting cases where $\omega \to 0$ (static dielectric constant ε_0) and $\omega \to \infty$ (high frequency dielectric constant ε_∞) can be expressed by

$$\frac{\varepsilon_0-1}{\varepsilon_0+2} = \frac{4\pi}{3v} \lim_{\omega \to 0} \alpha(\omega)$$

$$= \frac{4\pi}{3v}\left[\alpha_+ + \alpha_- + \frac{z^2e^2}{R}\right] \qquad (3\text{-}25)$$

and

$$\frac{\varepsilon_\infty - 1}{\varepsilon_\infty + 2} = \frac{4\pi}{3v} \lim_{\omega \to \infty} \alpha(\omega)$$

$$= \frac{4\pi}{3v}\,[\alpha_+ + \alpha_-] \qquad (3\text{-}26)$$

The relation (3-26) was used by Tessman et al.[52] and is known as the Lorentz-Lorentz equation.

The transverse optical frequency ω_0 occurs when the relation (3-15) for $\varepsilon(\omega)$ becomes infinite. Rearrangement of (3-24) shows that ω_0 occurs when

$$\alpha(\omega) = \frac{3v}{4\pi} \qquad (3\text{-}27)$$

Thus,

$$\frac{3v}{4\pi} = \alpha_+ + \alpha_- + \frac{Z^2e^2}{R - \bar{M}\omega_0^2}. \qquad (3\text{-}28)$$

The solution of this equation with the help of equations (3-25) and (3-26) can be expressed in terms of R, ε_0, and ε_α as under:

$$\bar{M}\omega_0^2 = R\left(\frac{\varepsilon_\alpha + 2}{\varepsilon_0 + 2}\right) \qquad (3\text{-}29)$$

The displacement polarization is the same as that of reduced charges moving with the nuclei. Szigeti[49] postulated that the ions during the vibrations, behave as if they carry an effective charge e^*, which is smaller than the full electronic charge, e. Szigeti derived the following expression

$$\varepsilon_0 - \varepsilon_\alpha = \frac{4\pi}{9v} \cdot \frac{(Ze^*)^2(\varepsilon_\alpha + 2)^2}{\bar{M}\omega_0^2} \qquad (3\text{-}30)$$

which defines the effective charge e*.

Although many phenomena in solid-state physics can be explained on the basis of the PPI model, it fails to account for the defect properties of solids. In defect simulations with the PPI model, a polarizability, α, is ascribed to each ion. The studies of defect involves two major inadequacies associated with the model. Firstly, if short-range forces are obtained by fitting to the elastic constants the static dielectric constant is overestimated by the model. The consequence of this error of dielectric constant is an underestimation of the energy of

formation of charged defects, due to the incorrect calculated relaxation energy. In a study Norgett[53] predicted a value 2.1 eV for the Frenkel formation energy. Whereas, the corresponding experimental value in 2.7 ev. A great failure occurs in the work of Tharmalingam[54], where negative values were estimated for Schottky formation energies.

The second major inadequancy of the PPI treatment is its succeptibility to the polarization catastrophe. This instability, an account of which has been given by Faux[55] occurs in the calculation when two dipoles increases without bound due to their mutual dipole-dipole interaction outweighing the self-energy of polarization. Faux also showed that the instabilities occurs in any PPI calculation in which any two ions with i and j are closer than a minimum separation:

$$r_{ij} = (4\ \alpha_i \alpha_j)^{1/6}$$

The origin of the above two errors associated with the PPI treatment is in the omission from the model of any description of the physical basis of ionic polarization. The polarization involved in the model has been considered to be due to a response of a point ion, solely to electrostatic forces. The ionic dipole, however, is owing to the distortion of the ionic charge cloud. This distortion may be effected by both the electrostatic and short-range force fields, hence polarization and short-range forces are interdependent. Thus the displacement of an anion in a static electric field causes an imbalance in the repulsive forces acting on that ion, and the corresponding

induction of a deformation dipole. This feature has not been included in the PPI model, and then a high value of static dielectric constant is predicted. Similarly the neglect of the damping of polarization by short-range force fields leads to the polarization catastrophe. The inclusion of some description of such polarization damping is necessary in a model to have wide application in defect studies.

3.4 The Shell Model:

A good model should consist of a few, but physically meaningful, parameters. The choice of the model depends on the type of binding between the atoms. In ionic crystals, strong Coulomb forces and short-range repulsive forces operate between the ions. In the rigid ion model, an account of which has been given in the previous section, the charges are approximated by point charges centred at the nuclei. In reality, the ions are not rigid but polarisable. In the course of a lattice vibration, the electric field set up by the displacement of the ions is modified by the electronic polarisability which modifies the forces and affects the phonon frequencies. The widely used model for ionic crystals with polarisable ions is the shell model.

The physical basis of polarizability is the displacement of electrons by an electric field. Such displacements will change the short-range interactions between ions due to overlapping charge clouds. Therefore, the models which treat polarization as being solely due to the electrostatic field on the ion, e.g. the PPI model, are inadequate [56]. A successful treatment of polarizability must include coupling between short-range

repulsion and polarization. The shell model of Dick and Overhauser [28] as shown in fig. 3.1, simulates such behaviour using a simple mechanical description. The core, in which the mass of the ion resides, is connected to a massless shell, which represents the polarizable valance electrons. Here, ionic polarization is described as the displacement of a shell relative to a core. This treatment of polarization, therefore, includes a simple description of the distortion of the ionic charge cloud, and as short-range forces are taken to act between shells the model includes the required inter-dependence of those forces and polarization. The shell model then correctly simulates both elastic and dielectric properties of the crystal.

The model has been extensively developed since the original work of Dick and Overhauser. Cowley [57] gave a comprehensive treatment in which expressions are derived for bulk crystal properties including elastic and dielectric constants. Later on, the model was found to work good in the treatments for the fluorite lattice, e.g. the model was used to account for the internal strain contribution to the difference between C_{12} and C_{44} and to derive expressions for third order elastic constants.

The most extensive use of the shell model has been in the studies of lattice dynamics. Woods et al.[29] presented an analysis of lattice dynamics for the alkali halides on the basis of the shell model. Also several studies on fluorite compounds have used this shell model to analyse inelastic neutron data, e.g. work is reported by Elcombe and Pryor[58] for CaF_2 , by Elcombe[59] for SrF_2, by Hurrell and Minkiewicz[60] for BaF_2 and by

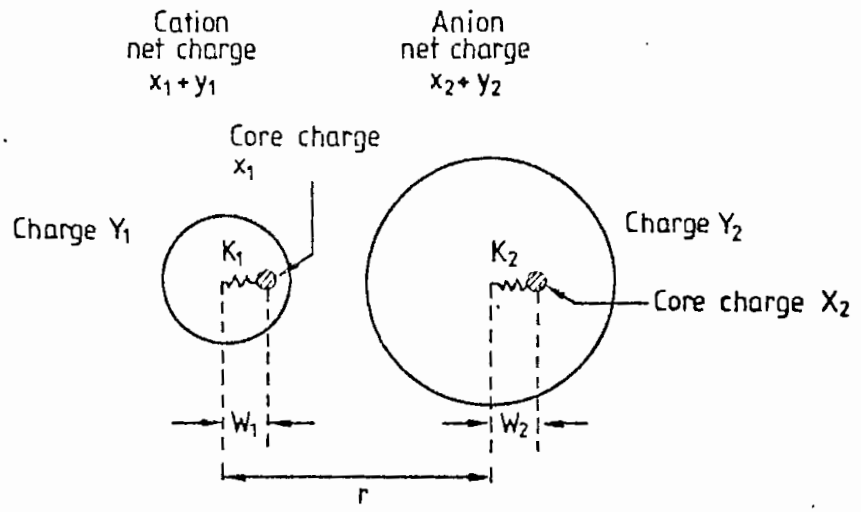

Fig. 3.1: The shell model.

Dolling et al.[61] for CO_2. The fit, however, obtained by the model to the experimental dispersion curves is generally fairly good.

In the Shell Model it is assumed that each ion consists of a spherical electronic shell which is isotropically coupled to its rigid-ion core by a spring of constant k; the charge of the shell is taken to be ye.

The free ion polarisability is given by

$$\alpha = \frac{(ye)^2}{k} \qquad (3\text{-}31)$$

The eqns. of motion on the basis of The Shell Model are given by:

$$-M_+\omega^2 u_1 = k_1(u_3 - u_1) + X_1 e E_{eff} \qquad (3\text{-}32)$$

$$0 = -k_1(u_3 - u_1) - R(u_3 - u_4) + Y_1 e E_{eff} \qquad (3\text{-}33)$$

$$-M_-\omega^2 u_2 = k_2(u_4 - u_2) + X_2 e E_{eff} \qquad (3\text{-}34)$$

$$0 = -k_2(u_4 - u_2) - R(u_4 - u_3) + Y_2 e E_{eff} \qquad (3\text{-}35)$$

where u`s denote the displacements of the positive and negative ion cores and the positive and negative ion shells. R is used to describe repulsive force constant.

Also $(X_1 + Y_1)e = Z_+e = (X_2 + Y_2) = Z_-e$ are the total charges on the ions.

E_{eff} = Effective field

P = polarization vector

$$= \frac{e}{v} [X_1 u_1 + Y_1 u_3 + X_2 u_2 + Y_2 u_4] \qquad (3\text{-}36)$$

The shell inertia forces are very small due to the relatively small mass of the electron and hence are omitted. Eqns. (3-32) to (3-35) can be written in the matrix form as follows:

$$\begin{bmatrix} -M_+w^2 & 0 & R & -R \\ 0 & -M_-w^2 & -R & R \\ -k_1 & 0 & k_1+R & -R \\ 0 & -k_2 & -R & k_2+R \end{bmatrix} \begin{bmatrix} u_1 \\ u_2 \\ u_3 \\ u_4 \end{bmatrix} \quad \begin{bmatrix} Z_1 \\ Z_2 \\ Y_1 \\ Y_2 \end{bmatrix} = eE_{eff} \qquad (3\text{-}37)$$

These eqns. are now solved to get u_1, u_2, u_3, and u_4 in terms of E_{eff} and then eqn.(3-36) is used to express P in terms of E_{eff} as:

$$P = \frac{\alpha(w)}{v} E_{eff} \qquad (3\text{-}38)$$

Now

$$E_{eff} = E + \frac{4\pi}{3} P, \text{ so that}$$

$$P = \frac{\alpha(w)/v}{1 - \frac{4\pi\alpha(w)}{3v}} E$$

Also

$$P = \frac{\varepsilon(\omega) - 1}{4\pi} E$$

where $\varepsilon(\omega)$ is the dielectric constant at frequency ω. Thus

$$\frac{\varepsilon(\omega) - 1}{\varepsilon(\omega) + 2} = \frac{4\pi}{3v} \alpha(\omega) \qquad (3\text{-}39)$$

The solution of (3-37) for $\alpha(\omega)$ is expressed by:

$$\alpha(\omega) = \frac{M_+M_-\omega^2[k_2Y_1^2+k_1Y_2^2+R(Y_1+Y_2)^2]-(M_++M_-)[Z^2k_1k_2+R(k_2X_1^2+k_1X_2^2)]}{M_-M_+\omega^2[k_1k_2+R(k_1+k_2)]-(M_++M_-)Rk_1k_2} \qquad (3\text{-}40)$$

where $Z = Z_+ = Z_-$.

The limiting values of (3-39) as $\omega \longrightarrow 0$ and $\omega \longrightarrow \infty$ are given by:

$$\frac{\varepsilon_0 - 1}{\varepsilon_0 + 2} = \frac{4\pi}{3v} \lim_{\omega \longrightarrow 0} \alpha(\omega)$$

$$= \frac{4\pi}{3v} \frac{Z^2k_1k_2+R(k_2X_1^2+k_1X_2^2)}{Rk_1k_2}$$

$$= \frac{4\pi}{3v}\left[\frac{Z^2}{R} + \frac{X_1^2}{k_1} + \frac{X_2^2}{k_2}\right] \qquad (3\text{-}41)$$

Taking $X_i = (Z-Y_i)$, the equation for ε_0 can be written as

$$\frac{\varepsilon_0 - 1}{\varepsilon_0 + 2}\frac{3}{4\pi} = \frac{1}{v}\left[\frac{(Z-Y_1)^2}{k_1} + \frac{(Z+Y_2)^2}{k_2} + \frac{Z^2}{R}\right] \qquad (3\text{-}42)$$

and

$$\frac{\varepsilon_\infty - 1}{\varepsilon_\infty + 2} = \frac{4\pi}{3v} \lim_{\omega \longrightarrow \infty} \alpha(\omega)$$

$$\frac{\varepsilon_\infty - 1}{\varepsilon_\infty + 2} \frac{3}{4\pi} = \frac{1}{v}\left[\frac{Y_1^2}{k_1} + \frac{Y_2^2}{k_2} - R_0\left(\frac{Y_1}{k_1} - \frac{Y_2}{k_2}\right)^2\right] \qquad (3\text{-}43)$$

where

$$\frac{1}{R_0} = \frac{1}{R} + \frac{1}{k_1} + \frac{1}{k_2} \qquad (3\text{-}44)$$

and

Anion polarizability is given by:

$$\alpha_2 = R_0\left[\frac{Y_2^2}{k_2}\left(\frac{1}{R} + \frac{1}{k_1}\right) + \frac{Y_1 Y_2}{k_1 k_2}\right] \qquad (3\text{-}45)$$

The dispersion frequency occurs when $\alpha(\omega) = \frac{3v}{4\pi}$

Thus,

$$\bar{M}\omega_0^2 = \frac{\alpha_0 - 3/4\pi}{\alpha_\infty - 3/4\pi} \frac{Rk_1k_2}{k_1k_2 + R(k_1+k_2)}$$

$$= \frac{\varepsilon_\infty + 2}{\varepsilon_0 + 2} \frac{Rk_1k_2}{k_1k_2 + R(k_1+k_2)} \qquad (3\text{-}46)$$

and the expression for the Szigeti charge using (3-40) is:

$$1 - \frac{e^*}{e} = \frac{R(Y_1k_2 - Y_2k_1)}{Z(k_1k_2 + R[k_1+_2])} \qquad (3\text{-}47)$$

3.5 Theoretical Techniques to Derive Interionic Interactions:

(a)Electron Gas Method:

For the calculation of forces between atoms it is convenient to divide the interactions into bonded and non-bonded types. It is known that bonded interactions occur between open cell atoms which involve considerably rearrangement of the electron density and the formation of covalent bonds. On the other hand, non-bonded interactions are between closed cell species, such as inert gas atoms or ions in crystals. They involve little distortion of the interacting species from spherical symmetry. In this part of the thesis an account is given on the method of calculating the non-bonded interactions.

For the purpose of calculation of the forces, a method is required which can be applied to a large range of interatomic separations. On the basis of the quantum mechanical theories, one can use perturbation theory at large distances and variational methods when the atoms are close together, but both the two techniques do not work satisfactorily at intermediate distances. Many authors worked on the problem and finally Gordon and Kim[62] presented a method as a solution. In modern implementations, the structures of the individual atoms are calculated accurately by quantum mechanical methods. The resulting charge densities are assumed to be unchanged when the atoms are brought together and the interaction energy of the two atoms is calculated using electron gas model, with the total charge density being a simple superposition of the individual atomic densities. In this technique, the electron kinetic energy in any small volume is

related by a simple power law to the local electron density. The total interaction energy $E_{ij}(r)$ of two interacting ions i and j is written as:

$$E_{ij}(r)=E_{ij}^{C}(r) +E_{ij}^{Ex}(r) +E_{ij}^{KE}(r) +E_{ij}^{Cor}(r) \qquad (3\text{-}48)$$

Where $E_{ij}^{C}(r)$ is the electrostatic interaction energy and $E_{ij}^{Ex}(r)$, $E_{ij}^{KE}(r)$ and $E_{ij}^{Cor}(r)$ denote the exchange, kinetic, and short-range correlation contribution to the interaction energy. Approximate expressions for all of the contributions are calculated in terms of the densities $\rho_i(r)$ and $\rho_j(r)$. A detailed description of the procedure and approximations, presented here, are given by Gordon and Kim[62]. Kim and Gordon[63], and Mackrodt and Stewart[24]. According to Gordon and Kim the energy of an isolated, closed-shell ion is given by

$$E(\rho) = C_k \int \left[\rho(r)^{5/3}\right] dr + C_e \int \rho(r)^{4/3}\, dr - Z \int \rho(r)/r\, dr + 1/2 \iint \rho(r)\, \rho(r')/|r - r'|\, dr\, dr' + \int \varepsilon_c [\, \rho(r)\,]\, \rho(r)\, dr \qquad (3\text{-}49)$$

where Z denotes the nuclear charge and

$$C_k = \frac{3}{10} (3\pi^2)^{2/3} ;$$

$$C_e = -\frac{3}{4} (3/\pi)^{1/3}$$

The first four terms of the eqn. represent the kinetic, exchange, and Coulomb energies respectively, while the last term is an approximation to the electron pair correlation energy and

can be determined simply by interpolating between the high and low density limits for a homogeneous electron gas. For a pair of ions, AB, the total electron density, $\rho_{AB}(r)$ is assumed to be the superposable sum of the separated ion densities, $\rho_A(r)$ and $\rho_B(r)$.The total energy of AB is, then, expressed by

$$E_{AB} = E [\rho_{AB}] = E [\rho_A + \rho_B] \qquad (3\text{-}50)$$

so that the interaction energy can be written as

$$E_{int} = E [\rho_A + \rho_B] - E [\rho_A] - E [\rho_B] \qquad (3\text{-}51)$$

Now, particularly at or near the minimum energy separation, is a small difference (~ 1 eV) between two considerably larger quantities. To minimise numerical errors in the evaluation of E_{int} Gordon and Kim proposed a re-arrangement of the integral expression in (3-49) and the expression for E_{int} takes the form

$$E_{int}(R) = Z_A Z_B/R - Z_B \int \rho_A(r_1)/ r_{1B}\, dr_1 - Z_A \int \rho_B(r_2)/ r_{2A}\, dr_2 + \iint \rho_A(r_1)\, \rho_B(r_2)/r_{12}\, dr_1\, dr_2 + \int \{[\rho_A(r) + \rho_B(r)]\, E_G\, [\rho_A(r) + \rho_B(r)] - \rho_A(r) E_G[\rho_A(r)] - \rho_B(r)\, E_G[\rho_B(r)]\}\, dr \qquad (3\text{-}52)$$

in which

$$E_G [\rho(r)] = C_k[\rho(r)]^{2/3} + C_e[\rho(r)]^{1/3} + E_c[\rho(r)] \qquad (3\text{-}53)$$

where r, r_{1B}, r_{2A} and r_{12} are functions of the inter-nuclear separation, R.

(b) Quantum Mechanical Method :

Fisher et al[4] performed a quantum mechanical calculation of the two-body SR interaction in LiH by taking determinantal wave functions consisting of various one-electron functions. They used the Heitler-London method to calculate the repulsive interaction energy, E_{rep} expressed by:

$$E_{rep}(r) = E(r) - E(\alpha) - q_a q_b/r \qquad (3\text{-}54)$$

Here, E(r) is used to denote the total energy as a function of internuclear distance, r.

$E(\alpha)$ gives the total energy of the separated pair, and q_a and q_b are the net charges of the ions a and b, respectively.

The energy E(r) is calculated from the relation:

$$E(r) = \int \Psi^* H \Psi \, d\tau \qquad (3\text{-}55)$$

where

$$H = \frac{1}{2} \sum_i \nabla_i - \sum_{i,a} \frac{Z_a}{r_{ia}} + \sum_{i>j} \frac{1}{r_{ij}} + \frac{Z_a Z_b}{r} \qquad (3\text{-}56)$$

The Hamiltonian involves the electronic kinetic energy, electron-nuclear, electron-electron, and nuclear-nuclear operators. The wave function Ψ is given as a linear combination of Slater functions of the form, $e^{-\delta r}$. Wave function parameters are then varied until the repulsive interactions obtained for the corresponding charge distributions result in a good fit to crystal data.

3.6 Present Potential Model:

The chosen form of the interionic potential has been developed on the basis of the points mentioned below with a view to describe, in a right manner, the lighter (lithium) and heavier (sodium) hydrides and deuterides (little work is available in literature for the heavier compounds). Short-range potential reported by Bowman[35] in the Born-Mayer form involving second neighbour interactions and van der Waals' terms is a two-body potential. As outlined in INTRODUCTION, this potential reproduces the perfect crystal data only in part but fails completely to describe a defect lattice. In this field, Hussain and Sangster[36] has extended the potentials for alkali halides to incorporate alkali hydrides. Here, also, it has been found that the potential is not suitable for a complete description (particularly defect properties) of the compounds under study.

In an exercise for the development of interionic potentials Catlow et al[22] reported that the contribution of many-body effects should be assessed. The effects as seen from the observed difference between C_{12} and C_{44}, must be equal for a compound with the rock salt structure under central pairwise interactions. However, this many-body effects as observed, generally, from the Cauchy violation may be erroneous owing to the over simplified treatment of the thermal contributions. This many-body effects may arise from the symmetric distortion of an ion or assymmetric distortions. It is known that the effects arising from the symmetric distortion contribute only to volume changing deformations but none to shear moduli, $1/2(C_{11}-C_{12})$ and C_{44}. On

the other hand, this effect that results from the assymmetric distortions of the ions or their environment does not contribute to the bulk modulus. Corish et al[25] also, from their work on the interionic potentials for alkali metal chlorides found that the best potential should be a central force potential in the Buckingham form with the repulsive part as hard as possible by omitting the van der Waals attraction between nearest neighbours. According to them the non-central forces do not improve the potential as judged by the criterion of the results of defect calculation.

It is known that dispersive interactions arise from the correlated motions of electrons on different atomic (or molecular) centres. This correlation, which is due to the Coulombic interaction of the electrons, results in an instantaneous dipole on each of the interacting species. The interaction of these dipoles and of the higher-order multipoles which they include gives rise to what is usually referred to as the van der Waals energy, Φ_{vdW}. Within the framework of perturbation theory it can be expressed as an asymptotic expansion of the form:

$$\Phi_{vdW}(r) = r^{-6} \sum_{n=0} C_n \, r^{-2n} \qquad (3\text{-}57)$$

where C_n are the so-called van der Waals coefficients.

From the above description, it is clear that the van der Waals interaction is a polarization phenomenon. The lowest energy can be expressed by :

$$(3\hbar/\pi r^6) \int_0^{\infty} \alpha_A\,(i\omega)\alpha_B\,(i\omega)d\omega \qquad (3\text{-}58)$$

where α_A and α_B are the polarizabilities of the two species at imaginary frequency ($i\omega$). Although the estimates of the coefficients, C_n, are available in literature, in general, the values are poorly known. Early work attempted to determine these coefficients from optical absorption data, but there are two difficulties associated with the approach. First, the energy of the optical excitations of anions and cations often overlap; second, it is uncertain as a to how much adjustment should be made for `local field` corrections in an ionic solid. Empirical estimates are given by:

$$-\frac{3}{2}\left[\frac{\delta_A\,\delta_B}{\delta_A+\delta_B}\right]\frac{\alpha_A\,\alpha_B}{r^6} \qquad (3\text{-}59)$$

Here the dependence is on the choice made for the average polarizabilities, α_A and α_B and the effective `excitation` energies δ_A and δ_B . Consequently there are large variations between the van der Waals coefficients reported by various authors using this approach. The methods, then, based on effective ionic polarizabilities and excitation energies, are unable to yield realistic values of the van der Waals coefficients. The study of dispersion energies in ionic solids is, thus,far from complete.

Taking into account these points and the points made by Corish et al[25] a potential model in the Buckingham form

including next near neighbour interactions has been developed. Here, complete quenching of the van der Waals' interactions between adjacent ions has been assumed.

The interionic potential energy based on the incompressible shell model is then expressed as a sum of pairwise terms as follows:

$$U_{ij}(r, W_i, W_j) = \frac{Z_i Z_j e^2}{|r|} + \frac{Y_i Y_j e^2}{|r+W_j-W_i|} + \frac{Y_i Z_j e^2}{|r-W_i|} + \frac{Y_i Z_j e^2}{|r+W_j|} + \frac{e^2}{2v}(k_i W_i^2 + k_j W_j^2) + \phi_{ij}(r, W_i, W_j) \qquad (3\text{-}60)$$

Where $r = (r_i - r_j)$ is the position of ion core j relative to ion core i, W_i and W_j the shell-core displacements, Y_i and Y_j the shell charges, k_i and k_j the spring constants, Z_i and Z_j the core charges of ions i and j, e the electronic charge, v the volume and ϕ_{ij}, the short-range part as discussed earlier is assumed to act between the shells only.

The short-range interaction between ions i and j is then given by:

$$\phi_{ij}(r) = B_{ij} e^{-a_{ij} r} - \frac{C_{ij}}{r^6} \qquad (3\text{-}61)$$

Where $\rho_{ij} = a_{ij}^{-1}$ is the hardness parameter. Here, C_{ij} (for anion-anion interaction) is a fitted quantity and all other C_{ij}'s e.g. C_{++} and C_{+-} are made equal to zero.

It may be mentioned here that in the potential of Bowman[35] and HS[36] a further term $-D_{ij}/r^8$ has been included.

The electron gas method is employed for the like particle (cation-cation) interaction. Because of the problem associated with diffused hydrogen wave function in using electron gas method for anion-anion interaction quantum mechanical method is then applied with the closed shell screened hydrogenic functions of the form $e^{-\delta r}$ involving the one electron functions with an adjustable screening parameter δ for the negative ion.

CHAPTER 4

PERFECT LATTICE

4.1 Static Properties:

Crystals are characterized by their various properties, viz. static, vibrational, and defect. The quantities which have been taken into consideration in the present work under the head of static properties are; lattice constant, lattice cohesive energy, second order elastic constants, static and high frequency dielectric constants, and transverse optic frequencies. The formulas for the second order elastic constants used in the present study are given as follows:

It is known that the matrices involved in the equations of motion (given in the later part of this chapter) which depend on the interactions between the different atoms and their associated dipole moments can be expressed as the sum of matrices which depend on the interactions between point charges and dipoles placed at the centers of the atoms and on the short-range forces. Thus, a matrix A is defined as the sum of a matrix R consisting of the short-range interaction and another involving the Coulomb interaction between point charges,

$$A = R + Z\mathscr{C}Z$$

where $\mathscr{C}$ is the matrix of Coulomb co-efficients. In a similar fashion:

$$\begin{aligned} B &= T + Z\mathscr{E}Y \\ C &= T^{T} + Y\mathscr{E}Y \\ D &= \mathscr{S} + Y\mathscr{E}Y \end{aligned} \qquad (4\text{-}1)$$

When the wave vector q of the normal mode is expressed in terms of an expansion parameter Δ as Δq, the matrices, A's, may be presented in the form of a series as follows:

$$A(\Delta q) = A^{(0)} + i\Delta \sum_{\gamma} A_{\gamma}^{(1)} q_{\gamma} + 1/2\,\Delta^2 \sum_{\gamma\lambda} A_{\gamma}^{(2)} q_{\lambda} q_{\gamma} + \ldots \tag{4-2}$$

Where $A^{(0)}$ is the matrix A for q=0 and $A_{\gamma}^{(1)}$ is the first derivative of A with respect to iq_{γ}.

Using similar expression for the other matrices the following relations can be written:

$$\begin{aligned}
&A^{(0)} = (A^{(0)})', \\
&B^{(0)} = (C^{(0)})', \\
&D^{(0)} = (D^{(0)})', \\
&\\
&A_{\gamma}^{(1)} = -(A_{\gamma}^{(0)})', \\
&B_{\gamma}^{(1)} = -(C_{\gamma}^{(0)})', \\
&D_{\gamma}^{(1)} = -(D_{\gamma}^{(0)})', \\
&\\
&A_{\gamma\lambda}^{(2)} = (A_{\gamma\lambda}^{(2)})' = A_{\lambda\gamma}^{(2)} \\
&B_{\gamma\lambda}^{(2)} = (C_{\gamma\lambda}^{(2)})' = B_{\lambda\gamma}^{(2)} \\
&D_{\gamma\lambda}^{(2)} = (D_{\gamma\lambda}^{(2)})' = D_{\lambda\gamma}^{(2)}
\end{aligned} \tag{4-3}$$

When the whole crystal is translated by a constant vector, the equations of motion and dipole moments remain the same on the basis of

$$\left.\begin{aligned}
&\sum_{k'} C_{\alpha\beta}^{(0)}(kk') = 0 \\
&\sum_{k} B_{\alpha\beta}^{(0)}(kk') = 0 \\
&\sum_{k} A_{\alpha\beta}^{(0)}(kk') = \sum_{k'} A_{\alpha\beta}^{(0)}(kk') = 0
\end{aligned}\right| \quad \text{for all } \alpha \text{ and } \beta, \tag{4-4}$$

The macroscopic equations of motion for a small element of the crystal is given by

$$\rho \ddot{u}_\alpha = \sum_{\beta\gamma\lambda} C_{\alpha\gamma,\beta\lambda} \frac{\partial^2 u_\beta}{\partial x_\gamma \partial x_\lambda} - \sum_{\beta\gamma} e_{\beta,\alpha\gamma} \frac{\partial E_\beta}{\partial x_\gamma} \tag{4-5}$$

where, ρ is the density of the crystal, u_α is the α-component of the three dimensional displacement vector, E_β is the β-component of the macroscopic field, $C_{\alpha\gamma,\beta\gamma}$ and $e_{\beta,\alpha\gamma}$ are used to denote the elastic and piezo-electric constants. If the displacement vector u and the macroscopic field E are expanded as plane waves, then

and

$$u(x,t) = u_0 \, e^{(2\pi i q.x - i\omega t)}$$
$$E(x,t) = E_0 \, e^{(2\pi i q.x - i\omega t)} \tag{4-6}$$

the macroscopic equation of motion then takes the form

$$\rho w^2 u_\alpha = 4\pi^2 \sum_{\beta\gamma\lambda} C_{\alpha\gamma,\beta\lambda} q_\gamma q_\lambda u_\beta + 2\pi i \sum_{\beta\gamma} e_{\beta,\alpha\gamma} q_\gamma E_\beta \tag{4-7}$$

The second-order elastic constants $C_{\alpha\alpha,\alpha\alpha}$, $C_{\alpha\alpha,\beta\beta}$, and $C_{\alpha\beta,\alpha\beta}$ which in Voigt's notation are C_{11}, C_{12}, and C_{44} are then estimated on the basis of the relation that satisfies all the symmetry:

$$C_{\alpha\gamma,\beta\lambda} = [\alpha\beta,\gamma\lambda] + [\beta\gamma,\alpha\lambda] - [\beta\lambda,\alpha\gamma] + [\alpha\gamma,\beta\lambda] \tag{4-8}$$

In this context, the short-range force constant between nearest-neigbour is estimated from:

and

$$\frac{e^2 A}{2v} = \left(\frac{d^2 \phi(r)}{dr^2} \right)_{r=r_0}$$

$$\frac{e^2 B}{2v} = \frac{d\,\phi(r)}{rdr}\Bigg|_{r=r_0} \qquad (4\text{-}9)$$

The second-nearest neighbour interaction is presented by

$$e^2/2v \begin{bmatrix} 1/2\,(A_1+B_1) & 1/2\,(A_1-B_1) & 0 \\ 1/2\,(A_1-B_1) & 1/2\,(A_1+B_1) & 0 \\ 0 & 0 & D_1 \end{bmatrix} \quad \text{for (1,1) interaction}$$

and

$$e^2/2v \begin{bmatrix} 1/2\,(A_2+B_2) & 1/2\,(A_2-B_2) & 0 \\ 1/2\,(A_2-B_2) & 1/2\,(A_2+B_2) & 0 \\ 0 & 0 & D_2 \end{bmatrix} \quad \text{for (2,2) interaction}$$

(4-10)

The co-efficients for the short-range interaction can be written as:[57]

$$R_{\alpha\alpha}(1\ 2) = -\frac{e^2}{v}\left[A\ \mathrm{Cos}2\pi q_\alpha\ r_0 + B\ (\mathrm{Cos}2\pi q_\beta r_0 + \mathrm{Cos}2\pi q_\gamma\ r_0)\right]$$

$$R_{\alpha\alpha}(1\ 1) = \frac{e^2}{v}\Big[A+2B+2A_1+2B_1+2D_1 - (A_1+B_1)\ (\mathrm{Cos}2\pi q_\alpha r_0)$$

$$(\mathrm{Cos}2\pi q_\beta\ r_0 + \mathrm{Cos}2\pi q_\gamma\ r_0) - 2D_1\ \mathrm{Cos}2\pi q_\beta r_0 \mathrm{Cos}2\pi q_\gamma\ r_0\Big]$$

$$R_{\alpha\alpha}(2\ 2) = \frac{e^2}{v}\left[A+2B+2A_2+2B_2+2D_2-(A_2+B_2)\,(\cos 2\pi q_\alpha r_0)\right.$$

$$\left.(\cos 2\pi q_\beta\ r_0 + \cos 2\pi q_\gamma\ r_0) - 2D_2\ \cos 2\pi q_\beta r_0 \cos 2\pi q_\gamma\ r_0\right]$$

$$R_{\alpha\beta}(1\ 2) = 0$$

$$R_{\alpha\beta}(1\ 1) = \frac{e^2}{v}\left[A_1 - B_1\right]\ \sin 2\pi q_\alpha r_0\ \sin 2\pi q_\beta r_0$$

$$R_{\alpha\beta}(2\ 2) = \frac{e^2}{v}\left[A_2 - B_2\right]\ \sin 2\pi q_\alpha r_0\ \sin 2\pi q_\beta r_0$$

(4-11)

Neglecting the inner strain and using the coefficients for the short-range interactions and the relation

$$[\alpha\beta,\gamma\lambda] = (1/8\pi^2 v) \sum_{kk'} (A_{\alpha\beta}{}^{(2)})_{\gamma\lambda}$$

(4-12)

the elastic constants for the compounds under study with the van der Waals' contribution and also taking $B_1 = D_1$ and $B_2 = D_2$ in the case of central forces can, then, be represented by [64]

$$C_{11} = \frac{e^2}{Vr_0}\left[\frac{1}{2}\,(A+A_1+A_2+B_1+B_2)-2.55604Z^2\right] - \frac{V_{11}}{v} \qquad (4\text{-}13)$$

$$C_{12} = \frac{e^2}{Vr_0}\left[\frac{1}{4}\,(A_1+A_2-5B_1-5B_2-2B)+0.11298Z^2\right] - \frac{V_{12}}{v} \qquad (4\text{-}14)$$

$$C_{44} = \frac{e^2}{Vr_0}\left[\frac{1}{4}(2B+A_1+A_2+3B_1+3B_2)+1.27802Z^2\right] - \frac{V_{44}}{v} \quad (4\text{-}15)$$

Where

$$V_{11} = r^{-6}[3.4759\ C_{+-} + 1.3831\ (C_{++} + C_{--})] + r^{-8}[1.3162\ D_{+-} + 0.4353\ (D_{++} + D_{--})],$$

$$V_{12} = r^{-6}[3.6171\ C_{+-} + 0.6881\ (C_{++} + C_{--})] + r^{-8}[1.4784\ D_{+-} + 0.1498\ (D_{++} + D_{--})]$$

and

$$V_{44} = r^{-6}[1.2367\ C_{+-} + 0.0747\ (C_{++} + C_{--})] + r^{-8}[0.7016\ D_{+-} + 0.0162\ (D_{++} + D_{--})]$$

The general equations for the elastic constants presented here involve all co-efficients of C_{ij}'s and D_{ij}'s. These have been included to facilitate some calculations made in chapter 6 with Bowman[35] and HS[36] potentials which contain C and D terms.

The relations for the dielectric constants and transverse optic frequencies have already been derived in the previous chapter.

4.2 Dynamic Properties:

4.2.1 Introduction:

Lattice dynamics is an old branch of Solid State Physics owing to: the research on`Planck's Theory of Radiation and the Theory of Specific Heat' reported by Einstein in 1907, `Vibrations in Space Lattice' by Born and von Kerman in 1912 and on the `Theory of Specific Heat` by Debye in the same year. Other early papers on lattice dynamics included those by Debye[65] and by Waller[66] on the effect of temperature on the scattering of X - rays by a crystal.

Inspired with the work of Einstein on his model of independent atomic oscillators Debye[67] developed a more meaningful model of coupled atomic oscillators. He presented a frequency spectrum in which each normal mode possesses the mean energy of a Planck oscillator and the normal modes of vibration were treated as if they were waves in a continuous isotropic medium instead of in a system in which the mass is concentrated at discrete points. Debye's theory considers the solid to be continuous and due to this continuous background the model ignored dispersion, polarization, and isotropy of the waves in the lattice. Debye's theory of specific heat was generally in good agreement with most of the experimental data till 1930 when deficiencies of the theory began to be noticed in comparison with the experimental results.

In 1912, Born and von Kerman [68] introduced a model of lattice dynamics. According to them the atoms are arranged in a periodic three-dimensional array. In such an array, the force on an atom

depends not on its displacements from its equilibrium position but on its displacements relative to its neighbours. They introduced the periodic boundary conditions which greatly simplifies the calculations without affecting the bulk properties. Here, the motion of the system is described not in terms of the vibrations of individual atoms but in terms of collective motions in the form of travelling waves called lattice vibrations by Born. Each lattice vibration is characterized by a wave vector, a frequency and certain polarization properties. A quantised lattice vibration is called a phonon which has particle-like properties analogous to photon which is a quantised electromagnetic wave.

In Debye and Waller's study on the theory of the influence of thermal motion on the scattering of X-rays on crystals, the thermal motion of the atoms causes a decrease in the intensity of the Bragg reflections with increasing temperature. The part of intensity lost from the main beam appears as diffusely scattered radiation which is observed in directions not allowed by Bragg's law. In 1938, Laval[69] experimentally detected this thermal diffuse scattering and correctly explained in terms of the Born-von Kerman theory. Olmer[70] and Walker[71] continued the research and deduced dispersion curves for aluminium. Other workers used this technique and obtained the dispersion curves of iron, copper, and zinc. Born[72] presented comprehensive theoretical investigation on the relationship between crystal dynamics and the scattering of X-rays.

Rubens and Hollnagel[73] and Barnes[74] first performed experimental investigations on the electromagnetic waves with wavelengths from the visible to the infra red region and found that the waves interact in various ways with lattice vibrations. From the experimental research they reported that these long wave length lattice vibrations which produce an oscillating dipole moment interact strongly with light in the infra and far-infrared regions and lead to absorption and reflection bands in narrow frequency regions. The wavelengths corresponding to the absorption frequencies are termed as Reststrahl wavelengths.

Light in the visible region is scattered by both acoustic sound waves and by certain optical phonons. Brillouin[75] estimated the spectrum of light scattered by density fluctuations associated with sound waves. He observed that the spectrum consists of a double split symmetrically around the frequency of the incident light. The splitting, which is very much smaller than the frequency of the incident light, is determined by the velocity of those sound waves whose wavelength is close to that of the light and the experimental technique is known as Brillouin scattering.

In 1923, Smekal[76] studied the scattering of light by a system with two quantised energy levels and predicted the existence of sidebands in the spectrum. Subsequently, in 1928 Raman Krishnan[77] observed this effect and they reported that light scattered by liquids contains sharp side bands symmetrically arranged around the incident frequency with shifts identical to the frequencies of some of the infrared vibrational absorption bands. This

inelastic scattering of light by molecular and crystal vibrations is known as the Raman effect. This is caused by those long wavelength optical phonons which modulate the electronic polarizability of the system.

Brockhouse[78] used inelastic scattering of thermal neutrons and presented the first dispersion curves for lattice vibrations in aluminium. At present, inelastic scattering of neutrons is the most important technique for studying phonons for the reason that in contrast to X-rays, neutrons which have come into thermal equilibrium with matter at about room temperature have energies of the same order of magnitude as phonons. The wave length associated with a beam of monochromatic neutrons in this range is of the same order of magnitude as interatomic distances and the beam will be diffracted by a crystal. As in the case of X-rays, there is again elastic scattering according to Bragg`s law. The neutron beam is, however, also diffracted in other directions by travelling waves and exchanges energy with them in units of the phonon energy, which is directly proportional to the frequency. Consequently, by measuring the change in direction and in energy of the scattered neutrons, it is possible to get the phonon frequency as a function of the wave vectors for all the acoustic and optic branches and on the basis of this new technique it is also possible to obtain detailed information about the inter-atomic forces. The next section describes the dynamics of a Three Dimensional Crystal. Section 4.2.3 is concerned with the Phonon Dispersion and Interionic Forces on the basis of Rigid Ion Model and Shell Model.

4.2.2 Dynamics of a Three Dimensional Crystal:

(a) Equations of Motion and Atomic Force Constant:

A crystal is considered to be composed of an infinite number of unit cells, each of which is a parallelopiped defined by three non-coplaner vectors a_1, a_2, and a_3 (Fig.4.1). The equilibrium position vector of the lth unit cell relative to an origin located at some atom is expressed by

$$r(l) = l_1 a_1 + l_2 a_2 \; l_3 a_3 \qquad (4\text{-}16)$$

where l_1, l_2, l_3 are any three integers, positive., negative, or zero and collectively taken as l. The vectors a_1, a_2, a_3 are the primitive translation vectors and they define the primitive unit cell which is the cell with the smallest volume from which the crystal structure can be generated by the translations of the lattice (4-16). If the primitive unit cell consists of only one atom, the vector r(l) given by (4-16) defines the equilibrium positions of the atoms. If there are n>1 atoms in the primitive unit cell, this group of n atoms constitute the basis of the crystal structure. The equilibrium positions of the n atoms within the unit cell are given by the vectors r(k) with k = 1,2, ...,n. Thus, the equilibrium position of the kth atom in unit cell l is given by

$$r\begin{pmatrix} l \\ k \end{pmatrix} = r(l) + r(k) \qquad (4\text{-}17)$$

The atoms in a crystal are capable of executing vibrations about their equilibrium positions owing to the thermal fluctuations at non-zero temperatures and the zero-point motion at absolute zero. In vibrating states, the instantaneous position

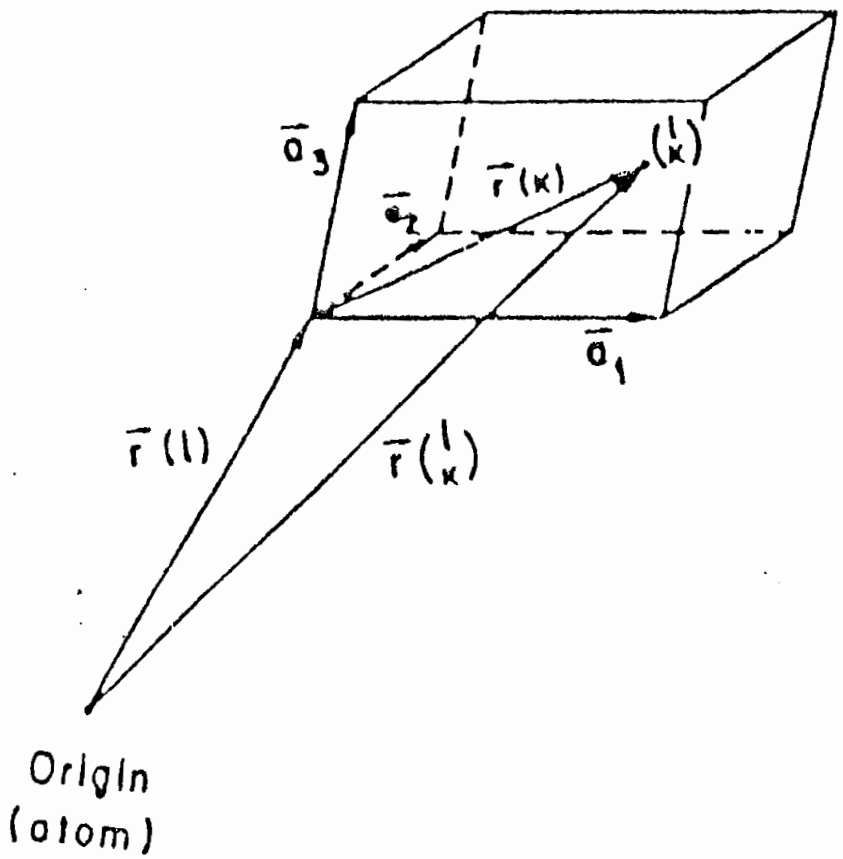

Fig. 4.1: The unit cell with equilibrium positions of atoms.

of the atom, $\begin{pmatrix} l \\ k \end{pmatrix}$ is given by

$$R\begin{pmatrix} l \\ k \end{pmatrix} = r\begin{pmatrix} l \\ k \end{pmatrix} + u\begin{pmatrix} l \\ k \end{pmatrix} \qquad (4\text{-}18)$$

where $u\begin{pmatrix} l \\ k \end{pmatrix}$ denotes displacement of the atom $\begin{pmatrix} l \\ k \end{pmatrix}$ from its equilibrium position $r\begin{pmatrix} l \\ k \end{pmatrix}$.

$$u\begin{pmatrix} l \\ k \end{pmatrix} = \left[u_x \begin{pmatrix} l \\ k \end{pmatrix}, u_y \begin{pmatrix} l \\ k \end{pmatrix}, u_z \begin{pmatrix} l \\ k \end{pmatrix} \right] \qquad (4\text{-}19)$$

Here, $u_\alpha\begin{pmatrix} l \\ k \end{pmatrix}$ expresses the displacement of the atom $\begin{pmatrix} l \\ k \end{pmatrix}$ in the direction α (α=x,y,z).

The kinetic energy of the vibrating crystal is

$$T = \frac{1}{2} \sum_{l,k,\alpha} m_k \dot{u}_\alpha^2 \begin{pmatrix} l \\ k \end{pmatrix} \qquad (4\text{-}20)$$

where m_k is the mass of the atom $\begin{pmatrix} l \\ k \end{pmatrix}$. The potential energy Φ, is assumed to be some function of the instantaneous positions of all atoms:

$$\Phi = \Phi \left[..r\begin{pmatrix} l \\ k \end{pmatrix} + u\begin{pmatrix} l \\ k \end{pmatrix} ..... \right]$$

For small displacements, Φ may be expressed in a Taylor`s series in powers of atomic displacements $u\begin{pmatrix} l \\ k \end{pmatrix}$ as follows:

$$\Phi = \Phi\left(r\begin{pmatrix} l \\ k \end{pmatrix}\right) + \sum_{lk\alpha} \Phi_\alpha\begin{pmatrix} l \\ k \end{pmatrix} u_\alpha\begin{pmatrix} l \\ k \end{pmatrix} + 1/2 \sum_{\substack{l\,k\,\alpha \\ l'k'\beta'}} \Phi_{\alpha\beta}\begin{pmatrix} l\ l' \\ k\ k' \end{pmatrix} u_\alpha\begin{pmatrix} l \\ k \end{pmatrix} u_\beta\begin{pmatrix} l' \\ k' \end{pmatrix}$$

$$+ 1/6 \sum_{\substack{lk\alpha \\ l'k'\beta l''k''\gamma}} \Phi_{\alpha\beta\gamma}\begin{pmatrix} l\ l'\ l'' \\ k\ k'\ k'' \end{pmatrix} u_\alpha\begin{pmatrix} l \\ k \end{pmatrix} u_\beta\begin{pmatrix} l' \\ k' \end{pmatrix} u_\gamma\begin{pmatrix} l'' \\ k'' \end{pmatrix} + \ldots \qquad (4\text{-}21)$$

The terms beyond third represent the anharmonic contributions to the crystal potential energy and are neglected in the description of the lattice dynamics in the harmonic approximation. Since Φ_0 is the static potential energy of the crystal (i.e. independent of the displacement coordinates), it is ignored for the time being. The coefficients

$\Phi_\alpha\begin{pmatrix} l \\ k \end{pmatrix}$ and $\Phi_{\alpha\beta}\begin{pmatrix} l\ l' \\ k\ k' \end{pmatrix}$ are defined by

$$\Phi_\alpha\begin{pmatrix} l \\ k \end{pmatrix} = \left[\frac{\partial \Phi}{\partial u_\alpha\begin{pmatrix} l \\ k \end{pmatrix}}\right]_0 \qquad (4\text{-}22)$$

$$\Phi_{\alpha\beta}\begin{pmatrix} l\ l' \\ k\ k' \end{pmatrix} = \left[\frac{\partial^2 \Phi}{\partial u_\alpha\begin{pmatrix} l \\ k \end{pmatrix} \partial_\beta\begin{pmatrix} l' \\ k' \end{pmatrix}}\right]_0 \qquad (4\text{-}23)$$

where the subscript zero indicates that the derivatives are evaluated in the equilibrium configuration (4-17). The force that acts on the atom $\begin{pmatrix} l \\ k \end{pmatrix}$ in the α-direction due to the displacements of all atoms $\begin{pmatrix} l' \\ k' \end{pmatrix}$ is given by

$$F_\alpha\begin{pmatrix} l \\ k \end{pmatrix} = - \frac{\partial \Phi}{\partial u_\alpha \begin{pmatrix} l \\ k \end{pmatrix}} \qquad (4\text{-}24)$$

Now, eqn. (4-21) takes the form:

$$F_\alpha\begin{pmatrix} l \\ k \end{pmatrix} = - \Phi_\alpha \begin{pmatrix} l \\ k \end{pmatrix} - \sum_{l'k'\beta} \Phi_{\alpha\beta} \begin{pmatrix} l\ l' \\ k\ k' \end{pmatrix} u_\beta \begin{pmatrix} l' \\ k' \end{pmatrix} \qquad (4\text{-}25)$$

If all the atoms are in their equilibrium positions, i.e. the displacements $u_\beta\begin{pmatrix} l' \\ k' \end{pmatrix}$, are zero then the following condition must hold, i.e.

$$\Phi_\alpha\begin{pmatrix} l \\ k \end{pmatrix} = 0 \qquad (4\text{-}26)$$

In the harmonic approximation (4-25)then can be written as

$$F_\alpha \begin{pmatrix} l \\ k \end{pmatrix} = \sum_{l'k'\beta'} -\Phi_{\alpha\beta} \begin{pmatrix} l\ l' \\ k\ k' \end{pmatrix} u_\beta \begin{pmatrix} l' \\ k' \end{pmatrix} \qquad (4\text{-}27)$$

Hence the potential energy is given by:

$$\Phi = \frac{1}{2} \sum_{\substack{l,k,\alpha \\ l,k,\beta}} \Phi_{\alpha\beta} \begin{pmatrix} l\ l' \\ k\ k' \end{pmatrix} u_\alpha \begin{pmatrix} l \\ k \end{pmatrix} u_\beta \begin{pmatrix} l' \\ k' \end{pmatrix} \qquad (4\text{-}28)$$

The Hamiltonian of the system is then written as:

$$H = \frac{1}{2} \sum_{lk\alpha} m_k \dot{u}_\alpha^2 \begin{pmatrix} l \\ k \end{pmatrix} + \frac{1}{2} \sum_{\substack{l\ k\ \alpha \\ l'k'\beta}} \Phi_{\alpha\beta} \begin{pmatrix} l\ l' \\ k\ k' \end{pmatrix} u_\alpha \begin{pmatrix} l \\ k \end{pmatrix} u_\beta \begin{pmatrix} l' \\ k' \end{pmatrix} \qquad (4\text{-}29)$$

The eqn. of motion of an atom of mass m_k is given by

$$m_k \ddot{u}_\alpha \begin{pmatrix} l \\ k \end{pmatrix} = - \sum_{l'k'\beta} \Phi_{\alpha\beta} \begin{pmatrix} l\ l' \\ k\ k' \end{pmatrix} u_\beta \begin{pmatrix} l' \\ k' \end{pmatrix} \qquad (4\text{-}30)$$

The coefficients, $\Phi_{\alpha\beta}\begin{pmatrix} l\ l' \\ k\ k' \end{pmatrix}$ termed as atomic force constants indicate the negative force exerted in the α-direction on the atom $\begin{pmatrix} l \\ k \end{pmatrix}$ when the atom $\begin{pmatrix} l' \\ k' \end{pmatrix}$ is displaced a unit distance in the β direction, while all other atoms are kept at their equilibrium positions.

(b) Dynamical Matrix and Eigen Vectors:

The eqns. of motion (4-30) represent an infinite set of simultaneous linear differential eqns. The wave like solution of the system can be expressed in the form:

$$u_\alpha \begin{pmatrix} l \\ k \end{pmatrix} = U_\alpha(k/q) \exp\left[i\{q.r \begin{pmatrix} l \\ k \end{pmatrix} - \omega(q)t\}\right] \qquad (4\text{-}31)$$

Here, $U_\alpha(k)$ is independent of l, q, and $\omega(q)$ are used to indicate the wave vector and angular frequency associated with the wave, respectively. Since the lattice is translationally invariant, the solution of the eqns. depends only on the difference between cell indices l and l'. Thus a solution for one ion is in fact a solution for all ions of the given sublattice in the whole crystal. Substitution of (4-31) in (4-30) leads for each value of q to set of 3n simultaneous eqns.

$$\omega^2(q) m_k U_\alpha(k/q) = \sum_{k'\beta} D_{\alpha\beta}(kk'/q)\ U_\beta(k'/q) \qquad (4\text{-}32)$$

in terms of the wave amplitude $U_\alpha(k/q)$.

In matrix notation (4-32) can be written as:

$$\omega^2(q)\ \mathbf{m}\ U(q) = D(q)\ U(q) \qquad (4\text{-}33)$$

where $U(q)$ is a column matrix containing 3n elements and $D(q)$ is a square Hermitian matrix known as the dynamical matrix. This matrix consists of 3nX3n elements given by:

$$D_{\alpha\beta}(kk'/q) = \sum_{l'} \phi_{\alpha\beta}(l-l',\ kk')\ \exp[iq.R(lk;l'k')] \qquad (4\text{-}34)$$

The condition for (4-33) to have a solution is that

$$\left| D(q) - \omega^2(q)\ mI \right| = 0 \qquad (4\text{-}35)$$

where I is a unit matrix of order 3n and m is a (3nX3n) diagonal matrix defined by

$$m_{\alpha\beta}\ (kk') = m_k\ \delta_{\alpha\beta}\ \delta_{kk'} \qquad (4\text{-}36)$$

Eqn.(4-35) is an eqn. of 3nth degree in $\omega^2(q)$ and the 3n solutions for each value of q will be denoted by $\omega_j^2(q)$ where j=1,2,....,3n. These are the eigen values of the dynamical matrix. The corresponding eigen vectors are $U_{\alpha j}(k/q)$. These determine the pattern of displacement of the atoms in a particular mode of vibration and the $U_j(k/q)$ may be referred to as polarization vectors. The relation given by

$$\omega = \omega_j(q) \qquad (4\text{-}37)$$

is called the dispersion relation. The curves obtained from (4-37) are the dispersion curves and depend on the crystal structure and the nature of the interionic forces. Translational invariance of the potential ensures that three branches of the spectrum are acoustic, i.e. they have $\omega_j(q)$ proportional to q

when q is small. The remaining 3(n-1) branches, generally, tend to finite frequencies as q tends to zero. Such modes in binary crystals are found to interact strongly with light and hence they are called the optic modes.

(c) Reciprocal Lattices and Brillouin Zones:

The discussion on vibrational properties was started with an infinitely extended crystal. For the purpose of periodic boundary conditions the crystal is subdivided into macrocrystals; these are parallelopipeds defined by the vectors $N_1 a_1, N_2 a_2, N_3 a_3$ where a_1, a_2, a_3 are the primitive translation vectors and N_1, N_2, N_3 are large integers. Each macrocrystal contains $N = N_1 N_2 N_3$ primitive unit cells. The periodic boundary conditions require that the atomic displacements for atoms separated by a translation $N_i a_i$, or a sum of such translations, must be the same

$$u\begin{pmatrix} l+N_i \\ k \end{pmatrix} = u\begin{pmatrix} l \\ k \end{pmatrix} \qquad (4\text{-}38)$$

also

$$\exp(i q N_i a_i) = 1 \qquad (4\text{-}39)$$

this relation specifies the possible values of q for i = 1,2,3. Using reciprocal lattice the conditions can be expressed in the manner as follows:

The primitive translation vectors of the reciprocal lattice are the three vectors b_1, b_2, and b_3 defined by

$$a_i . b_j = 2\pi\delta_{ij} \qquad (4\text{-}40)$$

these eqns. can be satisfied by putting

$$\left.\begin{aligned} b_1 &= \frac{2\pi}{v}\,(a_2 \times a_3) \\ b_2 &= \frac{2\pi}{v}\,(a_3 \times a_1) \\ b_3 &= \frac{2\pi}{v}\,(a_1 \times a_2) \end{aligned}\right\} \qquad (4\text{-}41)$$

where

$$v = a_1 \cdot (a_2 \times a_3) \qquad (4\text{-}42)$$

is the volume of the primitive unit cell of the direct lattice. A lattice vector in the reciprocal lattice is given by

$$\tau(n) = n_1 b_1 + n_2 b_2 + n_3 b_3 \qquad (4\text{-}43)$$

where the n_i are arbitrary integers which can be positive, negative, or zero. The scalar product between a direct lattice vector $r(l) = l_1 a_1 + l_2 a_2 + l_3 a_3$ and a reciprocal lattice vector is given by

$$r(l) \cdot \tau(n) = 2\pi \sum_i l_i n_i = 2\pi \times (\text{integer}) \qquad (4\text{-}44)$$

Hence an expression for q which satisfies (4-39) is given by

$$q = \frac{n_1}{N_1} b_1 + \frac{n_2}{N_2} b_2 + \frac{n_3}{N_3} b_3 \qquad (4\text{-}45)$$

Also

$$w_j(q+\tau) = w_j(q) \qquad (4\text{-}46)$$

and

$$u\left(\begin{array}{c|c} l & q+\tau \\ k & j \end{array}\right) = u\left(\begin{array}{c|c} l & q \\ k & j \end{array}\right) \qquad (4\text{-}47)$$

Therefore, all the distinct solutions can be obtained if the allowed values of q are restricted to lie in one unit cell of the reciprocal lattice defined by the three vectors b_1, b_2, b_3, in other words, the integers n_i in (4-46) are restricted to:

$$n_i = 0,1,2,.....,N_i - 1$$

or,

$$n_i = 1,2, ...,N_i$$

The unit cell described by b_1, b_2, b_3 does not, in general, reflect the symmetry of the reciprocal lattice. It is, however, possible to construct a primitive unit cell in such a way that the point symmetry of the reciprocal lattice can be made. This is achieved by taking a point, q=0, in the reciprocal lattice and then constructing vectors to neighbouring points of the reciprocal lattice and bounding the unit cell by planes which are perpendicular bisectors of the vectors to the neighbouring points. Such a cell is termed as Brillouin zone and the volume of the zone is given by:

$$v_b = b_1 \cdot (b_2 \times b_3)$$

$$= \frac{(2\pi)^3}{v} \qquad (4\text{-}48)$$

In Fig. 4.2 the Brillouin zone of the compounds under study, is exhibited.

4.2.3 Interionic Forces and Phonon Dispersion :

Phonon dispersion curves $\omega(q)$ can be determined by inelastic neutron scattering techniques. These experimentally measured curves are mainly of interest owing to the fact that they provide chance of testing various models of interionic forces. The forces

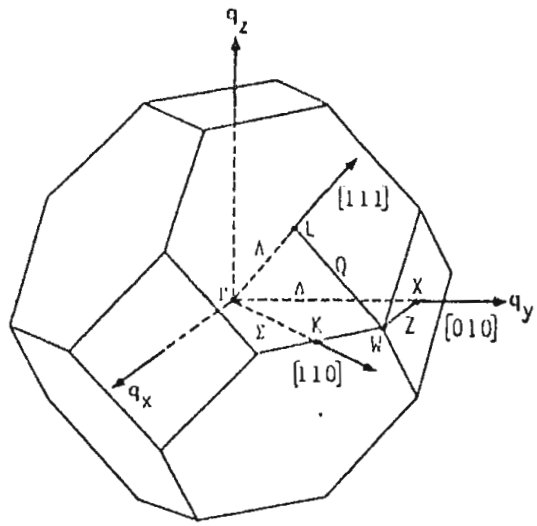

Fig. 4.2: The Brillouin zone of the f.c.c. lattice.

between the ions are governed by the electronic structure of the atoms involved. The vibrational properties of the ionic crystals has been given here on the basis of the Rigid Ion Model and the Shell Model in sections (a) and (b), respectively.

(a) The Rigid Ion Model:

In the rigid ion model an ion of type k carries a point charge $Z_k e$, where e denotes the magnitude of the electronic charge; the ions are, therefore, not polarizable. The interaction energy of two ions $i = \begin{pmatrix} l \\ k \end{pmatrix}$ and $k = \begin{pmatrix} l' \\ k' \end{pmatrix}$ separated by a distance R_{ik} is expressed by

$$\Phi(R_{ik}) = \phi^{(R)}(R_{ik}) + \phi^{(C)}(R_{ik}) \qquad (4\text{-}49)$$

where $\phi^{(R)}$ is a short-range repulsive or overlap energy and $\phi^{(C)}$ represents the long-range Coulomb energy. In this case of central forces, the total force constants are :

$$\phi_{\alpha\beta}(ik) = \phi^{R}{}_{\alpha\beta}(ik) + \phi^{C}{}_{\alpha\beta}(ik) \qquad (4\text{-}50)$$

Here, $\phi^{R}{}_{\alpha\beta}(ik)$ and $\phi^{C}{}_{\alpha\beta}(ik)$ denote the force constants derived from the repulsive and Coulomb energy, respectively. The dimensionless short-range parameters are given by

$$\phi^{(R)''}(r_{ik}) = \frac{e^2}{2v} A_{ik} \qquad (4\text{-}51a)$$

$$\frac{1}{r_{ik}} \phi^{(R)'}(r_{ik}) = \frac{e^2}{2v} B_{ik} \qquad (4\text{-}51b)$$

where r_{ik} is the equilibrium distance between the ions i and k and v is used to represent the volume of the primitive unit cell.

The repulsive force constants for $i \neq k$ can be expressed by

$$\phi^{R}_{\alpha\beta}(ik) = -\frac{e^2}{2v}\left[(A_{ik}-B_{ik})\frac{r_{ik\alpha}\, r_{ik\beta}}{r_{ik}} + \delta_{\alpha\beta}B_{ik}\right] \tag{4-52a}$$

also

$$\phi^{R}_{\alpha\beta}(ii) = -\sum_{k}{}' \phi_{\alpha\beta}(ik) \tag{4-52b}$$

Similarly, the force constants of the Coulomb forces for $i = k$ are given by

$$\phi^{C}_{\alpha\beta}(ik) = Z_i Z_k e^2 \frac{\delta_{\alpha\beta} r_{ik}^{-3} r_{ik\alpha} r_{ik\beta}}{r_{ik}} \tag{4-53a}$$

and

$$\phi^{C}_{\alpha\beta}(ii) = -\sum_{k}{}' \phi_{\alpha\beta}(ik) \tag{4-53b}$$

The dynamical matrix can be written as

$$D_{\alpha\beta}\begin{pmatrix} q \\ k\ k' \end{pmatrix} = \sum_{l'} \phi_{\alpha\beta}\begin{pmatrix} l\ l' \\ k\ k' \end{pmatrix} \exp\left[iq\left(r\begin{pmatrix} l' \\ k' \end{pmatrix} - r\begin{pmatrix} l \\ k \end{pmatrix}\right)\right] \tag{4-54}$$

The corresponding secular eqn. is

$$\left| D(q) - m\omega^2(q) \right| = 0 \tag{4-55}$$

Using (4-50) in (4-54), the eqn. takes the form

$$\mathbf{D = R + ZCZ} \tag{4-56}$$

The eqn. of motion for RIM is then given by

$$\omega^2 \mathbf{mu = Ru + ZCZu} \tag{4-57}$$

Here R(q) is the matrix of the repulsive forces given by

$$R_{\alpha\beta}\begin{pmatrix} q \\ k\ k' \end{pmatrix} = \sum_{l'} \phi_{\alpha\beta}\begin{pmatrix} l\ l' \\ k\ k' \end{pmatrix} \exp\left[iq\left(r\begin{pmatrix} l' \\ k' \end{pmatrix} - r\begin{pmatrix} l \\ k \end{pmatrix}\right)\right] \tag{4-58}$$

and C(q) is the Coulomb matrix, the elements of which are given by

$$Z_k Z_{k'} C_{\alpha\beta}\begin{pmatrix} q \\ k\ k' \end{pmatrix} = \sum_{l'} \Phi_{\alpha\beta}\begin{pmatrix} l\ l' \\ k\ k' \end{pmatrix} \exp\left[iq\left(r\begin{pmatrix} l' \\ k' \end{pmatrix} - r\begin{pmatrix} l \\ k \end{pmatrix} \right) \right] \qquad (4\text{-}59)$$

The repulsive matrix R(q) is evaluated directly due to the rapid convergence of the series (section 4.1). On the other hand, it is very difficult to evaluate the series (4-59) due to the reason that, it does not tend to a unique value as q-->0, but to a value which depends on the relative directions of q and the electrical polarization associated with the mode concerned. However, the problem is solved using Ewald`s method (an account of which has been given earlier). The condition for the solubility of the set of eqns. given by (4-57) presents a determinantal relation for w(q),

$$\left| (R + ZCZ) - w^2 mI \right| = 0 \qquad (4\text{-}60)$$

This determinant is of order six for a cubic diatomic crystal. Along principal symmetry directions, the determinant factorises and yields three different (2X2) determinants which can be solved as a quadratic eqn. to determine $w_j(q)$ for every q. In case of a face-centred cubic lattice, when q is in a special direction of high symmetry such as (1 0 0), the matrix C(q) is also diagonal in α and ß. Thus,when $q = (q_x,0,0)$, one finds that the dynamical matrix has the following structure:

$$D(q) = \begin{bmatrix} D_{xx} & 0 & 0 \\ 0 & D_{yy} & 0 \\ 0 & 0 & D_{zz} \end{bmatrix} \qquad (4\text{-}61)$$

where $D_{\alpha\alpha}(q)$ are two dimensional and real matrices. In this case, the direction of the eigen vectors are determined by symmetry and the modes are purely longitudinal or purely transverse. If $q = (q_x,0,0)$, the matrix $D_{xx}(q)$ gives the dispersion $\omega(q)$ for the longitudinal modes LA and LO, while $D_{yy}(q)$ and $D_{zz}(q)$ yield identical solutions for the doubly degenerate TA and TO-modes. The two principal frequencies, longitudinal and transverse, thus, determined are given by:

$$\mu\omega^2_{LO} = R_0 + \frac{8\pi Z^2 e^2}{3v} \qquad (4\text{-}62)$$

$$\mu\omega^2_{TO} = R_0 - \frac{4\pi Z^2 e^2}{3v} \qquad (4\text{-}63)$$

where μ is the reduced mass, given by:

$$\mu = \frac{m_1 m_2}{m_1 + m_2} \qquad (4\text{-}64)$$

The optical splitting between the LO and TO modes is written as

$$\mu(\omega^2_{LO} - \omega^2_{TO}) = \frac{4\pi Z^2 e^2}{v} \qquad (4\text{-}65)$$

and the Lorentz field is

$$E(L) = \frac{4\pi}{3} P \qquad (4\text{-}66)$$

The macroscopic field $E^{(M)}$ have values which are different for the TO and LO - modes. For a TO - mode, (q perpendicular to P), the macroscopic field vanishes while for the LO-mode (q parallel to P), the macroscopic field is

$$E^{(M)} = - 4\pi P.$$

The effective fields are thus:

$$E^* = \frac{4\pi}{3} P \text{ (TO-mode)} \qquad (4\text{-}67)$$

$$E^* = -\frac{8\pi}{3} P \text{ (LO-mode)} \qquad (4\text{-}68)$$

Macroscopic field is, therefore, responsible for the result

$$\omega_{LO} > \omega_{TO}.$$

(b) The Shell Model:

A description of this model has been presented in chapter 3. As shown in fig 3.1, k_1 and k_2 denote spring constants which couple the shells to the ion cores. The core charges are given by X_1e and X_2e while Y_1e and Y_2e are used to express shell charges. The net charge on the cation and anion are

$Ze = (X_1 + Y_1)e$ and $-Ze = (X_2 + Y_2)e$,

respectively. As the unit cell as a whole is electronically neutral

$$\sum_k Z_k e = \sum_k (X_k + Y_k)e = 0 \qquad (4\text{-}69)$$

If the spring constant between core and shell be k_k, the polarizability is given by

$$\alpha_k = \frac{Y_k^2 e^2}{k_k} \qquad (4\text{-}70)$$

Here the interaction of a shell has been considered with the core of the same atom and of neighbouring atoms.

The harmonic potential energy of the crystal is expressed by

$$\Phi = \frac{1}{2}\sum_{l,k,\alpha}\Bigg\{\sum_{l',k',\beta}\Bigg(\Phi_{\alpha\beta}\begin{pmatrix} l & l' \\ k & k' \end{pmatrix} u_\alpha\begin{pmatrix} l \\ k \end{pmatrix} u_\beta\begin{pmatrix} l' \\ k' \end{pmatrix} +$$

$$\Phi_{\alpha\beta}\begin{pmatrix} l & l' \\ k & k' \end{pmatrix} u_\alpha\begin{pmatrix} l \\ k \end{pmatrix} W_\beta\begin{pmatrix} l' \\ k' \end{pmatrix} + \Phi^{T}_{\beta\alpha}\begin{pmatrix} l'l \\ k'k \end{pmatrix} u_\beta\begin{pmatrix} l' \\ k' \end{pmatrix} W_\alpha\begin{pmatrix} l \\ k \end{pmatrix}\Bigg) +$$

$$\Phi_{\alpha\beta}\begin{pmatrix} l & l' \\ k & k' \end{pmatrix} W_\alpha\begin{pmatrix} l \\ k \end{pmatrix} W_\beta\begin{pmatrix} l' \\ k' \end{pmatrix} + k_k W_\alpha\begin{pmatrix} l \\ k \end{pmatrix} -$$

$$\left[Y_k e W_\alpha\begin{pmatrix} l \\ k \end{pmatrix} + Z_k e u_\alpha\begin{pmatrix} l \\ k \end{pmatrix}\right] E_\alpha\begin{pmatrix} l \\ k \end{pmatrix}\Bigg\} \qquad (4\text{-}71)$$

Here, **W** gives the displacement of the shell relative to the core.

Relation (4-71) yields the dynamical eqn. for the shell model and can be written as:

$$\omega^2(q)\,\mathbf{m}\mathbf{U} = (\mathbf{R} + \mathbf{Z}\mathbf{C}\mathbf{Z})\mathbf{U} + (\mathbf{T} + \mathbf{Z}\mathbf{C}\mathbf{Y})\mathbf{W} \qquad (4\text{-}72a)$$

$$0 = (\mathbf{T}^{T} + \mathbf{Y}\mathbf{C}\mathbf{Z})\mathbf{U} + (\mathcal{Y} + \mathbf{Y}\mathbf{C}\mathbf{Y})\mathbf{W} \qquad (4\text{-}72b)$$

The shell masses have been taken to be zero and this assumption is equivalent to the adiabatic approximation which expresses that the electron distribution is always that appropriate to the instantaneous configuration of the nuclei, in this case, of cores.

Here, **Y** is a (3n X 3n) diagonal matrix of shell charges (Y_k), **m** and **Z** re the ionic mass and and charge matrices, respectively. **U** and **W** are the 3n-component column matrices represented by the core and relative core-shell displacements such that

$$U\begin{pmatrix} l \\ k \end{pmatrix} = U^{C}\begin{pmatrix} l \\ k \end{pmatrix} \text{ and } W\begin{pmatrix} l \\ k \end{pmatrix} = U^{S}\begin{pmatrix} l \\ k \end{pmatrix} - U^{C}\begin{pmatrix} l \\ k \end{pmatrix} \tag{4-73}$$

R,T, and $\mathcal{S}$ denote, as shown in Fig. 4.3, the short-range core-core , core-shell, and shell-shell interaction matrices such that

$$R = D + S + 2F \quad \text{and} \quad T = S + F \tag{4-74}$$

and T^{T} gives the transpose conjugate of T.

Here, D, S, and F represent (3n X 3n) matrices on the basis of interactions exhibited in Fig. 4.3 and is related to S by

$$\mathcal{S}_{\alpha\beta}\begin{pmatrix} q \\ k\ k' \end{pmatrix} = S_{\alpha\beta}\begin{pmatrix} q \\ k\ k' \end{pmatrix} + k_{K}\,\delta_{\alpha\beta}\,\delta_{kk} \tag{4-75}$$

Here, $\mathcal{S}$ = (S + K) with S as the short-range interaction matrix (3n X 3n) and K is the diagonal matrix (3n X 3n) specified by the core-shell spring force constant k_K. C is a (3n X 3n) Coulomb interaction matrix. The short-range forces are assumed to act through the shells and under this condition the matrices R, T, and S are taken to be equal. Elimination of W from (4-72b) yields

$$\omega^{2}(q)\ mU = D(q)\,U \tag{4-76}$$

where the dynamical matrix corresponding to the shell model is expressed by

$$D(q) = (R + ZCZ) - (R + ZCY)(S + K + YCY)^{-1}(T^{T} + YCZ) \tag{4-77}$$

The first term of (4-77) is the dynamical matrix found with the RIM model. The second term gives contributions arising from the electronic polarization. It is, however, interesting to note

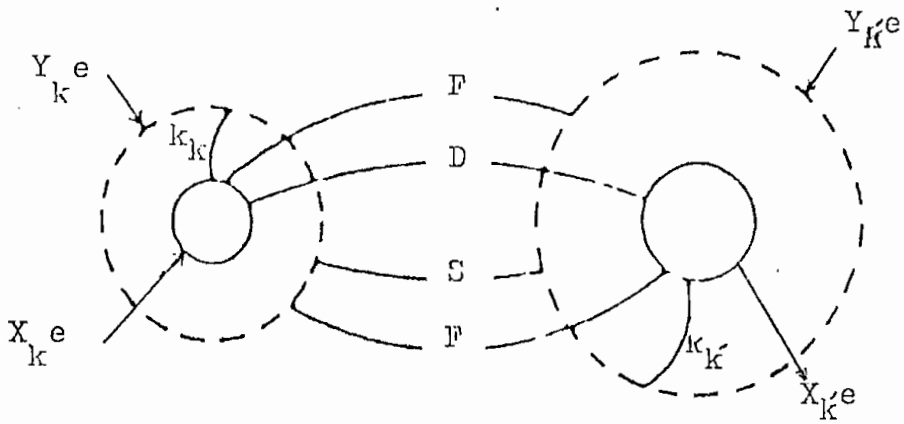

Fig. 4.3: The shell model showing interactions between two neighbouring ions, k and ḱ.

that many-body forces are present in the second term although R, T, and S involve only two-body forces.

A substitution of the dynamical matrix (4-77) in the secular equation (4-35) and its solution then, yields 3n vibration frequencies $w_j^2(q)$ corresponding to each phonon wave vector q. Along the principal symmetry directions Δ , Σ , λ the determinant reduces to, as in the case of RIM, lower order determinant, (2 X 2), for diatomic cubic crystals.

It should be pointed that The Shell Model treatment of dielectric behaviour satisfies the Lyddane-Sachs and Teller and Clausius-Mosotti relations. The additional polarization mechanism associated with the shell model which arises owing to the electronic distortions does not have any effect on the dielectric constant. The frequencies for the TO and LO-modes can be written as:

$$\mu w^2_{TO} = R_0' - \frac{4\pi(\varepsilon_\alpha+2)(Z'e)^2}{9v} \qquad (4\text{-}78a)$$

$$\mu w^2_{LO} = R_0' + \frac{8\pi(\varepsilon_\alpha+2)(Z'e)^2}{9v\varepsilon_\alpha} \qquad (4\text{-}78b)$$

The optical splitting is then given by:

$$\mu\,(w^2_{LO} - w^2_{TO}) = \frac{4\pi(Z'e)^2(\varepsilon_\alpha+2)^2}{9v\varepsilon_\alpha} \qquad (4\text{-}79)$$

where, $R_0' = R_0 - e^2\{(d_1^2/\alpha_1) + (d_2^2/\alpha_2)\}$ and

$$Z' = Z + d_1 - d_2 \qquad (4\text{-}80)$$

and the electrical and mechanical polarizabilities, α_k and d_k are given by:

$$\alpha_k = \frac{\gamma_k e^2}{k_k + [R(kk)]_{q\to 0}} \; ; \qquad d_k = \frac{-\gamma_k [R(kk)]_{q\to 0}}{k_k + [R(kk)]_{q\to 0}} \tag{4-81}$$

CHAPTER 5

DEFECT LATTICE

5.1 Introduction:

A perfect lattice may be defined as one in which all the atoms are at rest on their correct lattice positions in the crystal structure. Such a perfect crystal can be obtained, theoretically, only at absolute zero. As the temperature of a crystal is raised, the amplitude of the thermal vibrations of the atoms about their mean positions increases. Lattice vibrations, also referred to as phonons, constitute an important defect in solids since they are the agents whereby the lattice reaches a state of thermal equilibrium. The energy distribution of the phonons is important in problems involving optical absorption, heat capacity, electrical resistivity, X-ray diffraction, line broadening, luminescence and many others. The changes in the phonon spectrum accompanying the formation of atomic defects in solids contribute to the entropy of the solid. Apart from the fact that atoms are vibrating, a number of atoms are inevitably misplaced in a real crystal. According to Frenkel[79] Wagner et al[80], and Jost[81] there exist in a crystal in themodynamical equilibrium a number of vacant lattice points also a number of ions will be situated in interstitial positions. In some crystals, the number of defect present may be very small, e.g. high purity diamond or quartz crystals. In other crystals, very high defect concentrations may be present. In highly defective crystals, the question arises as to whether or not the defects themselves should be regarded as forming a fundamental part of

the crystal structure rather than as some imperfections in an otherwise ideal structure.

Various schemes have been proposed for the classification of defects. They are broadly divided into two parts: (a) stoichiometric defects: In this category the crystal composition is unchanged on introducing the impurities and (b) non-stoichiometric defects: This type of defect is a consequence of a change in crystal composition. Alternatively, the size and shape of the defects can be used as a basis for classification and accordingly described as:

(i) Point Defects: This type of defects includes: vacant lattice sites, interstitial atoms, impurity atoms, atoms on wrong sub-lattices, and ions with different valencies.

(ii) Line Defects: Here the defects are:

(a) Edge dislocation: Row of atoms marking edge of a crystallographic plane extending only part way in crystal, and

(b) Screw dislocation: Row of atoms about which a normal crystallographic plane appears to spiral.

(iii) Plane Defects: Under this head the defects are:

(a) Linear Boundary: Boundary between two adjacent perfect regions in the same crystal that are slightly tilted with respect to each other,

(b) Grain Boundary: Boundary between two crystals in a polycrystalline solid,

(c) Stacking Fault: Boundary between two parts of a closest packing having alternate stacking sequences, and

(iv) Volume Defects includes: clusters of atoms of different chemical composition; ordered regions; clusters of point defects; divacancies; trivacancies; impurity atom vacancy or interstitial complexes; small regions of disorder; extended, long range configurational defects and initial stages of spinodal decomposition.

Many of the important properties of ionic crystals are largely influenced and often determined by the defect structure and in particular by the properties of the point defects (Crawford et al.[82], Stoneham[83]). Point defects play an important part in determining the physical properties of most crystalline substances, most notably those controlling the transport of matter and the properties that stem from it. They also strongly influence the resistivity of metals by scattering conduction electrons, the low temperature thermal conductivity of all crystalline solids by scattering the phonons, the electronic conduction and related properties of semi conductors by acting as donors or acceptors and the optical properties in ionic solids by introducing electron states with optical transitions. The knowledge of defect properties of solids will be applicable in the fields where technical requirements demand materials with high ionic conduction, e.g. (a) there are ion monitors in which the presence of a low concentration of some species is measured electrochemically as a voltage across a suitable electrolyte. The important features are discrimination and low electronic conductivity, to avoid dissipating the potential generated in driving an electric current, (b) high ionic conductivity can be

valuable in electrolytes for batteries and fuel cells. These electrolytes need low electronic conductivity to avoid leakage losses. The batteries are being tested in several countries for use in, viz. electric cars and for power station load levelling. For these processes the various energies of the defects are some of their most important parameters. The energies needed to form the defects determine the concentrations in which they are present in thermal equilibrium, while the activation energies needed for them to jump from one lattice position to another determine the rates of their migration through the lattice. Because defects do determine many of the technologically important properties, an ever increasing amount of attention is being devoted to their study. The next section of this chapter is concerned with the concentration of defects in crystals. Section 5.3 describes the calculation of defect energies.

5.2 Concentration of Defects:

5.2.1 Schottky Defect:

The Schottky defect which is stoichiometric in ionic crystals is a pair of vacant sites, a cation vacancy and an anion vacancy. For a cation vacancy in a normal lattice to occur, a positive ion must some how migrate out of its proper position in the structure to the crystal's exterior. If only positive ions migrate out of the crystal and collect on its surface the surface will become positively charged. This positive surface charge opposes the migration of additional positive ions out of the crystal's interior. Simultaneously, the excess negative charge created inside the crystal is conducive to the formation of negative

vacancies. In the absence of external forces, therefore, the number of oppositely charged vacancies inside a crystal tends to be equal.

If there are N ions in the crystal and n Schottky defects are produced by removing n cations and n anions from the crystals interior, the different ways in which each kind of ion can be removed is given by

$$\frac{N!}{(N-n)!n!} \tag{5-1}$$

As the number of cation and anion vacancies are equal the different ways in which Schottky defects can be formed is then obtained by squaring (5-1). According to the Boltzmamn formula, the increase in entropy on creating n Schottky defects is

$$S = k \log\left[\frac{N!}{(N-n)!n!}\right]^2 \tag{5-2}$$

This in turn produces a change in the Hemholtz free energy

$$\begin{aligned} F &= E - TS \\ &= nE_p - kT\log\left[\frac{N!}{(N-n)!n!}\right]^2 \end{aligned} \tag{5-3}$$

where E_p is the energy required to remove a pair of ions from the crystal's interior to sites on the surface so that nE_p represents the total energy in its internal energy. When equilibrium is attained at a given temperature, F must be a minimum with respect to changes in n. The condition for this is that

$$\left(\frac{\delta F}{\delta n}\right)_T = 0 \tag{5-4}$$

eqn. (5-4) then gives

$$\frac{N - n}{n} = \exp\,(E_p/2kT) \qquad (5\text{-}5)$$

In practice, $n \ll N$ and $N-n \sim N$; eqn. (5-5) can, then, be written as

$$n \simeq N \exp(-E_p/2kT) \qquad (5\text{-}6)$$

the concentration of Schottky defects is, thus, given by

$$C_S = \frac{n}{N} \simeq \exp\,(-E_p/2kT) \qquad (5\text{-}7)$$

The concentration of Schottky defects, thus, increases exponentially with temperature.

5.2.2 Frenkel Defect:

Frenkel defect is also a stoichiometric defect and involves an atom displaced off its lattice site into an interstitial site that is normally empty.

Let E_i be the energy required to displace an atom from its proper position to an interstitial position in a perfect crystal. Then, if there are N atoms in the crystal and N_i interstitial positions in its structure, there are

$$\frac{N!}{(N-n)!n!} \cdot \frac{N!}{(N-n)!n!} \qquad (5\text{-}8)$$

ways in which n Frenkel defects can be formed. The increase in entropy of the crystal due to putting the ions into interstitial position becomes

$$S = k \left[\log \frac{N!}{(N-n)!n!} + \log \frac{N!}{(N-n)!n!} \right] \qquad (5\text{-}9)$$

The change in the Helmholtz free energy produced by the creation of n Frenkel defects is

$$F = nE_i - kT \left[\log \frac{N!}{(N-n)!n!} + \log \frac{N!}{(N-n)!n!} \right] \qquad (5\text{-}10)$$

Differentiation of (5-10) with respect to n using Stirling's formula yields

$$\left(\frac{\delta F}{\delta n} \right)_T = E_i - kT \log \frac{(N-n)\ (N_i-n)}{n^2} \qquad (5\text{-}11)$$

At equilibrium the free energy should be a minimum with respect to changes in n. The condition for this is given by

$$\left(\frac{\delta F}{\delta n} \right)_T = 0 \quad \text{and since } N>>n \text{ and } N_i>>n,$$

$$n = (NN_i)^{1/2} \exp(-E_i/2kT) \qquad (5\text{-}12)$$

the equilibrium concentration of Frenkel defects taking $N = N_i$ is then expressed by

$$C_F = \frac{n}{N} \simeq \exp(-E_i/2kT) \qquad (5\text{-}13)$$

Usually both kinds of defects are present in all solids; however, there is always a tendency for one type of defect to predominate since their energies of formation are generally unequal. On the basis of the experimental evidence and theoretical calculations, as shown in Table 6.11 of Chapter 6, next, it has been established that the predominant defects present in the compounds under study, are Schottky defects.

5.3 Method of Evaluation of Defect Energy:

The various defect energies which have been reported in the thesis were estimated using the minimisation method (described in subsequent sections). What happens in the region of crystal where the vacancy has been created is shown schematically in fig. 5.1. Removal of the cation will have the same effect on the neighbours as the substitution of a negative charge. The interionic distances in the crystal are governed by the balance of positive and negative charges. Extraction of the cation will allow the cations surrounding the vacancy to relax inward because of repulsion from neighbours surrounding the ions. Conversely, the anions will move outward. The ions that are far removed from the defect site also move inwards or outwards according to the effective charge on the defect because of the long range nature of the Coulomb field. In this context, the relaxation of the ions in case of saddle point configuration required to evaluate migration energy is shown in fig. 5.2. The main problem associated with the defect calculation is the treatment of lattice relaxation. The dominant contribution to the lattice response is due to the effective charge of the defect. The ions immediately adjacent to point defect, initially at their regular sites on the perfect crystals, suffer displacements which are too large to be adequately described in terms of linear elastic theory. Because of this, these ions, in the presence of the defect at the centre of the region, are treated as discrete particles. Ions, which lie well away from the defect are displaced by small amounts and are susceptible to treatment by the elastic theory. In other words, the dielectric response in

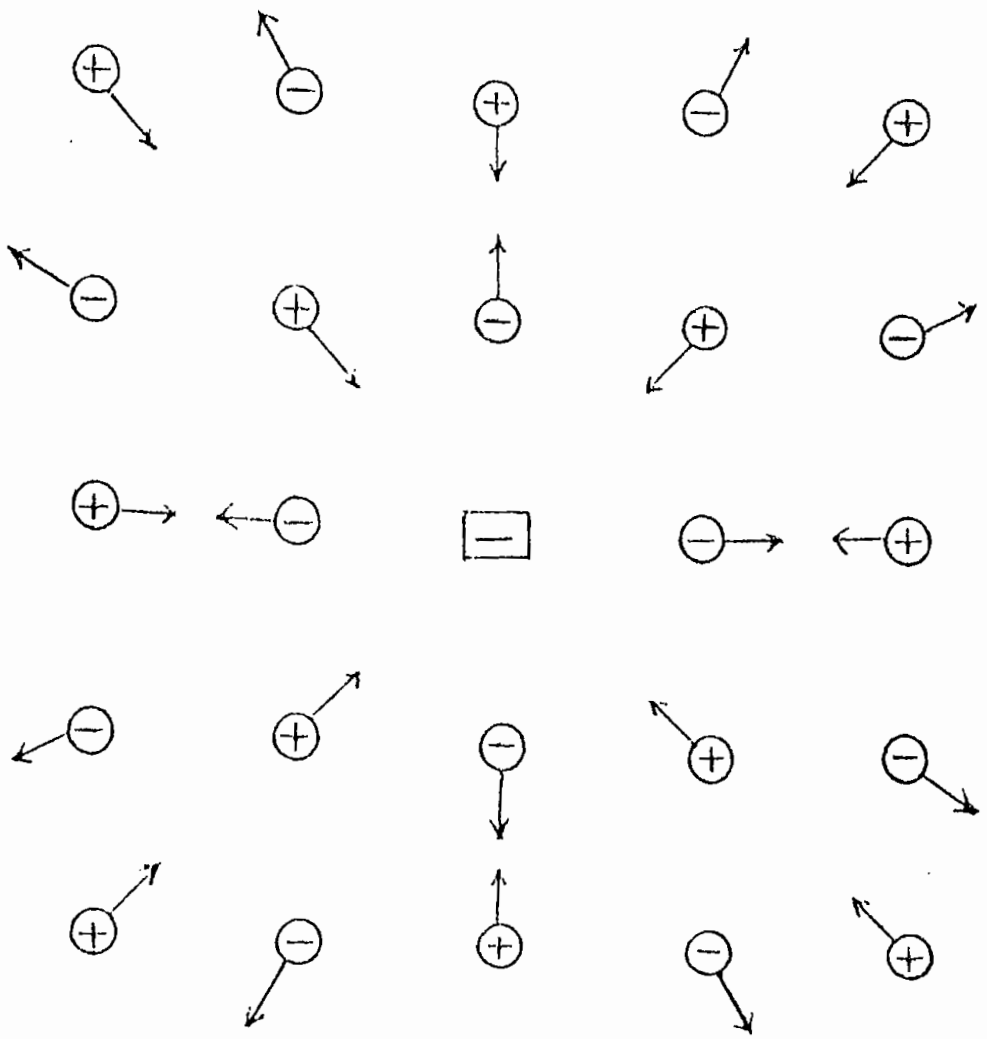

Fig. 5.1: Displacements of ions around a vacancy.

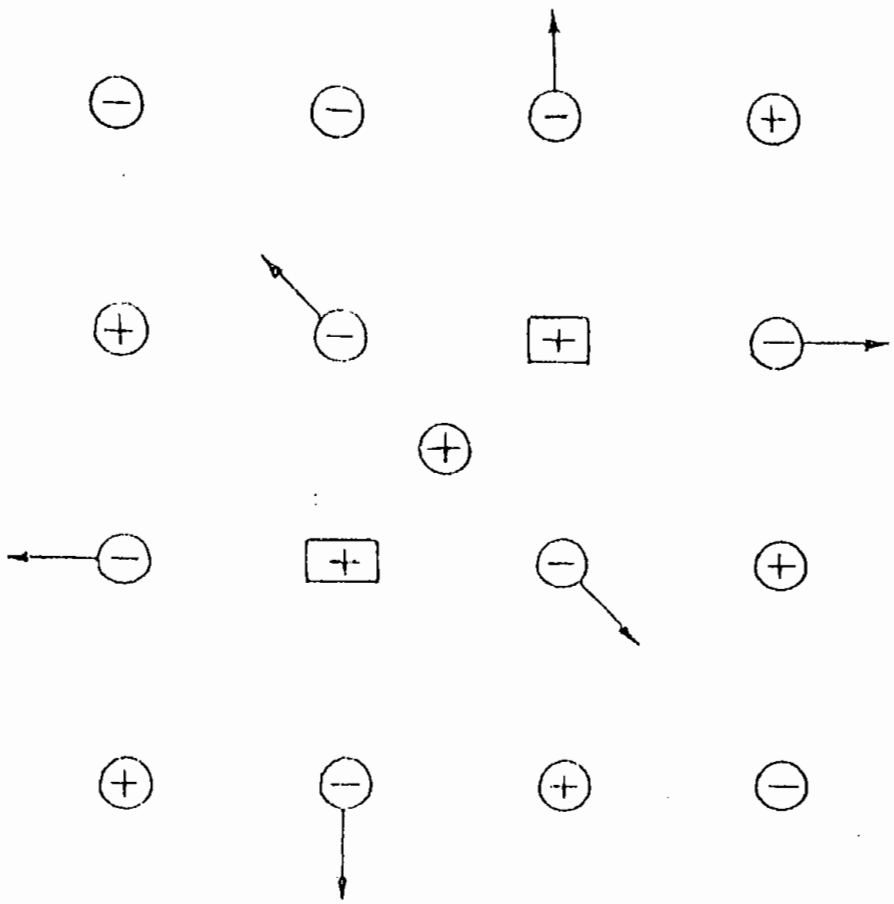

Fig. 5.2: Saddle point configuration for migration of a cation.

the strong field region close to the defect is incorrectly represented by any continuum approach based on the macroscopic dielectric constant. On the other hand, the calculation of the relaxation of the more distant weak field region by the continuum methods is quite adequate. As a result, the crystal containing charged defects is considered to be divided into an inner strong field and an outer weak field regions. In the inner region, termed as region I, the displacements are treated independently and determined by allowing it to interact with surrounding ions according to a pairwise central force law. In the outer region, region II, the ions are also regarded as discrete particles embedded in an elastic continuum. Here the relaxation is taken to arise solely from interaction of the polarizable medium with the defect at the origin. Region II has further been subdivided into two zones: Region IIa forms an annulus about region I, within this, the deformations due to its polarization interaction with the defect are assigned to the lattice sites of the crystal, i.e. in IIa the discrete ions are relaxed by amounts determined by the relaxation of the polarizable continuum of Mott and Littleton[84]. According to Mott and Littleton, the macroscopic polarization P, at a distance r from a defect of effective charge Z, is given by:

$$P = \frac{1}{4\pi}\left(1-\frac{1}{\varepsilon_0}\right)\frac{Zer}{r^3} \qquad (5\text{-}14)$$

The polarization per unit cell is then divided into constituent polarization terms. For the shell model, the polarization is broken down into core and shell displacements.

5.3.1 Division of the Lattice into two Regions:

Proceeding formally, the crystal is divided into two regions. The energy of defect formation is then expressed by

$$E = E_1(x) + E_2(x,y) + E_3(y) \qquad (5\text{-}15)$$

Here **x** and **y** are vectors of shell and core coordinates for region I and region II, respectively. $E_1(x)$ is the energy of the inner region depending only on the independent coordinates **x** describing the configuration of region I, $E_3(y)$ is the energy of the outer region and is a quadratic function of the displacements of region II. The interaction energy between the two regions is included in E_2 and

$$E_3(y) = \frac{1}{2}\, y,A.y \qquad (5\text{-}16)$$

where **A** is the force constant matrix and the components of **y** describe all the displacements in the outer region. On the basis of the equilibrium condition:

$$\frac{\delta E_2}{\delta y} = - A,y \qquad (5\text{-}17)$$

and then

$$E_3(y) = - \frac{1}{2}\, y \frac{\delta E_2}{\delta y} \qquad (5\text{-}18)$$

5.3.2 Short-Range Potential:

Here the SR potential function that acts between ions i and j is denoted by

$$\Phi_{ij}(|r_i - r_j|) \qquad (5\text{-}19)$$

where r_i is the position of the ith ion. All the ions, including

those removed from the crystal to form vacancies and also those added to the crystal to form interstitials are numbered. Substitutional ions are regarded as vacancies plus interstitials. Each lattice ion and interstitial now has a position denoted by r_i. In the sum over actual ions, those which are removed to infinity to form vacancies are always excluded. It is visualised by implicitly assigning a lattice position to the removed ions at some distance far from the crystal. The potential interaction is then becomes zero. Analogously, the sum over lattice sites denoted by R_i which excludes term corresponding to interstitials and whose lattice sites are assigned at infinity are required. Unrelaxed or ideal positions in the crystal are described by R_i and relaxed ion positions by r_i.

Also

$$R_{ij} = |R_i - R_j|$$
$$r_{ij} = |r_i - r_j| \qquad (5\text{-}20)$$

The convention then used corresponds to the process of removing ions to infinity to form vacancies and bringing ions from infinity to form interstitials. Also a notation $\Sigma'_{\substack{i\varepsilon I \\ j\varepsilon I}}$ is used to imply summation only over pairs of ions in region I where prime denotes restriction to i>j is used. On the basis of the convention the perfect crystal energy is expressed by

$$E^P = \Sigma'_{\substack{i\varepsilon I\&II \\ J\varepsilon I\&II}} \phi(R_{ij}) \qquad (5\text{-}21)$$

The energy of the defect lattice formed by the addition or removal of ions for an arbitrary configuration is then given by

$$E^d = \sum'_{\substack{i\varepsilon I\&II \\ J\varepsilon I\&II}} \phi(r_{ij}) \qquad (5\text{-}22)$$

The summation implicitly excludes vacancies but includes interactions with interstitials. E_3 is the quadratic relaxation energy of region II and on the basis of:

$$\frac{\delta E_3}{\delta y}\Big|_{y=0} = 0 \qquad (5\text{-}23)$$

E_3 gives the energy of a lattice in which every region II ion is at equilibrium when all displacements in the outer region is zero. It is the energy of a displaced region II with all ions in the inner region held at their perfect lattice sites, i.e. without defects. The expression for E_1 and E_2 then stands as:

$$E_1 = \sum'_{\substack{i\varepsilon I \\ J\varepsilon I}} \{ \phi(r_{ij}) - \phi(R_{ij}) \} \qquad (5\text{-}24)$$

and

$$E_2 = \sum'_{\substack{i\varepsilon I \\ J\varepsilon II}} (\phi(r_{ij}) - \phi(R_i - r_i) \qquad (5\text{-}25)$$

The summations are now restricted to ions in region I and region IIa. E_3 is then expressed in the form:

$$E_3 = -\frac{1}{2}\frac{\delta E_2}{\delta y}.y$$

$$= -\frac{1}{2}\sum'_{\substack{i\varepsilon I \\ j\varepsilon IIa}} \{ \frac{\delta \phi(r_{ij})}{\delta r_j} - \frac{\delta \phi_{ij}(|R_i - r_{ij}|)}{\delta r_j} \}. (r_j - R_j) \qquad (5\text{-}26)$$

5.3.3 Coulomb Potential:

The formalism for the energies is extended when the potential is a long range Coulomb interaction. The basic aim here, is to modify the summations to separate off interactions between explicit ions in a finite region of the crystal. The remaining long range part involves Madelung energy and it is calculated analytically by Ewald's method (described in chapter 2). Here, the expressions for E_1 and E_2 can be written as:

$$E_1 = \Sigma' \sum_{\substack{i\varepsilon I \\ j\varepsilon I}} \left[\frac{q_i^c q_j^c}{|r_i^c - r_j^c|} + \frac{q_i^c q_j^s}{|r_i^c - r_j^s|} + \frac{q_i^s q_j^c}{|r_i^s - r_j^c|} + \frac{q_i^s q_j^s}{|r_i^s - r_j^s|} - q_i \frac{q_j^c}{|R_i - R_j|} + \frac{q_j^s}{|R_i - R_j|} \right] \qquad (5\text{-}27)$$

and

$$E_2 = \Sigma' \sum_{\substack{i\varepsilon I \\ j\varepsilon II}} \left[\frac{q_i^c q_j^c}{|r_i^c - r_j^c|} + \frac{q_i^c q_j^s}{|r_i^c - r_j^s|} + \frac{q_i^s q_j^c}{|r_i^s - r_j^c|} + \frac{q_i^s q_j^s}{|r_i^s - r_j^s|} - q_i \left(\frac{q_j^c}{|R_i - r_j^c|} + \frac{q_j^s}{|R_i - r_j^s|} \right) \right] \qquad (5\text{-}28)$$

According to the Ewald's method, as the potential due to the complete Gaussian lattice is evaluated using a transformation to a rapidly convergent reciprocal lattice summation, the point charge lattice sum is estimated by correcting the value for the Gaussian distribution lattice only for lattice sites close to the point where the sum is evaluated. The situation is different and complex in case of a lattice with defect where ions are

displaced. To get comprehensive formulae for energies of a defect lattice, the evaluation of the potential $\Psi(r)$ at r due to a normalised charge density is carried out with the help of:

$$\rho(r') = \frac{\eta}{\pi^{1/2}} \exp(-\eta^2 r^2) \qquad (5\text{-}29)$$

The total charge nearer the origin than r may be considered to act at the origin and the potential due to the charge outside r is uniform at all points nearer the origin than r itself and it is conveniently evaluated at the origin. The potential of a lattice of Gaussian charge distribution evaluated at each ion in region I is subtracted from the lattice summations and the same contribution evaluated at each lattice site is then added to the summations. These terms are subsequently estimated analytically as a reciprocal lattice sum and the potential of the Gaussian lattice is, thus, removed. In terms of lattice summation, the extra term is given by

$$\Sigma'' q_i \left[q_j{}^c \left(- \frac{\mathrm{erf}(\eta |r_i{}^c - R_j|)}{|r_i{}^c - R_j|} + \frac{\mathrm{erf}(\eta |R_i - R_j|)}{|R_i - R_j|} \right) \right.$$
$$i \varepsilon I \quad j \varepsilon I \& II$$
$$\left. + q_j{}^s \left(- \frac{\mathrm{erf}(\eta |r_i{}^s - R_j|)}{|r_i{}^s - R_j|} + \frac{\mathrm{erf}(\eta |R_i - R_j|)}{|R_i - R_j|} \right) \right] \qquad (5\text{-}30)$$

The summation associated with the formulae is different with respect to convention . It excludes vacancies and interstitials (where appropriate) and extends over all values of i and j independently, including i = j. Before collecting this term with

other lattice sums, it is expressed in terms of the restricted summation over pairs of ions. Here difficulty arises only when ions i and j are in the same region. Now the extra term is given by

$$\sum_{\substack{i\varepsilon I\\ j\varepsilon I}}{}'' \left[q_i \left(-q_j{}^c \frac{\mathrm{erf}(\eta|r_j{}^c - R_j|)}{|r_i{}^c - R_j|} - q_j{}^s \frac{\mathrm{erf}(\eta|r_i{}^s - R_j|)}{|r_i{}^s - R_j|} \right) + q_i . q_j \frac{\mathrm{erf}(\eta|R_i - R_j|)}{|R_i - R_j|} \right]$$

$$= \sum_{\substack{i\varepsilon I\\ j\varepsilon I}}{}' q_i \left[q_j{}^c \left(- \frac{\mathrm{erf}(\eta|r_i{}^c - R_j|)}{|r_i{}^c - R_j|} - \frac{\mathrm{erf}(\eta|r_j{}^c - R_i|)}{|r_j{}^c - R_j|} + 2 \frac{\mathrm{erf}(\eta|R_i - R_j|)}{|R_i - R_j|} \right) + q_j{}^s \left(- \frac{\mathrm{erf}(\eta|r_i{}^s - R_j|)}{|r_i{}^s - R_j|} - \frac{\mathrm{erf}(\eta|r_j{}^s - R_i|)}{|r_j{}^s - R_i|} + 2 \frac{\mathrm{erf}(\eta|R_i - R_j|)}{|R_i - R_j|} \right) \right]$$

$$\sum_{i\varepsilon I}{}' q_i \left(-q_i{}^c \frac{\mathrm{erf}(\eta|r_i{}^c - R_i|)}{|r_i{}^c - R_i|} - q_i{}^s \frac{\mathrm{erf}(\eta|r_i{}^s - R_i|)}{|r_i{}^s - R_i|} \right) - q_i{}^2 \lim_{r \longrightarrow 0} \frac{\mathrm{erf}(\eta r)}{r} \qquad (5\text{-}31)$$

The summation Σ' accounts for terms in Σ'' when $i = j$. The term which is a function of $|r_i - R_i|$ excludes both vacancies and interstitials. From the assignment of coordinates at infinity for vacancies and interstitials, this term, in both the cases, is

zero. The term involving $|R_i-R_j|$ is zero only for interstitials.

For small argument the error function yields:

$$\frac{\mathrm{erf}(\eta r)}{r} = \frac{2\eta}{\pi^{1/2}} \left[1 - \frac{(\eta r)^3}{3} + \frac{(\eta r)^4}{10} - \frac{(\eta r)^6}{42} + \frac{(\eta r)^8}{216} - .. \right] \qquad (5\text{-}32)$$

then using $\lim_{r \to 0} \frac{\mathrm{erf}(\eta r)}{r} = \frac{2\eta}{\pi^{1/2}}$, the expression for E_1 and E_2 can be written as:

$$E_1 = \sum_{\substack{i\varepsilon I \\ j\varepsilon I}}{}' \left[\frac{q_i^c q_j^c}{|r_i^c - r_j^c|} + \frac{q_i^c q_j^s}{|r_i^c - r_j^s|} + \frac{q_i^s q_j^c}{|r_i^s - r_j^c|} + \right.$$

$$\frac{q_i^s q_j^s}{|r_i^s - r_j^s|} - q_i^c q_j \frac{\mathrm{erf}(\eta|r_i^c - R_j|)}{|r_i^c - R_j|}$$

$$q_i^s q_j \frac{\mathrm{erf}(\eta|r_i^s - R_j|)}{|r_i^s - R_j|} - q_i q_j^c \frac{\mathrm{erf}(\eta|R_i - r_j^c|)}{|R_i - r_j^c|}$$

$$\left. -q_i q_j^s \frac{\mathrm{erf}(\eta|R_i - r_j^s|)}{|R_i - r_j^s|} + 2 \frac{\mathrm{erf}(\eta|R_i - R_j|) - 1}{|R_i - R_j|} \right]$$

$$+ \sum_{i\varepsilon I}{}'' q_i \left(-q_i^c \frac{\mathrm{erf}(\eta|r_i^c - R_i|)}{|r_i^c - R_i|} - q_i^s \frac{\mathrm{erf}(\eta|r_i^s - R_i|)}{|r_i^s - R_i|} \right.$$

$$\left. + \frac{2q_i\eta}{\pi^{1/2}} \right)$$

The summation, Σ'', in this formula excludes vacancies and interistitials. It extends over all values of i and j independently, including i=j.

$$E_2 = \sum_{\substack{i\in I \\ i\in II}}{}' \left[\frac{q_i^c q_j^c}{|r_i^c - r_j^c|} + \frac{q_i^c q_j^s}{|r_i^c - r_j^s|} + \frac{q_i^s q_j^c}{|r_i^s - r_j^c|} + \right.$$

$$\frac{q_i^s q_j^s}{|r_i^s - r_j^s|} - q_i^c q_j \frac{\mathrm{erf}(\eta|r_i^c - R_j|)}{|r_i^c - R_j|}$$

$$-q_i^s q_j \frac{\mathrm{erf}(\eta|r_i^s - R_j|)}{|r_i^s - R_j|} - \frac{q_i q_j^c}{|R_i - r_j^c|}$$

$$\left. - \frac{q_i q_j^s}{|R_i - r_j^s|} + \frac{\mathrm{erf}(\eta|R_i - R_j|)}{|R_i - R_j|} \right] \qquad (5\text{-}34)$$

As given, the eqn. for E_1 contains a term corresponding to the Gaussian lattice potentials which have been added and then subtracted to these explicit lattice sums. These are evaluated by expressing the charge density due to the lattice of Gaussian charges as follows:

$$\rho(r) = \left(\frac{\eta}{\pi^{1/2}} \right)^3 \sum_{\substack{i \\ \text{all ions}}} \exp((-\eta^2 |r_i - R_i|^2)$$

$$= \frac{1}{v} \sum_{g} \rho(g) \exp(2\pi i g.r) \qquad (5\text{-}35)$$

reciprocal lattice vectors

except $g = 0$

Here the summation extends over reciprocal lattice vectors excluding $g=0$ because of the overall charge neutrality of the lattice. Then

$$\rho(g) = \{ \sum_{\substack{s \\ \text{ions in} \\ \text{unit cell}}} q_s \exp(2\pi i g.R_s) \} \exp(-\frac{\pi^2 |g|^2}{\eta^2}) \qquad (5\text{-}36)$$

Denoting the structure factor $\Sigma\, q_s \exp(2\pi i g.R_s)$ by $S(g)$ the expression for $\rho(r)$ can be written as:

$$\rho(r) = \frac{1}{v} \sum_{g} S(g) \exp\left(-\frac{\pi^2 |g|^2}{\eta^2}\right) \exp(2\pi i g.r) \qquad (5\text{-}37)$$

and then using Poisson's eqn. the expression for $\Psi(r)$ due to a lattice of Gaussian charge distributions is expressed by :

$$\Psi(r) = \frac{1}{\pi v} \sum_{g} \frac{S(g)}{|g|^2} \exp\frac{-\pi^2 |g|^2}{\eta^2} \exp(2\pi i g.r) \qquad (5\text{-}38)$$

The reciprocal lattice summation converges rapidly if n is chosen sufficiently small.

The expression for E_1 is then made complete with the help of the reciprocal lattice summation expressions to remove the potential of the Gaussian lattice added to the direct lattice expressions.

5.3.4 Approximation of Region II:

As discussed earlier, for the calculation of E_2 and E_3, region II is subdivided into two parts: the inner part, region IIa, is taken to be large enough so that all the error function terms involving ions in region I and ions outside IIa are essentially equal to 1. For this region the displacements are estimated from the sum of those due to each component charged defect acting separately. E_2 and $\delta E_2/\delta y$ are then calculated by explicit summation over all pairs of ions in region I and IIa. In the outer section, IIb, the displacements are calculated by the Mott-Littleton approximation using the net charge of the defect, localised at the most symmetric part, at the origin, of the

defect configuration. The energy due to these displacements arises solely from polarization term and is of the form:

$$E_2^{\,b} = \sum_{\substack{i\varepsilon I \\ j\varepsilon IIb}} q_i q_j \left(\frac{1}{|r_i - r_j|} - \frac{1}{|r_i - R_j|} - \frac{1}{|R_i - r_j|} + \frac{1}{|R_i - R_j|} \right) \qquad (5\text{-}39)$$

It is evident from the expression that if $r_j = R_j$, i.e. if there is no displacement of ions in the outer region, the contribution from this section becomes zero. The calculation is, however, made tractable through separating the summation into a part by removing those terms corresponding to defect in region I, i,e, term where contribution of the form

$$\frac{1}{|r_i - r_j|} \quad \text{and} \quad \frac{1}{|R_i - r_j|}$$

do not cancel for zero displacement. All the remaining terms involve interaction of displacement dipoles in region I with displacement dipoles in region IIb. These terms are small and the region IIa can be extended to such a size that dipole-dipole interactions from region IIb are negligible. At a greater distance from the defect, the dominant perturbation of region II arises due to the electric field produced by any net charge on the defect. The outer region is regarded as a continuum and in the case of these ionic crystals under study, this outer region is uniformly polarized in a radial direction. The uniform polarization, thus, produced generates no electric field within the continuum region and consequently there is no interaction

with displacement dipoles in region I. It is required to perform explicit summation only over limited region close to the inner region. However, there remain the terms due to the interaction of region IIb with the defect in the system. The remaining part of E_2^b can be written as:

$$E_2^b = \sum_{\substack{i \text{ over interstitials in region I} \\ j \varepsilon IIb}} q_i q_j \left(\frac{1}{|r_i - r_j|} - \frac{1}{|r_i - R_j|} \right)$$

$$- \sum_{\substack{i \text{ over vacancies in region I} \\ j \varepsilon IIb}} q_i q_j \left(\frac{1}{|R_i - r_j|} + \frac{1}{|R_i - R_j|} \right) \qquad (5\text{-}40)$$

Considering the polarisation effect of the monopole field which is due to the total charge Q of the defect at the origin, E_2^b is expanded to first order in the displacements, y_j as follows:

$$E_2^b = -Q \sum_{j \varepsilon IIb} (q_j^c y_j^c + q_j^s y_j^s) \cdot \frac{R_j}{|R_j|^3}$$

where $y_j = (r_j - R_j)$. (5-41)

The other term associated with the region IIb is

$$- \frac{1}{2} \frac{\delta E_2^b}{\delta y} \Big|_{y=\tilde{y}} \cdot \tilde{y} \qquad (5\text{-}42)$$

where $\tilde{y}$ are the equilibrium values for the y corresponding to arbitrary values of x. The total contribution of region IIb is

then obtained from

$$E_2{}^b - \frac{1}{2}\frac{\delta E_2{}^b}{\delta y}\Big|_{y=\tilde{y}} \cdot \tilde{y}$$

$$= -\frac{1}{2} Q \sum_{j\varepsilon IIb} (q_j{}^c y_j{}^c + q_j{}^s y_j{}^s) \cdot \frac{R_j}{|R_j|^3} \cdot \qquad (5\text{-}43)$$

Expressing the displacements by

$\tilde{y}_j = K_j R_j / |R_j|^3$, where K_j is a parameter characteristic of each sublattice, the above eqn. can be written as

$$-\frac{1}{2} Q \sum_{j\varepsilon IIb} (q_j{}^c K_j{}^c + q_j{}^s K_j{}^s) \cdot \frac{1}{|R_j|^4} \qquad (5\text{-}44)$$

The energy which is solely due to the polarization terms is, thus, estimated analytically and the sum over all lattice ions converges as

$$\frac{1}{R^4} \cdot$$

5.3.5 Minimisation Techniques:

The equilibrium configuration of a lattice in the presence of defects is calculated by minimising the energy of the defect lattice. The minimisation may be performed in two ways:

(a) Minimisation of the total energy, E(x), with y taken as an explicit function of x, is carried out by solving the eqns.

$$\frac{dE}{dx} = 0 \qquad (5\text{-}45)$$

Here the use of total derivative equations implies rigorous differentiation of the $\tilde{y}$ which are implicit functions of the

x's, the displacements in region I. Although this approach is consistent it is difficult to apply. The complicated nature of E(x) effectively precludes any analytic evaluation of dE/dx which is a necessary step in the application of fast numerical methods to the optimisation problem.

(b) Minimisation of the energy of the defect lattice and the equilibrium configuration may be obtained through solving the partial differential eqns.

$$\left.\frac{\partial E}{\partial x}\right|_{y=\text{const.}} = 0 \ . \qquad (5\text{-}46)$$

These eqns. are satisfied only when the force on each ion is zero. This force balance relation is used in the program [85] to calculate defect energy. It is found that for a sufficiently large size of region I, the equilibrium configurations estimated on the basis of both the above two methods are essentially equivalent. For simple defects the displacements in region II are left unchanged throughout the minimisation. But in case of more complex defects with substitutionals or interstitials which may be displaced during the minimisation, the forces

$$\frac{\partial E_2}{\partial y}$$

may vary appreciably with the change of the defect configuration and the corresponding displacements are then recalculated each iteration. An important feature in the use of computational methods in these calculations is the efficiency of the numerical minimisation methods. The numerical problem is essentially an

optimisation problem. There are several approaches, mainly in three classes to treat this optimisation problem. These are (a) direct searches, in which E(x) is evaluated for many possible displacements; (b) conjugate-gradient methods, which evaluates first derivatives

$$\frac{\partial E}{\partial x}$$

and which, after each iteration, concentrate on those displacements which appear to offer the largest energy reduction at the next step ; and (c) Newton-Raphson methods, in which both first and second derivatives are used.

In the simplest Newton-Raphson method, expansion of the function about any point x to second order is made and then the minimisation of the function to this order is carried out.

Thus,

$$E(x^*) = E(x) + g.\delta + 1/2\ \delta .^{T} W.\delta \qquad (5\text{-}47)$$

where $g = \frac{\partial E}{\partial x}$, $\delta = x^* - x$ and

$$W_{ij} = \frac{\partial^2 E}{\partial x^i\ \partial x^j} \qquad (5\text{-}48)$$

Here, the superscript T denotes the matrix transpose. E(x) has a minimum when $g=-W.\delta$ and hence the optimum displacement is evaluated from

$$\delta = - W^{-1}.g \qquad (5\text{-}49)$$

If the energy is perfectly harmonic, then eqn. (5-49) would immediately yield the equilibrium positions for the components of the crystal. However, this assumption is only partially correct

and so values of δ must be repeated through several iterations to obtain an overall minimum in the function. Updating of the coordinates results in a configuration closer to the minimum. The condition for reaching the equilibrium configuration is that the displacements between successive iterations are less than a present accuracy factor.

The method is extremely efficient and it requires few iteration to perform minimisation, but it has also serious difficulties which severely limit its use. The method is unstable if the matrix **W** is not positive definite. It also requires a large amount of computer storage to preserve the matrix. In addition to this, computation time is the central problem associated with the method. There is also a practical difficulty that the calculation of the second derivative of the lattice energy for an arbitrary lattice configuration is extremely tedious.

The problem of excessive computer time is removed through the procedure of Fletcher and Powell[86]. The matrix of second derivatives (second derivatives of the energy with respect to the lattice relaxation variables) after initial calculation, is updated at each iteration without recalculation and conversion. At each iteration a better geometry is calculated. The new coordinate positions for the *th iteration are then estimated using the Hessian,

$$H = W^{-1} \text{ and are given by}$$

$$x^* = x - H.g \qquad (5\text{-}50)$$

If H is positive definite and the step reduces the function so that $E(x^*) < E(x)$, then a better approximation to H evaluated at x^* can be estimated on the basis of the new gradients g^*, given by:

$$H^* = H + \frac{\delta.\delta^T}{\delta^T.\delta g} - \frac{H.\delta g.\delta g^T.H}{\delta g^T.H.\delta g} \qquad (5\text{-}51)$$

where $\delta = x^* - x$ and $\delta g = g^* - g$

Using the appropriate substitutions in (5-51) the new coordinate positions for the (*+1)th iteration can be evaluated. Reinversion of **W** is performed after a specified number of iterations in order to maintain accuracy and the process continues until the equilibrium configuration is reached. This fast matrix method discussed by Norgett and Fletcher[87], is used to carry out minimisations which combine rapid convergence with reasonably low computer time per iteration. An important feature associated with the method is the time required for calculation is only a slowly varying function of the number of variables and this makes feasible calculations on large low symmetry defects.

5.3.6 Displacements in Region II:

One of the most important factors to be considered to start the iterative relaxation is the displacements in region II. In the present potential model only the shells are massless and follow a high frequency electric field. If the matrix **R** is the repulsive part of the dynamical matrix and if **K** is a diagonal matrix containing the spring constants for each ion of the sublattice then the change in repulsive energy per unit cell is given by

$$\Delta U^R = 1/2\ (x^S)^T\ .\ (R + K)\ .\ x^S$$

(5-53)

where x^S is the vector of shell displacements for the unit cell.

If the displacements are due to the effective electric field E^{eff} acting at each ion then the total energy change is given by

$$\Delta U = -(q^S)^T\ .\ X^S\ E_X^{eff} + 1/2\ (X^S)^T\ .\ (R + K)\ .\ x^S$$

(5-54)

Here q^S denotes vector of the shell charges for the unit cell.

The equilibrium solution for the displacements in the effective field is then given by:

$$x^S = \{(R + K)^{-1}\ .q^S\}\ E_X^{eff}$$

(5-55)

To eliminate E_X^{eff} conveniently, the Lorentz field expression for E_X^{eff} is used. This is valid for a cubic material and gives an expression for the displacements, x^S, in terms of the dielectric constants.

The polarization P_X is given by:

$$P_X = \frac{1}{V}\ \{(q^S)^T\ .\ (R + K)^{-1}\ .q^S\}\ E_X^{eff}$$

$$E_X^{eff} = E_X + \frac{4\pi}{3} P_X$$

$$= \frac{\varepsilon_\alpha + 2}{3\varepsilon_\alpha}\ D_X \qquad (5\text{-}56)$$

The displacements are, then, expressed by

$$x^S = (R + K)^{-1}\ .\ q^S\ \frac{\varepsilon_\alpha + 2}{3\varepsilon_\alpha}\ D_X$$

(5-57)

where, $$D_X = 4\pi P_X \frac{\varepsilon_\infty}{\varepsilon_\infty - 1} \qquad (5\text{-}58)$$

It is known that in a static field, the displacements of cores also take place and the associated total energy change is given by

$$\Delta U = -\{(q^c)^T \cdot x^c + (q^s)^T \cdot x^s\} E_x^{eff} + 1/2\ (x^s)^T \cdot R \cdot x^s + 1/2\ (x^s - x^c)^T \cdot K \cdot (x^s - x^c) \qquad (5\text{-}59)$$

Finally, the relation describing the displacements is, then, given by

$$X = \frac{V}{4\pi} \frac{R'^{-1} \cdot Q}{Q^T \cdot R^{-1} \cdot Q} \left(1 - \frac{1}{\varepsilon_o}\right) D_X \qquad (5\text{-}60)$$

where

$$Q = \begin{pmatrix} q^c \\ q^s \end{pmatrix} ; \qquad X = \begin{pmatrix} x^c \\ x^s \end{pmatrix}$$

and

$$R' = \left(\begin{array}{c|c} K & -K \\ \hline -K & K + R \end{array}\right)$$

5.3.7 Description of the Computer Program:

The method employed in the program[85] to calculate defect energies is based on the division of the lattice into two regions, as described earlier, the outer has been treated by the Mott-Littleton approximation and inner by the explicit minimisation techniques. The program requires, as data, a specification of the lattice structure, an initial defect configuration so that the symmetry is retained throughout the

minimisation, specifications of regions I and II, and parameters to describe the crystal potential. Calculations are performed by the program on the basis of shell model. The program yields values of the rigid lattice energy for the defect, i.e. the energy before lattice relaxation and then the relaxation is calculated using the minimisation procedure about which a description has been presented earlier. Finally, the total defect energy, and the shell and core co-ordinates of ions in region I and II are obtained.

Detailed specification to run the program is given by Rowell[88]. The reported calculations were carried out on an IBM 4331 machine. It is to be noted here that due to the rather considerable storage required by the program, mainly due to the size of the matrix H, a large system was needed to work with the program.

CHAPTER 6

CALCULATIONS, RESULTS AND DISCUSSIONS

6.1 Parameters of the Present Model:

The potential which has been designed in the present study consists of short-range (SR) potentials, e.g. ϕ_{++}, ϕ_{--}, and ϕ_{+-} for the perfect lattice. Parameters are needed for these SR terms and the shell model description of polarization. They are derived and discussed as follows:

The two-body interionic potential, U must satisfy the following conditions[25,29,57,64,89-93]:

(i) Equilibrium Condition:

$$\left.\frac{dU}{dr}\right|_{r=r_0} = 0 \qquad (6\text{-}1)$$

(ii) Elastic Constants:

The second order elastic constants, C_{11} and C_{44} given by the eqns. (4-13) and (4-15).

(iii) Dielectric Constants:

The static and high frequency dielectric constants, ε_0 and ε_∞ presented by the eqns. (3-42) and (3-43).

(iv) Anion Polarizability:

The anion polarizability, α_2 given by the relation (3-45).

The eqns. which are satisfied by the potential represent six conditions. In the absence of the knowledge of many-body correction terms, C_{12} is not included in the fitting procedure. Since the dielectric properties are not affected by the usually considered deformations in the many-body contributions there is

no problem in using these properties. The present work is concerned with the study of four compounds, e.g. LiH, LiD, NaH, and NaD. The parameters associated with the eqns. are, then, given by:

$4B_{+-}$, $4B_{--}$, $4B_{++}$, $4a_{+-}$, $4a_{--}$, $4a_{++}$, $4Y_1$, $4Y_2$, $4K_1$, and $4k_2$

The total number of parameters to be determined is, thus, 40. Therefore, for the evaluation of the parameters at least 40 properties of the crystals are required. Although observed values of elastic and dielectric constants for LiH and LiD are available, these are lacking for heavier hydrides and deuterides. Therefore, some additional assumptions have to be made with a view to eliminate or fix some of the parameters and reduce the number to that value for which the system becomes solvable.

6.1.1 Reduction of the Parameters:

The like ion cation-cation potential has been obtained by applying electron gas theory, a description of which has been given in the next section. The anion-anion interaction (H^--H^-) was assumed to be independent of crystal environment. This should not lead to any serious error as the ionic separation varies by atmost 20% from one crystal to another. An account of how this interaction was obtained is presented in section 6.1.2(a). These non-empirical calculations with the above assumption reduce the number of parameters by 16.

The shell charges of Li^+ and Na^+ ions are taken from Catlow et at. [22,23] where shell parameters are from a set in which each parameter is specific to each ion. In order to reduce the number still further the shell charges of H^- and D^- have been taken to

be same, irrespective of whether H^-/D^- is in lithium or sodium compounds. This is due to the fact that nuclear mass substitution has negligible effect upon polarizability. The total number of parameters now becomes 15, e.g. $4B_{+-}$, $4a_{+-}$, Y_2, $2k_1$ and $4k_2$. The number is again reduced by assuming the same value for spring constant, k_2 associated with hydrides and deuterides[9], and finally there are only 13 unknown parameters.

6.1.2 Evaluation of the Parameters:

Two approaches have been used in determining the values of the unknown parameters. The first method is to theoretically derive the short-range parameters, a description of which is given below. The second method is through the procedure of empirical fitting which involves adjustment of parameters until the observed properties of a crystal are best reproduced. The technique employs a non-linear least squares procedure and is discussed later in this section .

(a) Non-empirical Methods :

The work of Catlow et al.[22,23] shows that the electron gas method gives adequate potentials for certain systems, but the procedure is developed on the basis of many approximations. In particular, the wave function does not include the effect of distortion of the ion charge clouds due both to the interaction between the two species and the environment of the solid. Both the two factors may considerably modify the wave functions of the ions, which in turn affect the calculated densities and then the interionic potential. A modified approach has been developed by Mackrodt and Stewart[94] and gives the solution of the problem of

interaction with crystal environment. They calculated the wave function for the ions in the presence of the electrostatic potential which is found at the crystal site. Using the crystal adapted wave functions in the electron gas procedure they obtained potentials that were structure dependent and were more relevant to the solid state. The like ion, cation-cation potential for NaH/NaD was obtained by applying electron gas theory developed by Wedepohl[62,95]. The method of Harding and Hareker[96] was utilized to evaluate the non-bonded Na^+-Na^+ interaction in NaH crystal[97]. The Li^+-Li^+ interactions were taken from the electron gas calculations of catlow et al[22,23]. The values are close to those of free Li^+ -Li^+ quoted by Wilson and Johnson[5]. This is due to the fact that cations having tightly bound charge distributions will not be much affected by the crystalline field and hence show no appreciable change from their free ion radial density distribution (and hence wave function). The approximation is therefore, taken to be reasonable.

An attempt was made to evaluate the like ion anion-anion interaction by applying electron gas theory. A run of the electron gas code of Harding and Harker[97] for this interaction in NaH gave values which was found to be not at all reliable. The calculations suggest that the short-range interaction is always attractive, even down to small distances. It approximately fits a vdW expression in the range 3.0-3.6 Å. The problem is probably the very diffuse H^- wave function. At likely interstitial position the total nearest neighbour H^--H^- contribution is found to be too large. Thus it is not clear that the electron gas

calculation approximation is particularly reliable in this case. Although some of the results of electron-gas calculation are encouraging one should emphasize that the theoretical methods for deriving electron gas model is crude [24]. A critical discussion of the electron gas density functional method has been given by Wood and Pyper[98].

Fisher et al.[4] performed a quantum mechanical calculation of the two-body SR interactions in LiH by using determinantal wave functions consisting of various one-electron functions. They utilised determinants made up of screened hydrogenic wave functions. Using the same screened hydrogenic charge distribution for the ions, semiclassical interactions were also obtained. The Wedepohl type of semi-classical values of the H^--H^- interaction were found to be ~40% too low compared to the diatomic quantum mechnical results. They also pointed out that the finer details of the ionic charge distributions turn out to be not very important when repulsive interactions are being calculated, and screened hydrogenic functions may yield adequately detailed charge distribution for the purpose[4]. For various values of screening parameter δ of the hydride ion, they obtained the H^--H^- interaction. The smallest value, δ=0.68, corresponding to a free H^--ion gives the most diffuse charge distributions and yields the most attraction. On the other hand, the most contracted H^--function with δ=0.95 results in the greatest repulsion. When relatively smaller screening constant than this is used, the results for the ranges of interest are somewhat similar to those obtained by `crystal adapted ' electron gas calculation of Pandey

and Stoneham[11]. Thus, the values of the screening parameter, δ has been chosen to be 0.721 and the resulting interactions obtained are well represented by a potential of type (3-61) with $D_{ij} = 0$.

The anion-anion interactions of NaH has been evaluated from the material LiH owing to the fact that LiH has been studied extensively and its bulk properties are known very well. This interaction is assumed to be independent of crystal environment. As it is small at equilibrium anion-anion separation, it should not cause any serious error. Pandey and Harding[99] in their calculations of defect structure of CaS took $S^- - S^-$ interaction from Na_2S by assuming ϕ_{SS} to be independent of crystal environment. Several authors[22-24] examined the possible use of common anion densities in series of similar ionic solids. The overall picture is that it can possibly be done with tolerable effect on various results of many systems.

The non-empirical method has two great advantages over the empirical procedure discussed in the next section. Firstly, empirical fitting yields a reliable potential for interionic separations close to those observed in the crystal. However, the reliabilities of the potential for separations that deviate from this value is questionable. On the other hand, non-empirical potentials can be derived for a range of separations. Secondly, the whole approach of empirical fitting relies upon there being sufficient experimental data whereas non-empirical methods can be used to obtain potentials for materials for which little data is available.

(b) Empirical Methods:

From a set of appropriate pair potentials for various interactions in a crystal, it is possible to calculate its properties, e.g. elastic, dielectric constants, phonon dispersion curves, etc. It is, however, important to note that the elastic and dielectric constants and the lattice vibrational frequencies do not depend on the inter-atomic potentials directly, but rather on first and second derivatives of the potentials with respect to the interionic separation. The extraction of information on the potential then requires the analytical form used to represent the interaction that reliably describe the variation of the potential with interionic separation. Cohesive energies do, of course, include direct information about the potential, but this is of limited value for the extraction of short-range potentials, for the lattice energy is normally dominated by the Coulomb term.

Empirical methods adjust variable parameters in order to get the best agreement between calculated and observed crystal properties. An initial estimate of the parameters involved in the potential is made and then the estimation of the crystal properties corresponding to the parameters is performed. The calculated and experimental properties are compared and the parameters adjusted accordingly using a non-linear least squares fitting routine[100]. The cycle is continued until the fitted parameters yield the best agreement between calculated and observed properties.

In the present study equilibrium condition (6-1) provides four eqns. whereas C_{11}, C_{44}, ε_0, ε_∞ (LiH) and α_2 (NaH) gives

eight eqns. In the least squares minimisation process[100] the value of k_1 (Li^+) was chosen first from

$$\alpha = \frac{Y^2}{k} \qquad (6\text{-}2)$$

and using the free ion polarizability of Pauling[101]. Fowler and Madden[93] showed that there is no significant difference between the free-ion and in-crystal polarizability values of cations like Li^+ and Na^+. Thus this, as has been shown later, does not affect the result in any way. The relation

$$\alpha = \frac{Y^2}{k + R} \qquad (6\text{-}3)$$

was employed for fitting k_1 for Na^+ in NaH using TKS polarizability[52]. This approximate relation can be used for cations with small polarizability values because k_1 is large compared to R[29,57,89]. The twelve eqns, were then utilised to fit the remaining 12 variables by keeping k_1 (Li^+) fixed at the above value. After a successful least-squares fit both the values of k_1 (Li^+) and $\alpha(Na^+)$ were varied in turn over a wide range to simulate any effect of crystal environments. The variation $\alpha(Na^+)$ was made due to the fact that the crystal polarizability of Na^+ in NaH may differ slightly from the TKS value. The procedure left output parameters virtually unaffected and the results thus obtained showed no noticeable change as expected. The sign of the anion shell charge is negative as expected but the cation shell charge taken from Catlow et al.[22,23], could be positive because of overlap polarization[102]. A positive cation shell charge has also been obtained in a fitting by Pandey and Stoneham[11]. The results of non-empirical calculations and empirical fitting procedures are shown in tables 6.1 and 6.2.

TABLE 6.1

Short-range potential parameters for interaction between ion-pairs

Source	Inter-action	a ($Å^{-1}$)	B (eV)	C (eV·$Å^6$)	D (eV·$Å^8$)
Present[1)]	Li-Li	7.3314	1153.80	0.0	0.0
	Li-H	3.1000	187.29	0.0	0.0
	Li-D	3.0915	181.93	0.0	0.0
	Na-Na	6.5232	1225293.0	0.0	0.0
	Na-H	2.7966	233.82	0.0	0.0
	Na-D	2.7659	216.81	0.0	0.0
	H - H	5.5411	915.50	4.986	0.0
Bowman[2)]	Li-Li	2.1598	15.98	0.05	0.02
	Li-H	2.1598	30.69	0.52	0.61
	Li-D	2.1598	30.34	0.52	0.61
	H-H	2.1598	54.61	13.94	28.25
	D-D	2.1598	53.99	13.94	28.25
	Na-Na	2.1598	61.00	3.29	2.21
	Na-H	2.1598	59.95	4.40	5.93
	Na-D	2.1598	59.27	4.40	5.93
	H-H	2.1598	54.61	10.81	21.88
	D-D	2.1598	53.99	10.81	21.88

1) Experimental values of C_{11}, C_{44}, ε_0, ε_∞(LiH), α_2(NaH) employed in the fitting procedure are from [11] and [92].

2) The potential parameters were obtained in this form using published data [35].

TABLE 6.2

Shell parameters

Source	Ion	Y(e)	k(eV/Å^2)
Present	Li	0.705	250.00
	Na	2.128	252.91
	H/D (LiH/LiD)	-0.9999	3.23
	H/D (NaH/NaD)	-0.9999	5.03
PS[1)]	Li(LiH)	0.998	40.08
	H	-1.005	4.24
	Li(LiD)	0.998	40.99
	D	-1.005	4.03

1) Ref.[11].

6.2 The Perfect Crystal:

6.2.1 Static Properties:

It is known that an accurate form of interionic potentials plays an important role in the study of structure and dynamics of ionic crystals. This part of the thesis is concerned with the static properties calculated on the basis of the derived potential.

The utility of the potential can be assessed in two ways: (i) directly by comparing with experiment or (ii) indirectly by comparing with alternative or previously derived potentials. Several physical quantities were estimated on the basis of the potentials which have been derived in the present study. The quantities calculated are: lattice cohesive energy Uo; the second order elastic constants, e.g. C_{11}, C_{12}, and C_{44}, static and high frequency dielectric constants (ε_0 and ε_∞), and transverse optic frequency ω_0. Values for the above quantities were also calculated utilizing two other potentials, e.g. Bowman and HS[35,36] and shown in Table 6.3. The available experimental data are also collected in the same table. The table shows that there is a reasonable agreement between the calculations performed in the present work and experiment where these are available. Since Coulomb-contribution dominates, agreement with Uo does not provide sensitive test of the SR potentials. Thus although the Bowman potentials yield good cohesive energy, these fail to give reasonable values (computed by the author) for both elastic and dielectric properties. For example, the computed C_{11} for LiH is found to be negative. The HS potential (fitted exactly for ε_0 and ε_∞) gives very high values of elastic constants. The

computed value of C_{11} for the same compound is ~ 40% higher compared to the observed value. On the other hand, the potential derived in the present study yields a value in reasonable agreement with experiment. C_{12} is overestimated and the Cauchy relation is obeyed since the potential used is central. This has to be allowed owing to the fact that there is uncertainty and inconclusive evidence for many body effects.[22,23,103]. It may be mentioned here that even the model of Verble et al.[12] and Jaswal et al.[6] underestimates or overestimates the values of C_{12}, respectively.

The estimated ε_o with Bowman potentials (using shell parameters from the present work) are found to be negative for all the compounds. On the other hand, the present potential produces ε_o, ε_∞ and W_o reasonably well for lithium compounds. The calculated values of these quantities for the sodium compounds when compared to those of HS[36] using S-A scheme are found to be very reasonable. It is to be noted that S-A reproduces dielectric properties well.

From a study on the interionic potential for alkali metal chloride, Corish et al.[25] suggested that the best effective potential is obtainable by fitting simultaneously the bulk elastic and dielectric properties. Further, they pointed that the best potential should ignore many-body forces and hardening of the short-range interaction between unlike particle shoulkd be made by completely neglecting the vdW effects. The initial qualitative agreement with experiment indicates that the present potential with the above characteristics is suitable (discussed later) for defect studies also.

TABLE 6.3

Properties of LiH, LiD, NaH, and NaD crystals.

Properties	Source	Values			
		LiH	LiD	NaH	NaD
r_0 (Å)	Present	2.0417	2.0346	2.44	2.434
	Bowman	2.0420	2.0340	2.44	2.434
	HS	2.0420	--	2.4836	--
	PS	2.0417	2.0324	--	--
	Exptl[1]	2.0417	2.0346	2.44	2.434
U_0 (eV)	Present	-10.38	-10.41	-8.81	-8.81
	Bowman	- 9.73	- 9.76	-8.46	-8.48
	HS	-10.22	--	-8.36	--
	PS	-10.36	-10.43	--	--
	Exptl[1)]	- 9.44	- 9.63	-8.21	-8.25
C_{11} (10^{11}dynes/ cm^2)	Present	7.89	7.86	4.73	4.60
	Bowman	-1.27	-1.41	1.30	1.24
	HS	10.25	--	5.27	--
	PS	7.98	7.78	--	--
	Exptl[1)]	7.41±0.2	7.68±0.2	--	--
C_{12} (10^{11}dynes/ cm^2)	Present	4.43	4.49	2.25	2.28
	Bowman	6.38	6.46	3.20	3.23
	HS	5.21	--	2.14	--
	PS	4.59	4.67	--	--
	Exptl[1)]	1.42±0.03	1.51±0.03	-	--

Contd.

Properties	Source	Values			
		LiH	LiD	NaH	NaD
C_{44} (10^{11} dynes/ cm^2)	Present	4.41	4.47	2.25	2.27
	Bowman	7.02	7.13	3.32	3.36
	HS	5.67	--	2.14	--
	PS	4.57	4.67	--	--
	Exptl[1)]	4.84±0.18	4.94±0.18	--	--
ε_0	Present	13.65	14.46	9.94	10.66
	Bowman[2)]	-4.91	-4.84	-9.37	-9.08
	HS	13.45[3)]	--	10.68	--
	PS	13.92	14.78	--	--
	Exptl[1]	12.9±0.5	14.0±0.5	--	--
ε_∞	Present	3.61	3.67	2.22	2.25
	Bowman[2)]	8.49	8.79	2.60	2.62
	HS	3.61[3)]	--	2.47	--
	PS	3.32	3.45	--	--
	Exptl[1)]	3.61±0.5	3.63±0.5	--	--
ω_0[4)] (10^{14} sec^{-1})	Present	0.855	0.629	0.7999	0.559
	HS	1.115[3)]	--	0.870	--
	PS	0.868	0.635	--	--
	Exptl[1]	1.115	0.860	--	--

1) Refs.[11, 12, 35].

2) Using shell parameters from the present work.

3) Fitted exactly.

4) ω_0 values with Bowman potential not reported because ω_0^2 were all negative.

6.2.2 Dynamic Properties:

This sub-section is concerned with the phonon dispersion relations for all the four compounds based on the present potential. The curves representing the dispersion of phonons along the principal symmetry directions are depicted in figures 6.1-6.4. Due to the non-availability of observed data for LiH, NaH, and NaD, the calculated frequencies are compared with those obtained by DJ[9] (based on the force constant model). The shell parameters of their model have been deduced from the force constants and the ionic charge of their best fit model DDM 13 for LiH/LiD. From fig. 6.1 (LiH) it is seen that although the dispersion curves for LiH in the optic branch bear little resemblance to those calculated by DJ, they are in good agreement in the acoustic branch. In the optic branch, the calculated frequencies are smaller throughout the zone whereas in the acoustic branch the agreement is much better except near the zone boundary. Figure 6.2 displays the phonon dispersion curves for LiD. From the fig. it is observed that, in spite of some discrepancies associated with the curves in the optic branch the agreement of the present calculation in the acoustic branch is excellent with the experimental values . However, it is interesting to note that the agreement of the frequency ratios, $\omega(LiH)/\omega(LiD)$ as shown in Table 6.4, when compared with those from the lattice-dynamic calculations of Verble et al.[12] based on shell model fitted to experimental neutron data, is amazingly well. The figures 6.3 and 6.4 consist of the phonon dispersion curves for the hydride and deuteride of sodium. From these two

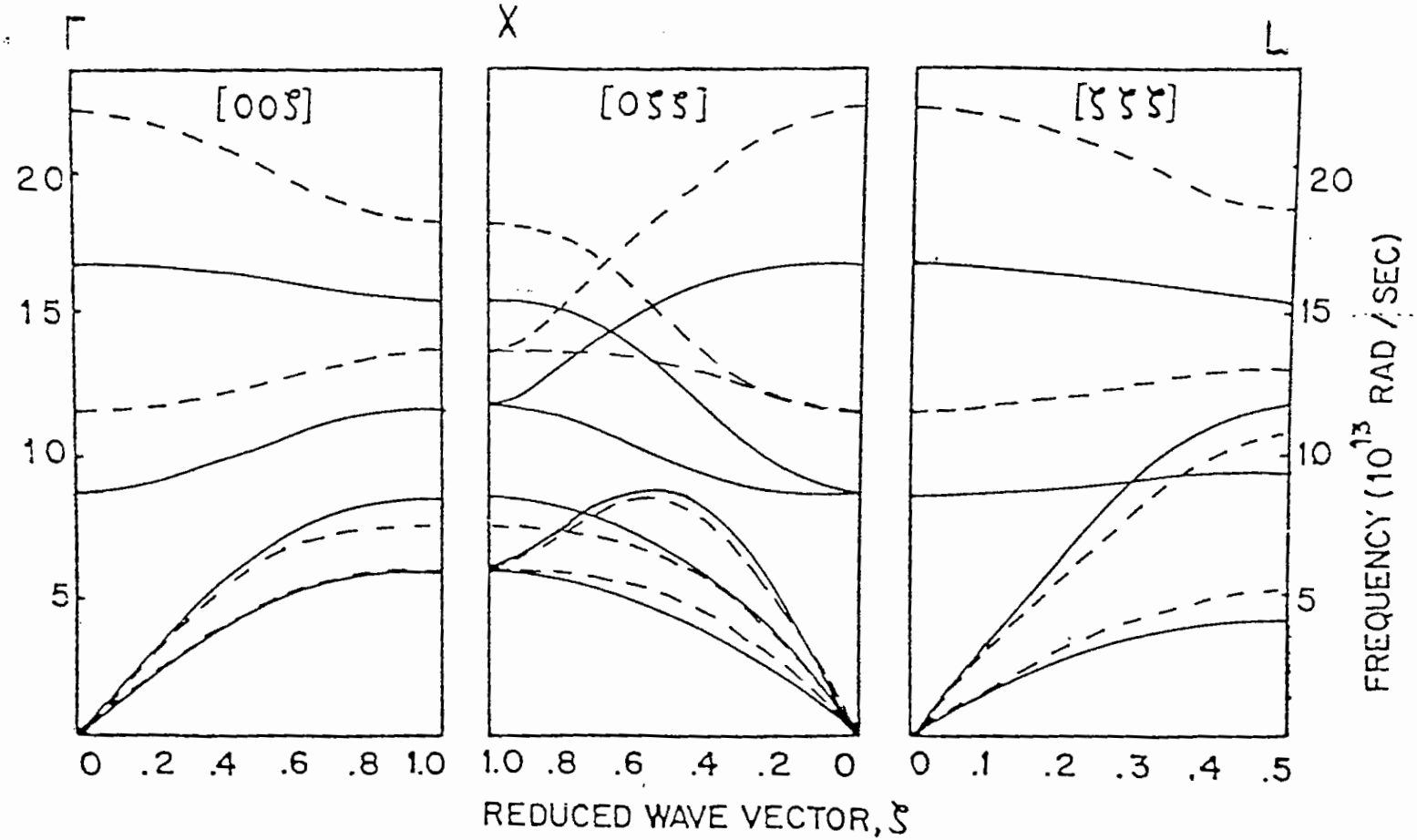

Fig. 6.1: Phonon frequencies for LiH (continuous curve) compared with the calculation of DJ (broken curve).

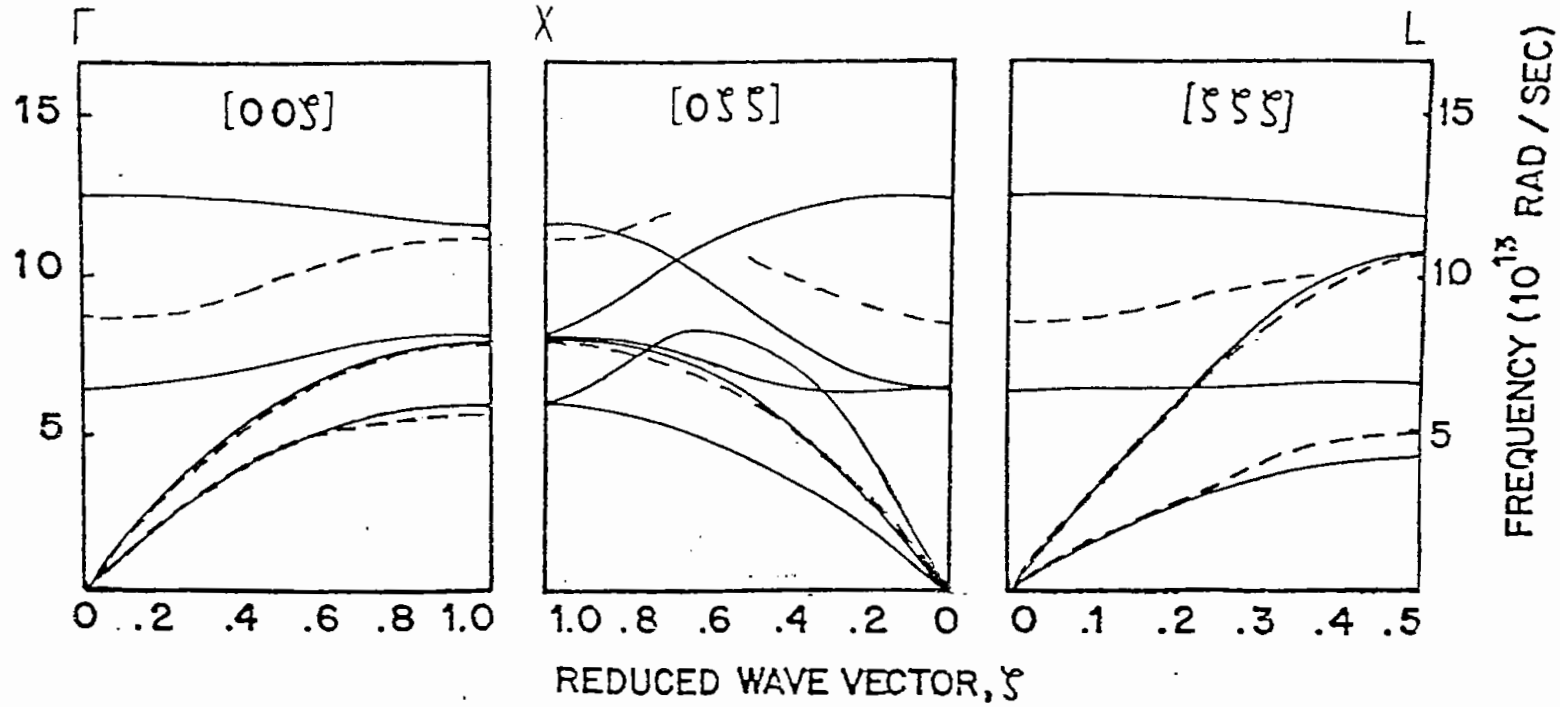

Fig. 6.2: Phonon frequencies for LiD (continuous curve) compared with the experimental data (broken curve).

TABLE 6.4

Frequency ratios w(LiH)/w(LiD) for Γ, X and L point phonons of LiH and LiD.

Phonon branch	Source	Γ	X	L
LO	Present	1.33	1.31	1.21
	PS	1.35	1.38	1.43
	VWY	1.33	1.39	1.40
TO	Present	1.35	1.41	1.42
	PS	1.36	1.42	1.44
	VWY	1.33	1.39	1.40
LA	Present	--	1.08	1.16
	PS	--	1.04	0.99
	VWY	--	0.99	0.97
TA	Present	--	1.00	1.01
	PS	--	1.00	1.01
	VWY	--	1.00	0.97

PS : Ref. [11]

VWY: Ref. [12]

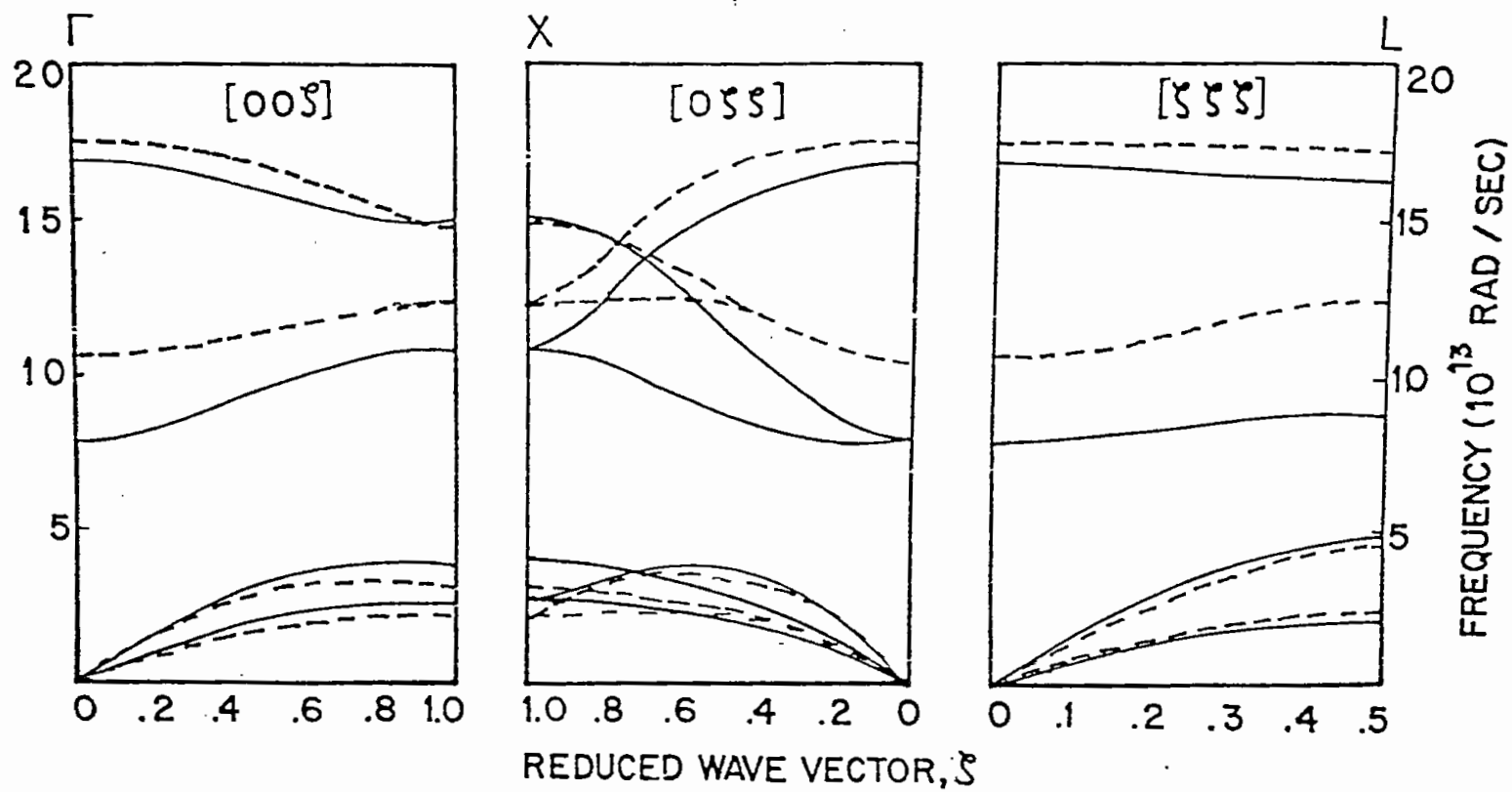

Fig. 6.3: Phonon frequencies for NaH (continucus curve) compared with the calculation of DJ (broken curve).

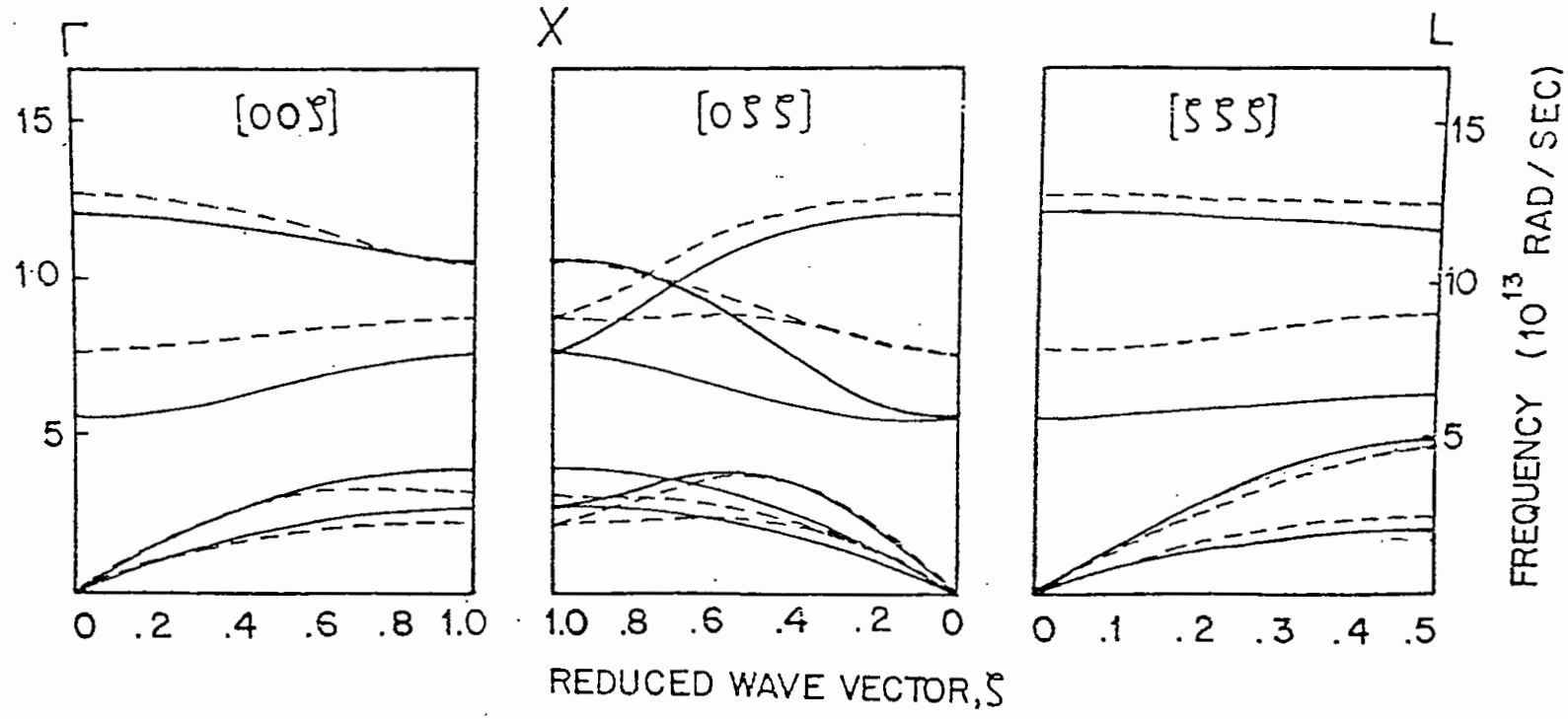

Fig. 6.4: Phonon frequencies for NaD (continuous curve) compared with the calculation of DJ (broken curve).

curves the discussion can be presented as follows:

(a) The increase in the mass of the vibrating cation yields somewhat flatter curves. On the other hand, since the D^- ion influences the acoustic branches, these branches fall in the same frequency range.

(b) The phonon dispersion curves for the hydrides differ from the ones for the corresponding deuterides in the optical mode only, the frequency of which can be calculated from

$$\omega_{OH} = (m_D/m_H)^{1/2} \omega_{OD}$$

(c) The influence of sodium polarizability ($\alpha_{Na} >> \alpha_{Li}$) can be seen in the lowering of the longitudinal branches in the [100] direction near the zone boundary.

(d) In the present model like-particle interactions are rather small. Despite the differences between the Li^+-Li^+ interaction and an unexpectedly strong interaction found by DJ[9], there is similarity of interaction strengths between other second neighbours. Thus, the dispersion curves presented here are mainly determined by the nearest neighbour interactions and also the effects arising from the electronic polarizability of ions. It is worth mentioning that the model is a simple one and is not like the complex lattice dynamical models specifically introduced to explain only the neutron data. However, one has to await future experimental investigations in order to make further comments regarding the dispersion curves.

6.3 The Defect Lattice:

The results obtained in the present study on various defect energies based on the derived potential are displayed in tables 6.5-6.13. The available observed data as well as other theoretical estimates are also listed in these tables.

The defect formation energies along with the first nearest-neighbour shell displacements are shown in Tables 6.5 and 6.6. From Table 6.5 it is seen that the extraction energy of a cation is less than the extraction energy of an anion. This is due to the fact that in these lithium and sodium ionic crystals the anions are larger in size than the cations and hence the polarization energy associated with the cation is more negative than the polarization energy for the anions. From the table it appears that the difference between the vacancy formation energies for cation and anion associated with the sodium compounds is smaller than those of lithium compounds. This is owing to the smaller differences in ionic radii of the sodium compounds in comparison to that of lithium values. The table also shows that in case of a cation vacancy the shell of the first-nearest-neighbour displaces through a much smaller distance in comparison to that of an anion. As the vacancy energy of a cation is less than that of an anion it can be inferred from this that due to the mismatch in size of the ions the cation vacancies are more probable in crystals under study.

TABLE 6.5

First-Nearest-Neighbour Shell Displacements, Extraction Energies and Lattice Energies

Compound	Vacancy	First-Nearest-Neighbour Shell Displacement*	Defect Energy (eV)	Lattice Energy (eV)
LiH	Li	0.020	5.882	-10.372
	H	0.650	6.037	
LiD	Li	0.020	5.876	-10.395
	D	0.650	6.034	
NaH	Na	0.010	5.169	-8.804
	H	1.490	5.222	
NaD	Na	0.010	5.138	-8.805
	D	1.500	5.192	

* In units of 10^{-3} r_o

From Table 6.6 it is seen that interstitial formation energies are negative. This is owing to the strong polarization in the lattice caused by the interstitial charge. In addition to this, van der Waals terms make a negative contribution. In case of an interstitial, the shell of the first-nearest-neighbour displaces, as shown in the Table, through almost the same extent with respect to both cation and anion.

The study of defect calculation involves consideration of the size of the inner region ; in this respect, an exercise was carried out with different sizes of the region. It is seen from table 6.7 that for the cation vacancy of a compound, e.g. LiH, the formation energy was found to change by ~1% due to the increase in size from 20 to 118 ions; the change was less than 0.2% if the size is changed from 82 to 118 ions and after that there is practically no change in the energy values. In case of an anion (table 6.8) the variation of the values with respect to the size of region I was exactly the same as those obtained in case of cation. For the estimation of lattice vacancies of the ionic crystals under study it is, therefore, sufficient to include 80-100 ions in the inner region. The errors in the calculations with this region size are smaller than the absolute errors in the defect energies which arise from other inadequacies in the model used. The size of region IIa has also been chosen in such a way that has only a negligible effect on the calculations.

For interstitial formation energy, as it is seen from tables 6.9 and 6.10 the number of ions in region I should also be around 100.

TABLE 6.6

First-Nearest-Neighbour Shell Displacements and Interstitial formation Energies.

Compound	Inter-stitial	First-Nearest-Neighbour Shell Displacement*	Defect Energy (eV)
LiH	Li	0.97	-3.118
	H	0.97	-3.365
LiD	Li	0.99	-3.149
	D	0.97	-3.400
NaH	Na	2.17	-2.366
	H	2.27	-2.595
NaD	Na	2.17	-2.419
	D	2.25	-2.645

* In units of 10^{-3} r_o

TABLE 6.7

Cation Vacancy Formation Energy (eV)

Compound	Number of Ions in Region I	Values
LiH	20	5.954
	34	5.900
	82	5.882
	118	5.893
	148	5.893
LiD	20	5.948
	34	5.895
	82	5.876
	118	5.888
	148	5.887
NaH	20	5.229
	34	5.185
	82	5.169
	118	5.177
	148	5.178
NaD	20	5.198
	34	5.152
	82	5.138
	118	5.145
	148	5.146

TABLE 6.8

		Anion Vacancy Formation Energy (eV)
LiH	20	6.106
	34	6.055
	82	6.037
	118	6.049
	148	6.049
LiD	20	6.104
	34	6.052
	82	6.034
	118	6.046
	148	6.046
NaH	20	5.277
	34	5.237
	82	5.222
	118	5.230
	148	5.232
NaD	20	5.246
	34	5.206
	82	5.192
	118	5.200
	148	5.201

TABLE 6.9

Cation Interstitial Formation Energy

Compound	Number of Ions in Region I	Values (eV)
LiH	22	-2.832
	58	-3.123
	78	-3.118
	114	-3.127
	150	-3.141
LiD	22	-2.859
	58	-3.154
	78	-3.149
	114	-3.158
	150	-3.172
NaH	22	-2.060
	58	-2.370
	78	-2.366
	114	-2.378
	150	-2.390
NaD	22	-2.101
	58	-2.417
	78	-2.413
	114	-2.425
	150	-2.438

TABLE 6.10

Anion Interstitial Formation Energy

Compound	Number of Ions in Region I	Values (eV)
LiH	22	-3.108
	58	-3.369
	78	-3.365
	114	-3.373
	150	-3.385
LiD	22	-3.140
	58	-3.405
	78	-3.400
	114	-3.408
	150	-3.421
NaH	22	-2.395
	58	-2.595
	78	-2.595
	114	-2.601
	150	-2.601
NaD	22	-2.442
	58	-2.646
	78	-2.645
	114	-2.651
	150	-2.660

The Schottky and Frenkel defect energies, E_S and E_F of a compound are estimated using the relations:

$$E_S = E_{V+} + E_{V-} - E_L$$

and

$$E_{F\pm} = E_{V\pm} + E_{i\pm}$$

where E_{V+} and E_{V-} are the defect energies associated with the extraction of a cation and an anion from the crystal respectively. $E_{i\pm}$ is the interstitial formation energy for the cation(anion) and E_L is used to denote the lattice cohesive energy.

Table 6.11 gives the Schottky, Frenkel, and antisite-pair defect energies. Schottky pair formation energy involves consideration of calculated value of lattice energy. The estimated lattice energies (for full ionic value, Z=1) for the lithium compounds differ from experimental values by 0.86 eV. This is reflected in the calculated Schottky energy and it is seen that the values of lithium compounds are lower than the reported data. The calculation shown under PS in Table 6.11 are much smaller than their earlier reported values[11]. This is because Pandey and Stoneham[11,104] used experimental rather than calculated cohesive energies in deducing the defect energies. The calculations, here, for lithium compounds give slightly better agreement with the experimental results than those achieved by PS[11].

TABLE 6.11

Intrinsic Defect Energies (eV)

Properties	Source	Values			
		LiH	LiD	NaH	NaD
Schottky Pair	Present	1.55	1.52	1.59	1.52
	PS[1]	1.49	1.48	--	--
	Exptl	2.30±0.3[2]	--	--	--
		2.33±0.01[3]	2.40±0.01[3]	--	--
Frenkel Pair					
Cation	Present	2.76	2.73	2.80	2.72
	PS	2.72	2.65	--	--
Anion	Present	2.67	2.69	2.63	2.55
	PS	2.70	2.61	--	--
Antisite Pair	Present	8.10	8.03	7.70	7.54
	PS	7.81	7.98	--	--

(1) PS[1] incorrectly reported these values as 2.42 eV and 2.29 eV, respectively. They used experimental rather than calculated cohesive energies. (Private communication with Dr. R. Pandey[104])

(2) Ref. [109].

(3) Ref. [110].

From an observation of the experimental results of the Schottky defect energies for alkali halide it is seen that for a particular alkali metal the defect energy of the corresponding halide increases in the sequence $I^- \longrightarrow Br^- \longrightarrow Cl^- \longrightarrow H^- \longrightarrow F^-$. A number of researchers worked on the dependence of the Schottky energy on the lattice properties and presented empirical expressions relating the defect energy with properties of the lattice involving numerical constants. According to Pathak and Vasavada[105]

$$E_S = 3.4 \times 10^{-13} \quad V/X \qquad (6\text{-}4)$$

where V is the mole volume, and X, the compressibility. The estimated Schottky defect energies using the above relation for the hydrides and deuterides of lithium and sodium are 1.18, 1.17, 1.13, and 1.11 eV, respectively. On the other hand, Shukla and Bansigir[106] presented a relation:

$$E_S = r_0^{\,3} \times H_V/1650 \quad (eV) \qquad (6\text{-}5)$$

where r_0 is the lattice constant and H_V denotes Vickers hardness. This relation also yields unsatisfactory results for the Schottky defect energies for alkali halides of NaCl structure. Likewise, according to Bollmann[107]

$$E_S = 0.0829 \ \frac{eV\ mol}{kJ} \ L \qquad (6\text{-}6)$$

where L is the heat of fusion. On the basis of this expression the estimated E_S values are 1.89 and 1.86 eV, for the lithium hydride and lithium deuteride, respectively. Thus, it is seen that the calculated defect energies (whether one uses rough empirical relation or detailed calculation) are always less than

the experimental values. This is because the empirical relations are not general formulae. The relation (6-4) holds only for some of the alkali halides in the right manner. Although the relation (6-4) shows $E_S \sim r_0^{-1}$, (as $v \sim r_0^3$ and $X \sim r_0^4$), the dependence is not strictly borne out experimentally. The relation (6-5) is also not suitable for all the compounds as the hardness which is influenced by the degree of purity of the crystal is not a real constant. Likewise, the numerical constant of relation (6-6) may be different for different compounds. On the other hand, estimation of Schottky defect energies using detailed calculation also yields a lower value. The reason is that the expression for E_S involves calculated lattice energy which turns out to be always larger for a fully ionic (Z=1) crystals. If one assumes a 95% ionicity, then the calculated E_L is closer to the experimental data. This in turn reproduces a value of E_S closer to the experimental one.

It is known that NaH decomposes before melting and the temperature at which decomposition occurs is 800°C. It can be inferred that the calculated Schottky energies for sodium compounds have the expected values based on the E_S versus T_m relationship and the corresponding Li-values[108].

Because of the paucity of experimental data for the Frenkel formation and antisite pair defect energies for all the four compounds, no useful comparison of these values seems possible. It is significant, however, that the calculated formation energies of Schottky pair are noticeably lower in comparison to both the Frenkel pairs. These confirm the suggestion of PS[11]

that vacancies, rather than interstitials, will be the most common defect species in these crystals. From the result of antisite-pair defect energies it is seen that the values are very high. It predicts that as the cations and anions in these compounds are of different sizes, the interchange of sites is least possible and hence this type of defect is unlikely to be observed.

The energy for vacancy migration is defined as the difference in the energy of the crystal in the saddle point configuration and the energy of the solid containing a single vacancy. In other words, it is given by the difference between the energy to extract two next nearest neighbour ions and to introduce one of them into the saddle point configuration between the two neighbouring vacancies and the energy to extract a single ion from a perfect crystal.

The migration energies for the movement of an ion by vacancy and interstitial mechanisms are calculated from:

$$E_{mv(i)} = E_{sv(i)} - E_{v(i)}$$

where $E_{sv(i)}$ is the saddle point energy for the vacancy (interstitial) mechanisms. $E_{v(i)}$ represents vacancy (interstitial) formation energy.

Table 6.12 presents results for cation and anion migration activation energies. It is observed that our calculated values of the migration of cation by vacancy mechanism in the lithium compounds are both equal to 0.43 eV. Though the results are slightly larger than those obtained by PS[11] they are smaller when compared with the available experimental data. It is

TABLE 6.12

Activation Energies for Migration (eV)

Compound	Source	Values	
		Vacancy Mechanism	Interstitial Mechanism
LiH			
Li^+	Present	0.43	0.17
	PS	0.42	0.17
	Exptl	0.54 ± 0.02[1]	--
H^-	Present	0.43	0.18
	PS	0.40	0.19
LiD			
Li^+	Present	0.43	0.17
	PS	0.33	0.18
	Exptl	0.52 ± 0.01[2]	--
D^-	Present	0.42	0.18
	PS	0.32	0.17
NaH			
Na^+	Present	0.44	0.15
H^-	Present	0.43	0.16
NaD			
Na^+	Present	0.43	0.15
D^-	Present	0.42	0.16

(1) Ref. [109].

(2) Ref. [110].

significant, however, that the analysis of the conductivity curves has been carried out taking cation vacancies as mobile species and treating them as extrinsic defects due to the presence of divalent cation in the lattice[109,110]. The values in the present work, on the other hand, are for free cation vacancy migration, and hence the results, as expected, are smaller [111].

Furthermore, analysis of the conductivity based on vacancy transport requires an anion vacancy activation energy that may be twice the cation value [112-114]. In contrast, the anion activation energies reported by PS[11] and those in the present work are almost equal to the cation value. There is, in addition, evidence that the two vacancy activation energies are more nearly comparable: anion tracer diffusion measurements, when corrected for the divacancy contribution yields values which are similar to the cation results [115,116], comparable and reliable estimates of anion transport are also obtained from conductivity measurements on materials which have been doped with divalent anions with a view to suppress the dominant cation contribution[117]. Beniere et al[118] also carried out research on both the diffusion and conductivity studies and presented similar values for the cation and anion activation energies. Thus, if the contribution in the conductivity is from both the vacancies with similar activation energies then the conductivity plot possesses a linear shape. This is contrary to experience and fails to separate cation and anion contributions in the curve. Hence the curvature in the plot requires some other explanation. For the sodium compounds the activation energies for the

migration of cation and anion in hydride and deuteride by vacancy mechanism are again comparable. The values for cation and anion migration energies for interstitial mechanism in case of lithium compounds are nearly same as those obtained by PS[11]. The corresponding values for sodium compounds are ~ 0.01 eV less than the lithium values. An examination of Table 6.12 further shows that although the Frenkel energies (Table 6.11) are higher, the activation migration energies in these compounds for both the ions by interstitialcy mechanism are significantly low. As the barrier heights for the interstitialcy mechanism are low, it is reasonable to infer following PS[11] that in addition to vacancy mechanism, interstitialcy also plays an important role in the conductivity at high temperature.

The Arrhenius energies, E_{AV} and E_{AI} for diffusion are given by:

$$E_{AV} = E_{mv} + 1/2\ E_S$$

and

$$E_{AI} = E_{mi} + 1/2\ E_F$$

where E_{AV} and E_{AI} are associated with vacancy and interstitial mode of migration, respectively.

Table 6.13 consists of Arrhenius energies for vacancy and interstitial mode of migration. From the comparison of the values reported in Table 6.13 it is seen that our results for the lithium compounds are slightly better than those of PS[11,104]. The calculated values are smaller in comparison to the available experimental data. This discrepancy is due to the lower values of Schottky defect energies which in turn are the results of the calculated E_L values as discussed earlier. Apart from Coulombic

TABLE 6.13

Arrhenius Energies of Migration (eV)

Compound	Source	Values	
		Vacancy Mechanism	Interstitial Mechanism
LiH			
Li^+	Present	1.21	1.55
	PS	1.18[1]	1.53
	Exptl	1.70±0.1[2]	--
		1.72±0.005[3]	--
H^-	Present	1.21	1.52
	PS	1.18[1]	1.54
LiD			
Li^+	Present	1.19	1.54
	PS	1.16[1]	1.51
	Exptl	1.695±0.005[3]	--
D^-	Present	1.18	1.50
	PS	1.16[1]	1.47
NaH			
Na^+	Present	1.25	1.55
H^-	Present	1.23	1.48
NaD			
Na^+	Present	1.19	1.51
D^-	Present	1.18	1.44

(1) Corrected values (See comment 1 of Table 6.11)

(2) Ref. [109].

(3) Ref. [11].

interaction the nearest-neighbour pairwise force is the dominant interaction. These forces are responsible for the similar values of activation and Arrhenius energies for cation and anion. Hence there is an ambiguity in the assumption of immobility of anion vacancies in the experimental analyses[109,110]. As the calculated Arrhenius energies presented in Table 6.13 are nearly equal for cation and anion in both the lithium and sodium compounds, it again confirms the suggestion of PS[11] that the ratio of cation and anion contributions to conductivity will be temperature independent. Estimates of interstitial Arrhenius energies for all the four crystals in Table 6.13 show that they are slightly larger than the vacancy values. Thus, as discussed earlier, although the Frenkel energies are large, the interstitial is also very mobile because of interstitialcy migration. Such a mechanism, in addition to vacancy mode of migration, presents a nearly linear shape in the conductivity curve. This sort of curve, in general, cannot be resolved in the analysis of conductivity curves associated with the ionic compounds.

An attempt was made to calculate various defect energies on the basis of two more potential models, e.g. Bowman[35] and HS[36]. The exercise failed due to the invalidity of minimization which happens owing to the excessive displacements of shells caused by the potentials. Although the two potentials describe, to some extent, the lattice properties of these four lithium and sodium compounds, they are not suitable for defect studies. On the other hand, the present potentials are able to give a unified description of all the properties, e.g. static lattice, dynamics,

and defect properties of the lithium hydride and deuteride. Although we believe that the various defect energies and other calculated values for the heavier hydrides and deuterides are also of expected magnitude, their experimental results on the latter crystals are needed in order to make a fruitful comparison.

CHAPTER 7

CONCLUSIONS

We have made an assessment of the derived potential by calculating the properties of the perfect and defect lattices of the hydrides and deuterides of lithium and sodium. The present potential has had the greatest degree of quantitative success for uniformly describing the static, dynamic and defect properties of the compounds under study. This is in contrast to the previous potential models of Bowman[35] and HS[36] which are partly suitable to reproduce the crystal data of alkali metal hydride and deuteride compounds. The former potential[35] fails to describe both the dynamic and defect properties and the latter one[36] is unable to model the defect lattices. Although the PS[11] potential describes only the lightest of the hydrides and deuterides, the degree of success with the present potential is much better. In addition, the present potential model has been extended to the heavier hydride and deuteride.

From the study of defect lattice properties (Schottky, Frenkel, and anti-site pair defect energies, activation and Arrhenius energies of migration) based on the present potential it is predicted that as the Schottky pair formation energies are smaller this type of defect will predominate in these hydrides and deuterides of lithium and sodium compounds . On the other hand, anti-site pair defect energies are very high and hence this sort of defect is least possible in the crystals under study. The estimated anion vacancy activation energies are smaller and

comparable with the cation values. The results, thus, obtained for the anion migration are insufficient to explain the reported curvature in the conductivity plot[109,110]. The prediction for defect lattice, here, shows that interstitial as well as vacancy play a significant role for ionic conduction in all these crystals and the relative contribution of both the ions to conductivity in the intrinsic region is temperature independent.

The parameters involved in the potential can further be refined if elastic and dielectric properties of heavier hydrides and deuterides are available. Thus, for a definitive study of heavier alkali metal hydrides and deuterides the need for the measurements of other quantities, e.g., elastic and dielectric properties is stressed.

REFERENCES

1. C.B. Magee, Metal Hydrides, Chap. 6, Ed. W.M. Mueller et al., Academic Press, New York, 1968.
2. F.E. Pretzel, G.V. Gritton, C.C. Rushing, R.J. Friauf, W.B. Lewis and P. Waldstein, J. Phys. Chem. Solids, 23, 325 (1962).
3. M.H. Brodsky and Burstein, J. Phys. Chem. Solids, 28, 1655 (1967)
4. C.R. Fisher, T.A. Dellin, S.W. Harrison, R.D. Hatcher, and W.D. Wilson, Phys. Rev. B1, 876 (1970)
5. W.D. Wilson and R.A. Johnson, Phys. Rev. B1, 3510 (1970)
6. S.S. Jaswal, T.P. Sharma, and G. Wolfram, Solid State Communication 11, 1151 (1972)
7. S.S. Jaswal and V.D. Dilly, Phys. Rev. B15, 2366 (1977)
8. H. Wendel and R. Zeyher, Phys. Rev. B21, 5544 (1980)
9. W. Dyck and H. Jex, J. Phys. C14, 4193 (1981)
10. B.W.James and H. Kheyrandish, J. Phys. C15, 6321 (1982)
11. R. Pandey and A.M. Stoneham, J. Phys. C18, 5289 (1985)
12. J.L. Verble, J.L. Warren and J.L. Yarnell, Phys. Rev. 168 980 (1968)
13. M.G. Zemlianov, E.G. Brooman, N.A. Chernopickov, and I.L. Shitikov, Inelastic Scattering of Neutrons, Vol. 2 (Viena: IAEA, 1965)
14. D. Laplaze, C. R. Acad. Sci., Paris 2768, 619 (1973)
15. D. Laplaze, J. Physique 37, 1051 (1976)
16. S. Haussuhl and W. Shorczyk, Z. Kristallogr. 130, 340 (1969)

17. M.W. Guinan and C.F. Cline, J. Nonmetals 1, 11 (1972)

18. D. Gerlich and C.S. Smith, J. Phys.Chem.Solids 35, 1567 (1974)

19. B. Yates, G.H. Wostenholm and J.L. Bingham, J. Phys. C7, 1769 (1974)

20. R.K. Singh, Solid State Communication 11, 559 (1972); J.Phys C7, 3473 (1974)

21. D. Laplaze, J. Phys. C10, 3499 (1977)

22. C.R.A. Catlow, K.M. Diller, and M.J. Norgett, J. Phys. C10, 1395 (1977)

23. C.R.A. Catlow, M.J. Norgett, and T.A. Ross, J. Phys. C10, 1627 (1977)

24. W.C. Mackrodt and R.F. Stewart, J. Phys. C12, 431 (1979)

25. J. Corish, M.C. Brenda, and P.W.M. Jacobs, Canada J. Phys. 54, 3839 (1976)

26. S. Bandopadhay, and A.K. Deb, Indian J. Phys. A57, 422 (1983)

27. E.W. Kellerman, Phyl. Trans. Roy. Soc. A238, 513 (1940)

28. B.G. Dick and A.W. Overhauser, Phys. Rev. 112, 90 (1958)

29. A.D.B. Woods, B.N. Brockhouse, R.A. Cowley, and W. Cochran, Phys. Rev. 131, 1025 (1963)

30. U. Schroder, Solid State Communication, 4, 347 (1963)

31. V. Nusslen and U. Schroder, Phys. Stat. Sol. 21, 309 (1967)

32. W. Bluthardt, W. Schneider, and M. Wagner, Phys. Stat. Sol. (b) 56, 453 (1973)

33. J.R. Hardy, Phil. Mag. 7, 315 (1962)

34. M.J.L. Sangster, J. Phys. Chem. Solids 34, 355 (1973); 35, 195 (1974)

35. R.C. Bowman, J. Phys. Chem 75, 1251 (1971)

36. A.R.Q. Hussain and M.J.L. Sangster, J. Phys. C19, 3535 (1986)

37. A.M. Stoneham and J.H. Harding, Ann. Rev. Phys.Chem. 37, 53 (1986)

38. P.P. Ewald, Ann. Physik 64, 253 (1921)

39. M. Born and K. Huang, Dynamical Theory of Crystal Lattices (Oxford University Press, 1954)

40. L. Pauling, Z. Kristallogr., 67, 377 (1928); J.A.C.S., 50, 1036 (1928)

41. M.L. Huggins and J.E. Mayer, J. Chem. Phys., 1, 643 (1933)

42. F.G. Fumi and M.P. Tosi, J. Phys. Chem. Solids, 25, 31 (1964)

43. M.P. Tosi and F.G. Fumi, J. Phys. Chem. Solids, 25, 45 (1964)

44. P.O. Lowdin, Ark. Mat. Astra. Fys. 35A, 30 (1947); J. Chem. Phys. 18, 365 (1950)

45. S.O. Lundqvist, Ark. Fys., 6, 25 (1952); 9, 435 (1955); 12, 263 (1957); 19, 113 (1961)

46. S.O. Lundqvist, V. Lundstrom, E. Tenerz and I. Waller, Ark. Fys., 15, 193 (1959)

47. B.N. Brockhouse, Can. J. Phys. 33, 889 (1955)

48. B.N. Brockhouse and P.K. Iyengar, Phys. Rev. 108, 894 (1957)

49. B. Szigeti, Trans. Farad. R. Soc. London 45, 155 (1949); Proc. R. Soc. London 204A, 51 (1950)

50. R.H. Lyddane, R. Sachs and E. Teller, Phys. Rev. 59, 673 (1941)

51. E.W. Kellermann, Phil. Trans. R. Soc. London 238A, 513 (1940); Proc. R. Soc. London 178A, 17 (1941)

52. J. R. Tessman, A.H. Kahn and W. Shockley, Phys. Rev.92, 890 (1953)

53. M.J. Norgett, J. Phys. C4, 298 (1971)

54. K. Thermalingam, Phil. Mag. 23, 181 (1971)

55. I.D. Faux, J. Phys. C4, L211 (1971)

56. C.R.A. Catlow and W.C. Mackrodt, Computer Simulation of Solids, Springer - Verlag, New York (1982)

57. R.A. Cowley, Proc. R. Soc. 268A, 121 (1962)

58. M.M. Elcombe and A.W. Pryor, J. Phys. C3, 492 (1970)

59. M. Elcombe, J. Phys. C5, 2702 (1972)

60. J.P. Hurrel and V.J. Minklewicz, Solid State Communication 8, 463 (1970)

61. G. Dolling, R.A. Cowley, and A.D.B. Woods, Can. J. Phys. 43, 1397 (1965)

62. R.G. Gordon and Y.S. Kim, J. Chem. Phys. 56, 3122 (1972)

63. Y.S. Kim and R.G. Gordon, J. Chem. Phys. 60, 1842 (1974); 60, 4332 (1974)

64. M.J.L. Sangster and M. Dixon, Adv. Phys. 25, 247 (1976)

65. P. Debye, Ann. Phys. 43, 49 (1914)

66. I. Waller, Z. Phys. 17, 398 (1923); 51, 213 (1928)

67. P. Debye, Ann.Phys. 39(4), 789 (1912)

68. M. Born and Th. v. Kerman, Z. Phys. 13, 297 (1912); 14, 65 (1913)

69. J. Laval, C.R. Acad. Sci. (Paris) 207, 169 (1938); 208, 1512 (1939); Bull. Soc. Franc. Miner. 62, 137 (1939)

70. P. Olmer, Acta. Cryst. 1, 57 (1948)

71. C.B. Walker, Phys. Rev. 103, 547,558 (1956)

72. M. Born, Rep. Progr. Phys. 9, 294 (1942-43)

73. H. Rubens and P. Hollnagel, Sitzungsber Berl. Akad. 26 (1910)

74. R.B. Barnes, Z. Phys. 75, 723 (1932)

75. L. Brillouin, Compt. Rend. 158, 1331 (1914); Ann. Phys. (Paris) 17, 88 (1922)

76. A. Smekal, Naturwiss. 11, 873 (1923)

77. C. V. Raman, K. S. Krishnan, Ind. J. Phys. 2, 387 (1928); Nature 121, 501 (1928)

78. B.N. Brockhouse, A.T.Stewart, Phys. Rev. 100, 756 (1955)

79. J. Frenkel, Zeits. f. Physik, 35, 652 (1926)

80. C. Wagner and W. Schottky, Zeits. f. Phys. Chem (B) 11, 163 (1930)

81. W. Jost, J. Chem. Phys. 1, 466 (1933)

82. J. H. Crawford Jr. and L.M. Slifkin, Point defect in Solids Vol. 1, (New York and London: Plenum, 1972)

83. A.M. Stoneham, The Theory of Defects in Solids (Oxford University press, 1975)

84. N.F. Mott and M.J. Littleton, Trans. Faraday Soc. 34, 485 (1938)

85. M.J. Norgett, AERE Report: AERE R- 7650 (1974)

86. R. Fletcher and M.J.D. Powell, Computer J. 6, 163 (1963)

87. M.J. Norgett and R. Fletcher, J. Phys. C3, L190 (1970)

88. D. Rowell, AERE Report, R - 10861 (1984)

89. W. Cochran, CRC. Crit. Rev. Sol.State Sc. 2, 1 (1971)

90. M.J.L. Sangster, U. Schroder, and R.M. Atwood, J. Phys. C11, 1523 (1978)

91. M.J.L. Sangster and R.M. Atwood, J. Phys. C11, 1541 (1978)

92. M.P. Tosi, Solid State Physics 16, 1 (1964)

93. P.N. Fowler and P.A. Madden, Phys. Rev. B29, 1035 (1984)

94. W.C. Mackrodt and R.F. Stewart, J. Phys. C10, 1431 (1977)

95. P.T. Wedepohl, Proc. Phys. Soc. 92, 79 (1967)

96. J.H. Harding and A.H. Harker, UKAEA Report R - 10425 (1982)

97. J.H. Harding, Private Communication (1988)

98. C.P. Wood and N.C. Pyper, Mol. Phys. 43, 1371 (1981)

99. R. Pandey and J.H. Harding, Phil. Mag. B49, 135 (1984)

100. J.P. Chandler, Subroutine STEPIT, Physics Department, Indiana University, Bloomington, Indiana, U.S.A.

101. L. Pauling, The Nature of the Chemical Bond, (Ithaco, Cornell University Press, 1945)

102. H. Blitz, M. Buchanan, K. Fisher, K. Haberkorn and U. Schroder, Solid State Commun. 16, 1023 (1975)

103. F.H. Ree and A.C. Holt, Phys. Rev. B8, 826 (1973)

104. R. Pandey, Private Communication (1989)

105. P.D. Pathak and N.G. Vasavada, J. Phys. D3, 1767 (1970)

106. M. Shukla and K.G. Bansigir, J. Phys. D9, L49 (1976)

107. W. Bollman, Phys. Stat. Sol(a). 61, 395 (1980)

108. L.W. Barr and A.B. Lidiard, Phy. Chem. 10, 152 (1970)

109. M. Ikeya, J. Phys. Soc. Japan, 42, 168 (1977)

110. P.A. Varotsos and S. Mouriksis, Phys. Rev. B10, 5220 (1974)

111. W.C. Mackrodt, Computer Simulation of Solids (New York : Springer - Verlag) 175, 1982

112. Ya.N. Parshits E.V. Pavlov, Fiz. Tverd Tela. 10, 1418 (1968)

113. P.W.M. Jacobs and P. Pantelis, Phys. Rev. B4, 3757 (1971)

114. C. Nadler and J. Rossel, Phys. Stat. Solidi(a) 18, 711 (1973)

115. R.G. Fuller, C.L. Marquardi, M.H. Reilly and J.C. Wells Phys. Rev. 176, 1036 (1968)

116. L.W. Barr and D.K. Dawson, AERE Harwell Rep., R-6234 (1969)

117. S. Chandra and J. Rolfe, Can. J. Phys. 48, 397,412 (1970); 49, 2098 (1971); 51, 236 (1973)

118. M. Beneire, M. Chemla and F. Beneire, J. Phys. Chem. Solids, 37, 525 (1976)

phys. stat. sol. (b) 158, 457 (1990)

Subject classification: 63.20; S2

Department of Physics, Rajshahi University[1]) *(a),*
and International Centre for Theoretical Physics, Trieste[2]) *(b)*

Hydrides and Deuterides of Lithium and Sodium

I. Model Potentials and Their Use in Perfect Lattice

By

E. HAQUE (a) and A. K. M. A. ISLAM (a, b)

An interionic potential model is developed for lighter and heavier alkali hydrides and deuterides. The method uses a combination of theoretical techniques, empirical fit, and a few plausible assumptions. An assessment of the derived potentials is made by calculating the lattice statics and dynamics of the crystals and by comparing both with experiment (where available) and with other calculations. The potentials are found to describe the elastic and dielectric properties reasonably well. The phonon dispersion curves of hydride and deuteride of sodium are compared with the calculations of Dyck and Jex based on force constant model approach and the results are discussed. The need for further experiments on heavier hydrides and deuterides is stressed.

Es wird ein Interionenpotentialmodell für leichtere und schwerere Alkalihydride und -deuteride entwickelt. Die Methode benutzt eine Kombination von theoretischen Techniken, empirischer Anpassung und einigen wenigen plausiblen Annahmen. Eine Einschätzung der abgeleiteten Potentiale wird durch Berechnung der Gitterstatik und -dynamik der Kristalle und durch Vergleich sowohl mit Experimenten (wenn vorhanden) als auch mit anderen Berechnungen durchgeführt. Es wird gefunden, daß die Potentiale die elastischen und dielektrischen Eigenschaften verhältnismäßig gut beschreiben. Die Phononendispersionskurven der Hydride und Deuteride von Natrium werden mit den von Dyck und Jex auf der Grundlage des Kraftkonstantenmodells durchgeführten Berechnungen verglichen und die Ergebnisse diskutiert. Die Notwendigkeit weiterer Experimente an schwereren Hydriden und Deuteriden wird hervorgehoben.

1. Introduction

Alkali metal hydrides possess properties that make them desirable for many applications in chemical and nuclear industries including high energy fuels. These hydrides are all quite similar in their overall physical and chemical properties. LiH is a material unique in its simplicity of electronic structure and its nuclear preparation. Thus it is not surprising to find that there are considerably more literature data pertaining to LiH and LiD [1 to 10] than to any of the other saline hydrides. Following LiH, more is known of NaH and CaH_2, simply because these hydrides were most readily available and least expensive for a particular application. This accounts for the fact that these hydrides arouse much interest for both theoretical and experimental studies.

The development of potentials for hydrides and deuterides, like other alkali halides, has been largely driven by the increased use of modelling methods in studying both structural and defect properties of these materials. The works of several investigators [10 to 14], have

[1]) Rajshahi-6205, Bangladesh.
[2]) P.O. Box 586, 34100 Trieste, Italy.